Doctoral Dissertations 1896 - February 2014

1-1-1995

Segmented polyurethane elastomers with liquid crystalline hard segments/

Weiming, Tang
University of Massachusetts Amherst

Follow this and additional works at: https://scholarworks.umass.edu/dissertations_1

SEGMENTED POLYURETHANE ELASTOMERS WITH LIQUID CRYSTALLINE HARD SEGMENTS

A Dissertation Presented

by

WEIMING TANG

Submitted to the Graduate School of the
University of Massachusetts Amherst in partial fulfillment
of the requirement for the degree of

DOCTOR OF PHILOSOPHY

September 1995

Department of Polymer Science and Engineering

SEGMENTED POLYURETHANE ELASTOMERS WITH
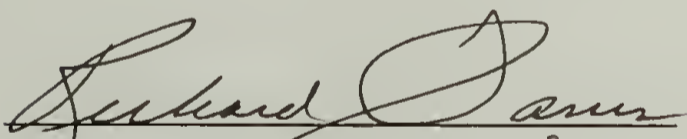LIQUID CRYSTALLINE HARD SEGMENTS

A Dissertation Presented

by

WEIMING TANG

Approved as to style and content by:
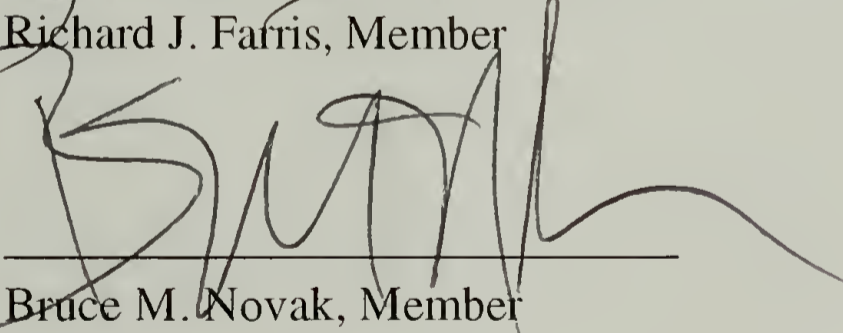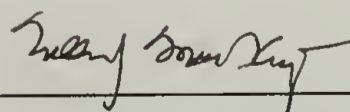
_____

William J. MacKnight, Chair

_____

Richard J. Farris, Member

_____

Bruce M. Novak, Member

_____

William J. MacKnight, Department Head
Polymer Science and Engineering

Dedicated to my parents

ACKNOWLEDGEMENTS

I would like to thank my advisor Professor William MacKnight for his guidance and support throughout my doctoral studies. He is the first person who introduced me the exciting field of polymer physical chemistry and to the meaning of scientific research. He has always encouraged me to seize the moment of graduate studies and pursue the research project with my own thoughts and intuitions. His belief in my ability has supported me to face the scientific challenges.

I would appreciate very much my other two committee members, Professors Richard Farris and Bruce Novak. Their criticism and suggestions during the work are important and valuable for the completion of this dissertation.

I would like to express my gratitude to my collaborators, Professor Claus Eisenbach and Dr. Heidi Hayne at Universität of Bayreuth, Germany. Their assistance has helped make my research and stay pleasant at Bayreuth. Our devotion to this project has led to a continuous cooperation between the two research groups.

It has been truly enjoyable to collaborate with Dr. Wolfgang Wedler, Professor Henning Winter, Professor Shaw L. Hsu. I am particularly indebted to Dr. Charles Dickinson, Dr. Alan Waldon and Mr. Louis Raboin for their assistance with NMR, X-ray, and electron microscopy, respectively.

I am grateful to the Army Research Office (Grant DAAL 03-91-G-0127) for financial support of this research. I acknowledge the Material Research Laboratory (MRL) for the use of the central facilities.

I especially thank Drs. Tee Yu, Hsin-Lung Chen, Wilson Cheung, Quinn Tong, Karla Gagnon, Fotis Papadimitrakopoulos and Ms. Wei Chen. I have

enjoyed our endurable friendship and support during both the good and bad times.

Finally, I would like to thank my parents. They have inspired my curiosity and desire to learn, and encouraged me to pursue the doctoral education in a foreign country. I will be forever indebted for their selfless love and constant support. I dedicate this dissertation to my parents.

ABSTRACT

SEGMENTED POLYURETHANE ELASTOMERS WITH LIQUID CRYSTALLINE HARD SEGMENTS

SEPTEMBER 1995

WEIMING TANG,

B.S., EAST CHINA UNIVERSITY OF SCIENCE AND TECHNOLOGY

M.S., UNIVERSITY OF MASSACHUSETTS AMHERST

Ph.D., UNIVERSITY OF MASSACHUSETTS AMHERST

Directed by: Professor William J. MacKnight

Segmented liquid crystalline polyurethanes (LCPUE) have been studied with hard segments composed of the mesogen 4,4'-bis(6-hydroxyhexoxy)-biphenyl, 2,4-tolylene diisocyanate, and 2,6-tolylene diisocyanate and soft segments composed of poly(tetramethylene oxides). Differential scanning calorimetry and wide-angle X-ray scattering experiments show the existence of an enantiotropic mesophase in the hard domains of the elastomer. Furthermore, the mesophase can be oriented by elastic deformation, and it forms a more ordered packing during this process. The tensile properties of these segmented polyurethanes are determined by their morphologies and can be manipulated by controlling the hard- and soft-segment concentration ratio.

The linear viscoelastic properties of a segmented polyurethane referred to as LCPUE 1000 have been studied. The rheological study indicates a broad transition from a viscoelastic solid to a viscoelastic liquid at the isotropization temperature of the mesophase. We conclude that the

aggregation of liquid crystalline hard segments does enhance the connectivity of the molecular structure, and this is supported by the results of a kinetic study with dynamic mechanical spectroscopy (DMS). Physical gelation studies identify a liquid/solid transition when cooled to 106 °C or below and show the characteristic critical behavior at the gel point with a power law relaxation spectrum at low frequencies.

Segmented liquid crystalline polyurethanes (LCPUE) have been further studied by infrared spectroscopy. The orientation function achievable in the hard segments results from the combination of mechanical strain and stress-softening. Furthermore, elastic deformation induces the rearrangement of some hard segments in the mesophase into a more ordered packing. High temperature infrared spectra have been correlated with thermal transitions of the LCPUE, and a liquid-liquid microphase separated morphology above the isotropization of the mesophase appears to exist.

Segmented polyurethane elastomers with monodisperse isomerically pure hard segments (PUE) and isomerically mixed hard segments (LCPUE) have been synthesized by treating amine-terminated hard segments with poly(oxytetramethylene) bischloroformate in the presence of an acid acceptor. Differential scanning calorimetry and wide-angle X-ray scattering experiments show the existence of crystalline phases in the isomerically pure hard domains of PUEs and a mesophase in the isomerically mixed hard domains of LCPUE, respectively. Copolymerization and/or blending of the pure isomers (PUE) destablize the crystalline phase, forming an enantiotropic mesophase in the elastomer.

TABLE OF CONTENTS

LIST OF TABLES

LIST OF FIGURES

CHAPTER 1

INTRODUCTION

1.1   Thermoplastic Polyurethane Elastomer

Polyurethane chemistry and technology opened the way to a new generation of high performance materials such as foams, coatings, adhesives, elastomers and fibers.   Based on a straightforward polyaddition reaction, the polyurethanes showed to be very versatile polymers. Materials with specified properties can be produced from the wide variety of the chemicals used. Today, thermoplastic polyurethane elastomers play a significant role within the family of thermoplastic elastomers.[1,2]

Pioneering polyurethane work was initiated by Otto Bayer and his coworkers in 1937.[3] Their original goal was to improve or duplicate the properties of synthetic nylon fibers. Subsequently, the elastomeric properties of polyurethanes were recognized by DuPont[4] and by ICI.[5] By the 1940's polyurethanes were manufactured on an industrial scale. Early polyurethane elastomers consisted of basically three components:

1. a polyether or polyester macrodiol

2. a chain extender such as water, a short-chain diol, or a diamine

3. a diisocyanate, e.g. naphthalene-1,5-diisocyanate (NDI).

However, these polyurethane elastomers were not yet real thermoplastic polyurethane elastomers in the proper sense of the definition, since their

melting temperature was higher than the decomposition temperature of the urethane linkages.

It was the great progress that NDI was replaced by diphenylmethane-4,4'-diisocyanate (MDI) in the above mentioned three component system. Schollenberger of B. F. Goodrich described a TPU in 1958.[6] Simultanously, DuPont announced a Spandex fiber called Lycra, a polyurethane based on MDI. By the early 1960's Goodrich marketed Estane, Mobay Texin, Upjohn Pellethane in the U.S.A. Bayer and Elastogran marketed Desmopan and Elastollan in Europe, respectively.

In the following years, much emphasis was spent to elucidate the nature of bonding, structure-property relationship, etc. It is well established now that TPU owe their unique properties to a domain structure which is achieved by the phase separation of these multi-block polymers.

One type of block, the hard segment, is formed by addition of the chain extender, e.g., butanediol, to the diisocyanate, e.g. MDI. The other type is the soft segment and consists of the flexible polyether or polyester chains which interconnect two hard segments. At room temperature, the soft segments are thermodynamically incompatible with the polar hard segments, which leads to a microphase separation. A part of the driving force for phase separation is attributed to the development of crystallinity of the hard domains. Upon heating above the melting temperature of the hard domains, the polymer forms a viscous melt which can be processed by thermoplastic processing techniques such as injection molding, extrusion, blow molding, etc. Subsequent cooling leads again to segregation of hard and soft segments.

In general, TPU are synthesized by mixing all of the reactants together at temperature above 80 °C. The reaction can be carried out in different ways. The so called "one-shot method" involves mixing all the ingredients together.

In the "prepolymer method" the polyol is reacted first with the diisocyanate to give an isocyanate endcapped prepolymer, which is further reacted with the chain extender.

TPU were the first polymeric materials to combine both rubber elasticity and thermoplastic characteristics. The soft segments usually form an elastomer matrix which accounts for the reversibly elastic properties of TPU, with the hard segments acting as multifunctional tie points functioning both as physical crosslinks and reinforcing fillers. However, these crosslinks can be reversibly overcome by heat or by solvation. Then by cooling or on desolvation a TPU network is reformed.

By varying the hard segment concentration, the Young's moduli of TPU range from 8 MPa up to about 2000 MPa and the strains at break up to 1000 percent.[7,8] These materials also process a high resistance to abrasion, up to ten times that of natural rubber, and excellent tensile strengths of up to 55 MPa.[9]

It is obvious that morphology of microphase separated systems plays an important role in determining the material ultimate properties. By controlling variation of the morphology, desired properties of a product can be obtained. Hence, the morphological investigation is essential for understanding structure-property relationships.

Cooper et al[10] studied polyester and polyether polyurethanes by using transmission electron microscopy (TEM). Iodine was used to stain the hard domain. It was concluded that the hard domains were from 30 to 100 Å for both the polyester and polyether urethanes. Schneider et al[11] studied the MDI/BDL based segmented polyurethanes by TEM and found spherulites on the order of one micrometer, which were believed to arise from the crystallizable hard segments. Briber and Thomas[12] found the crystal forms in

3

MDI/BDI hard segments in a polypropylene oxide based polyurethanes which were prepared by one-stage method.

Considerable efforts have been made to elucidate the nature of TPU hard segment domains.[13-17] Recently, Blackwell et al. extensively studied the structure of hard segments in MDI/diol/polytetramethylene adipate polyurethanes by X-ray diffraction. They used butanediol (BDO), propanediol (PDO), and ethylene glycol (EDO) as chain extenders.[18,19] Poly(MDI/BDO) was found to be the most crystallizable hard segment. Based on conformational analysis and model compound considerations, it was concluded that poly (MDI/BDO) existing in its fully extended chain conformation can form a hydrogen bonded network in two dimensions perpendicular to the chain axis. In contrast, poly (MDI/PDO) and poly(MDI/EDO) crystallized in higher energy contracted conformations, which are necessary for a nonstaggered packing of the chains. The above findings were confirmed by the results of Eisenbach[20] who reported on the synthesis and analysis of a series of soft and hard segments under strictly controlled conditions. Oligomers from MDI and BDO were synthesized and endcapped. By SAXS measurements it was shown that MDI/BDO based oligourethanes crystallize in an extended chain without chain folding.

Furthermore, interphase mixing phenomena in TDI-based polyurethanes were extensively studied by Schneider and coworkers.[21-24] Block polyurethanes were prepared from 2,4- and 2,6-TDI isomers. DSC, X-ray scattering, IR analysis and thermomechanical studies were used to investigate the structural organization and thermal transitions in these products. It was found that the degree of phase segregation strongly depended on the TDI symmetry and the soft segment molecular weight. The T_g of 2,4-TDI polyurethanes with polyether soft segment of M_n ca. 1000

4

showed a strong dependence on composition, indicating extensive phase mixing occurred. In contrast, comparable 2,6-TDI based polyurethanes displayed a highly ordered structure as revealed by a concentration independent T_g and a high temperature transition attributed to melting of the crystallizable hard segment. Changing the soft segment molecular weight from 1000 to 2000 led to phase segregation in the 2,4-TDI series and further improved phase segregation in the 2,6-TDI series. The results are in agreement with similar results obtained with a polycaprolactone diol-based TPU.[25,26] Furthermore, it was confirmed by a paper of Senich and MacKnight.[27]

1.2   Liquid Crystalline Polymer

Liquid crystalline polymers (LCP) are an important class of materials because of their ability to show spontaneous anisotropy and readily induced orientation in the liquid crystalline state. When polymers are processed in the liquid crystalline state, the anisotropy is maintained in the solid state and leads to the formation of materials that sustain great strength in the direction of orientation. An important example of utilizing this anisotropy is in the formation of aromatic polyamide fibers which are spun from shear oriented liquid crystalline solutions.[28,29]

These lyotropic mesogenic materials require the solvent presence in order to produce a mesophase, in contrast, thermotropic mesogenic compounds exhibit a mesophase in the melt state at temperatures above the crystalline solid state and before the formation of an isotropic melt.[30] Mesophase-forming polymers may either contain the mesogenic group

5

directly in the main chain, or the mesogen may be present as a pendant group in the side chain.

Flexible spacers have been extensively employed to separate mesogenic groups placed in the main chain from each other, and the backbone flexibility achieved by this approach has improved the solubility and lowered transition temperatures of materials in comparison to those of the pure rigid rod polymers of same composition.[31] In order to further improve their processability, thermotropic rigid rod polymers may be modified in other ways, and such polymers are receiving considerable interest for potential fiber applications because they can be processed by melt spinning techniques.[32]

Other methods can be used to reduce the transition temperatures of main chain LC polymers to a suitable range; these include: (1) the introduction of substituents, (2) the addition of an element of dissymmetry to the main chain by copolymerizing mesogenic units of different shapes and (3) copolymerizing non-linear, non-mesogenic units.[33] These mechanisms preserve the linearity and stiffness of the rigid rod polymer chain but hinder crystal or liquid crystal packing, and can produce materials with reduced transition temperatures without adversely affecting the range of mesophase stability.

Liquid crystals are classified into three major categories based on the type of ordering within the mesophase.[30] A nematic phase exhibits orientational order but no positional order; i.e., the centers of gravity of the molecules are randomly located; A cholesteric liquid crystalline phase consists of a helical stacking of nematic layers; A smectic phase possesses orientational order within the layers.

The principal techniques used to characterize liquid crystals are differential scanning calorimetry (DSC), polarized optical microscopy (POM),

and wide-angle X-ray scattering (WAXS). DSC can measure the thermal energy gained or lost by the system as phase transition occurs. Crystal to liquid crystal, liquid crystal to isotropic, and liquid crystal to liquid crystal transitions are all first order and therefore give rise to peaks in a DSC temperature scan. The enthalpy and entropy of each transition can be calculated from the peak areas.

POM is used to observe birefringent textures which result from spatial fluctuations of the director within the sample.[34] Nematic phases typically give rise to the so-called schlieren texture; smectic phases can produce several different types of textures, including schlieren, mosaic and fan-shaped textures.

WAXS measures the periodicity of electron density over a scale of about 4 Å-40 Å. In a three-dimensional crystal, the WAXS diffraction pattern consists of many sharp reflections, indicating a high degree of order that persists over a long range. In a liquid crystal, the WAXS reflections are fewer and less sharp. Nematic phases show only a single reflection, at a spacing on the order of 4 Å-5 Å, corresponding to the distance between the long axes of the molecules. The reflection is diffuse, indicating that the interchain distance is not uniform. Smectic phases show this reflection, plus an additional reflection at low angles, which corresponds to the spacing between layers. Ordering within the smectic layers can cause the outer reflection to sharpen and sometimes to resolve into two or more components. In samples that do not possess long-range orientation, the reflections are seen as rings; in oriented samples, the low-angle reflections are usually meridional spots or arcs and the high-angle reflections are usually equatorial arcs. Low molecular weight liquid crystals can be oriented by placing the sample in a magnetic field. Polymer liquid crystalline phases can be oriented by uniaxial stretching.

1.3   Liquid Crystalline Polyurethane

Of the many thermotropic liquid crystalline polymers that have been reported in the literature, only a few are polyurethanes. This is partly because of the chemical instability of the polyurethane functional groups at temperature above 180 °C. Liquid crystalline polyurethanes are of interest for their potential application as high-strength fibers and plastics because of the strong tendency of the formation of hydrogen bonds. Ordered phases that incorporate hydrogen bonds are likely to gain thermodynamic stability from these interactions. This may have a profound effect on the structure and thermal behavior of mesophases in these polymers.

In our previous studies, both the isomerically pure 2,4-tolylene diisocyanate- and 2,6-tolylene diisocyanate-4,4'-bis(6-hydroxyhex oxy)biphenyl polyurethanes were found to be crystallizable and also to display monotropic liquid crystalline phases.[35,36] Cocrystallization of the isomerically pure polymers does not occur. The crystalline phase can be destabilized relative to the liquid crystalline phase, thus forming an enantiotropic liquid crystalline phase by altering the structure of the polymer, for example, by copolymerization and/or blending of the isomers. Stenhouse and MacKnight[37] obtained an enantiotropic liquid crystalline polyurethane (referred to as LCPU) from 4,4'-bis(6-hydroxyhexoxy)biphenyl with 2,4-tolylene diisocyanate and 2,6-tolylene diisocyanate at equal molar ratio.

Tanaka and Nakaya reported main-chain thermotropic liquid crystalline polyurethanes derived from 4,4'-bis(2-hydroxyethoxy)biphenyl (DHB)[38] and bis(p-oxymethylphenyl)terephthalate (BOPT),[39] each with four isocyanates: hexamethylene diisocyanate (HDI), dicyclohexylmethane-4,4'-diisocyanate (H_{12}MDI), cyclohexane-1,3-di(methylisocyanate) (H_6XDI), and 2,4-tolylene

8

diisocyanate (TDI). In the first series, the polyurethanes DHB/HDI, DHB/H$_{12}$MDI, DHB/H$_6$XDI, and DHB/TDI were reported on the basis of DSC and optical microscopy to display mesophases within temperature ranges of 188-203 °C, 147-172 °C, 135-193 °C, and 151-193 °C, respectively.

Mormann[40] synthesized a series of poly(diesterurethane)s based on diisocyanatoesters and α,ω-alkanediols. Four of these polymers were reported to be liquid crystalline. The mesophases were declared nematic on the basis of miscibility studies with low molecular weight nematogens. The crystalline melting temperatures were between 226 °C and 285 °C; clearing temperatures were all slightly above or below T$_m$.

Mormann and Bramm[41] synthesized a series of polyurethanes using mesogenic diisocyanates. The mesogenic units consisted either of two aromatic rings, or one aromatic ring and one cyclohexyl ring, connected by an ester linkage. Some of the aromatic rings contained methyl substituents, the purpose of which was to lower the transition temperatures of the polyurethanes by inducing the structural irregularity and also by sterically hindering hydrogen bonding. However, only the polyurethanes made from unsubstituted diisocyanates showed liquid crystalline phases. The mesophases were monotropic and nematic, with T$_m$ close to 250 °C and T$_i$ in the range of 222-258 °C.

1.4   Dissertation Objectives and Overview

Segmented liquid crystalline polyurethane elastomers (LCPUE) are a new class of block copolymers composed of alternating liquid crystalline hard and amorphous soft segments. The thermodynamic incompability between

9

the hard and soft segments results in the aggregation of hard segments, forming physical cross-links in the network. Due to the formation and nature of the liquid crystalline hard domains, their response to an applied strain should be different than that in a system with crystalline domains, thus, LCPUEs may be sensitive to external mechanical, electric and magnetic fields, and exhibit properties characteristic of both physically cross-linked elastomers and liquid crystalline materials over a wide temperature range before the isotropization of the liquid crystalline hard domains occurs. One of the primary objectives of this dissertation is to establish a model system in the thermoplastic elastomers and to understand the formation of liquid crystalline phase acting as multifunctional physical cross-links. The emphasis is on the orientation and response of liquid crystalline phase under an applied strain which may achieve a highly oriented and perfected structure.

Chapter 2 details the synthesis, phase characterization and tensile properties of LCPUEs.[42] Differential scanning calorimetry and wide-angle X-ray scattering experiments show the existence of an enantiotropic mesophase in the hard domains of the elastomer. The comparison between the LCPUE and LCPU is made to elucidate the behavior of the mesophase in the elastomers.

Chapter 3 applies rheology[43] to characterize the linear viscoelastic properties of LCPUE, it indicates a broad transition from a viscoelastic solid to a viscoelastic liquid at the isotropization temperature of the mesophase. Furthermore, a physical gelation method is used to identify a critical liquid/solid transition in the vicinity of isotropization of mesophase.

Chapter 4 presents infrared spectroscopic analysis of LCPUEs.[44] The first section discusses the dichroism work performed on each of materials as a function of strain. The second section focuses on the highly localized mode

of the amide I region (carbonyl stretching), which is sensitive to conformation change under strain and temperature.

Chapter 5 discusses the structure-property relationships with regard to the hard domain ordering aspect in LCPUE.[45] Segmented polyurethane elastomers with monodisperse isomerically pure hard segments (PUE) and isomerically mixed hard segments (LCPUE) have been synthesized. Differential scanning calorimetry and wide-angle X-ray scattering experiments show the existence of crystalline phases in the isomerically pure hard domains of PUEs and a mesophase in the isomerically mixed hard domains of LCPUE, respectively.

Chapter 6 includes the conclusions of the dissertation and suggestions for future work.

References and Notes

(1)   Folkes, M. J. *Processing, Structure and Properties of Block Copolymers*; Elsevier Applied Science Publishers: New York, 1985.

(2)   Legge, N. R.; Holden, G.; Schroeder, H. E. *Thermoplastic Elastomers*; Hanser Publishers: New York, 1987.

(3)   Bayer, O.; Rinke, H.; Siefken, W.; Ortner, L.; Schild, H. Ger. Pat. 728981 **1937**.

(4)   Christ, A. E.; Hanford, W. E. US Pat. 2333639 **1940**.

(5)   Brit. Pat. 580524 **1941**; Brit. Pat. 574134 **1942**.

(6)   Schollenberger, C. S.; Scott, H.; Moore, G. R. *Rubber World* **1958**, *137*, 549.
       Schollenberger, C. S. US Pat. 2871218 **1955**.

(7)   Goyert, W.; Winkler, J.; Wagner, H.; Hoppe, H. G. Eur. Pat. Appl. 15049 **1981**.

(8)   Goldwasser, D. J.; Onder, K. US Pat. 4376834 **1981**.

(9)   Willwerth, L.; Anzuoni, A. *Modern Plastics Encyclopedia 97*; McGraw Hill: New York, 1988.

(10)   Koutsky, J. A.; Hien, N. V.; Cooper, S. L. *J. Polym. Sci., Polym. Lett. Ed.* **1970**, *8*, 353.

(11)   Schneider, N. S.; Desper, C. R.; Illinger, J. L.; King, A. O.; Barr, D. *J. Macromol. Sci. Phys.* **1975**, *B11(4)*, 527.

(12)   Briber, R. M.; Thomas, E. L. *J. Macromol. Sci., Phys.* **1983**, *B22(4)*, 509.

(13)   Cooper, S. L.; Tobolsky, A. V. *J. Appl. Polym. Sci.* **1966**, *10*, 1837.

(14)   Bonart, R. *J. Macromol. Sci.* **1968**, *B2*, 115.

(15)   Bonart, R.; Morbitzer, L.; Hentze, G. *J. Macromol. Sci.* **1969**, *B3*, 337.

(16)   Bonart, R.; Morbitzer, L.; Muller, E. H. *J. Macromol. Sci.* **1974**, *B9*, 447.

(17)   Wilkes, C. W.; Yusek, C. *J. Macromol. Sci.* **1973**, *B7*, 157.

(18)   Blackwell, J.; Nagarajan, M. R. *Polymer* **1981**, *22*, 202.

(19)   Blackwell, J.; Nagarajan, M. R.; Hoitink, T. B. *ACS Symp. Ser.* **1981**, *172*, 179.

(20)   Eisenbach, C. D.; Guenther, C. *Am. Chem. Soc., Org., Coat. Appl. Sci. Proc.* **1983**, *49*, 239.

(21)   Paik Sung, C. S.; Schneider, N. S. *Macromolecules* **1975**, *8*, 68.

(22)   Paik Sung, C. S.; Schneider, N. S. *Macromolecules* **1977**, *10*, 452.

(23)   Schneider, N. S.; Paik Sung, C. S. *Polym. Eng. Sci.* **1977**, *17*, 73.

(24)   Schneider, N. S.; Paik Sung, C. S.; Matton, R. W.; Illinger, J. L. *Macromolecules* **1975**, *8*, 62.

(25)   Seefried, C. G. Jr.; Koleske, J. V.; Critchfield, F. E. *J. Appl. Polym. Sci.* **1975**, *19*, 2493.

(26)   Seefried, C. G. Jr.; Koleske, J. V.; Critchfield, F. E. *J. Appl. Polym. Sci.* **1975**, *19*, 2503.

(27)   Senich, G. A.; MacKnight, W. J. *Advan. Chem. Ser.* **1979**, *176*, 97.

(28)   Kwolek, S. L.; Morgan, P. W.; Schaefgen, J. R.; Gulrich, L. W. *Macromolecules* **1977**, *10*, 1390.

(29)   Flory, P. J. *Proc. Roy. Soc.* **1956**, *A234*, 73.

(30)   Gray, G. W.; Winsor, P. A. *Liquid Crystals and Plastic Crystals*; John Wiley & Sons: New York, 1974.

(31)   Jackson, W. J; Kuhfuss, H. F. *J. Polym. Sci., Polym Chem. Ed.* **1976**, *14*, 2043.

(32)   Pearce, E. M.; Schaefgen, J. R. *Contemporary Topics in Polymer Science*; Plenum Press: New York, 1977.

(33)   Griffin, B. P.; Cox, M. K. *Brit. Polym. J.* **1980**, *12*, 147.

(34)   Hartshorne, N. H. *The Microscopy of Liquid Crystals*; Microscope Publications Ltd.: London, 1974.

(35)   Stenhouse, P. J.; Valles, E. M.; Kantor, S. W.; MacKnight, W. J. *Macromolecules* **1989**, *22*, 1467.

(36)   Papadimitrakopoulos, F.; Hsu, S. L.; MacKnight, W. J. *Macromolecules* **1992**, *25*, 4671.

(37)   Stenhouse, P. J. Ph.D. Thesis, University of Massachusetts at Amherst, Amherst, MA. 1992.

(38)   Tanaka, M.; Nakaya, T. *Kobunshi Ronbunshu* **1986**, *43*, 311.

(39) Tanaka, M.; Nakaya, T. *J. Macromol. Sci., Chem.* **1987**, *A24*, 777.

(40) Mormann, W. *Polym Prepr.* **1989**, *30(1)*, 291.

(41) Mormann, W.; Brahm, M. *Marcomolecules* **1991**, *24*, 1096.

(42) Tang, W.; Farris, R. J.; MacKnight, W. J.; Eisenbach, C. D. *Macromolecules* **1994**, *27*, 2814.

(43) Wedler, W.; Tang, W.; Winter, H. H.; MacKnight, W. J.; Farris, R. J. *Macromolecules* **1995**, *28*, 512.

(44) Tang, W.; MacKnight, W. J.; Hsu, S. L. *Macromolecules* June 1995, in press.

(45) Tang, W.; MacKnight, W. J.; Hayne, H.; Eisenbach, C. D. Submit to *Macromolecules*.

CHAPTER 2

SEGMENTED POLYURETHANE ELASTOMERS WITH LIQUID CRYSTALLINE HARD SEGMENTS.
1. SYNTHESIS AND PHASE BEHAVIOR

2.1   Abstract

Segmented liquid crystalline polyurethanes (LCPUE) have been studied with hard segments composed of the mesogen 4,4'-bis(6-hydroxyhexoxy)-biphenyl, 2,4-tolylene diisocyanate, and 2,6-tolylene diisocyanate and soft segments composed of poly(tetramethylene oxides). Differential scanning calorimetry and wide-angle X-ray scattering experiments show the existence of an enantiotropic mesophase in the hard domains of the elastomer. Compared with nonsegmented polyurethane containing the same mesogen, the isotropization temperature of the mesophase in the elastomer is depressed. This is a result of the oligomeric structure of the hard domains. The endotherm corresponding to the isotropization transition is also broadened, reflecting a lack of uniformity of the hard domains. Furthermore, the mesophase can be oriented by elastic deformation, and it forms a more ordered structure during this process. The tensile properties of these segmented polyurethanes are determined by their morphologies and can be manipulated by controlling the hard- and soft-segment concentration ratio.

2.2   Introduction

Segmented block copolymers with alternating sequences of hard and soft segments are an important class of thermoplastic elastomers. The thermodynamic incompatibility between the hard and soft segments normally results in a microphase-separated structure. The hard segments form glassy or crystalline domains which act as physical cross-links to form a network. For example, in polyurethane elastomers, the hard segments based on diphenylmethane-4,4'-diisocyanate and short-chain diols develop crystallinity in the hard domains which act as multifunctional junction points and fillers.

Elastomeric chemically cross-linked networks with liquid crystalline side chains have been described,[1,2] and a few studies in the literature report the introduction of mesogens into the hard segment in the physically cross-linked thermoplastic elastomers.[3,4] The resulting polymeric structure consists of alternating liquid crystalline and amorphous segments which form main-chain liquid crystalline elastomers, a new class of polymeric material. The elasticity of this novel material arises form the conformational entropy changes which the soft segments undergo upon stretching, and the mesophase can be oriented by mechanical strain. Due to the liquid crystalline nature of the hard domains, their response to an applied strain should be different than that in a system with crystalline domains, and such an applied strain may result in a highly oriented and perfected structure. At high elongations, the amorphous soft segments will tend to become anisotropic as well. Thus, this kind of elastomer may exhibit unusual anisotropic mechanical, electrical, and optical properties, leading to future technological applications.

Thermotropic liquid crystalline polyurethanes have been studied[5-9] for their potential application as high-strength fibers and plastics. In our previous

16

studies, both the isomerically pure 2,4-tolylene diisocyanate- and 2,6-tolylene diisocyanate-4,4'-bis(6-hydroxyhexoxy)biphenyl polyurethanes were found to be crystallizable and also to display monotropic liquid crystalline phases. Cocrystallization of the isomerically pure polymers does not occur. The crystalline phase can be destabilized relative to the liquid crystalline phase, thus forming an enantiotropic liquid crystalline phase by altering the structure of the polymer, for example, by copolymerization and/or blending of the isomers. Stenhouse and MacKnight[10] obtained an enantiotropic liquid crystalline polyurethane (referred to as LCPU) from 4,4'-bis(6-hydroxyhexoxy)biphenyl with 2,4-tolylene diisocyanate and 2,6-tolylene diisocyanate at equal molar ratio. The current elastomers (referred to as LCPUE) are based on this LCPU structure as the hard segment, and we have compared the properties of LCPUE with LCPU in view of the understanding of the behavior of the mesophase in the elastomers. Poly(tetramethylene oxide) with different molar masses (650, 1000, 2000) is used as the soft segment.

2.3   Experimental Section

2.3.1   Materials

2,4-Tolylene diisocyanate (2,4-TDI; Fluka) and 2,6-tolylene diisocyanate (2,6-TDI; Aldrich) were purified by vacuum distillation. Poly(tetramethylene oxides) (PTMO; M_w= 650, 1000, 2000; PolyScience) were dried in vacuo for 3 days at 50 $^\circ$C. Dimethylformamide (DMF) was dried over molecular sieves and distilled under reduced pressure. 6-Chloro-1-hexanol (97%), 4,4'-dihydroxybiphenyl, ethyl alcohol, and 1,4-dioxane were used as received.

17

The syntheses of the mesogenic chain extender 4,4'-bis(6-hydroxy hexoxy)biphenyl (Diol-6) and of liquid crystalline polyurethane elastomers (LCPUE) are outlined in Figures 2.1 and 2.2.

2.3.2 4,4'-Bis(6-hydroxyhexoxy)biphenyl (Diol-6)

A total of 90 mL of ethyl alcohol was placed in a 250-mL three-necked flask equipped with a dropping funnel, a reflux condenser, and a magnetic stirrer. To this flask were added NaOH (6.72g, 0.168 mol) and 4,4'-dihydroxybiphenyl (7.7g, 0.042 mol), and the mixture was heated to 70 $^\circ$C. 6-Chloro-1-hexanol (25g, 0.183 mol) was added dropwise. The reaction mixture was refluxed for 24 h and poured into water. The precipitated material was filtered off and recrystallized three times from dioxane to yield a white powdery compound. Mp: 174.0-174.5 $^\circ$C. ^{1}H NMR (DMF-d_7): δ 1.33-1.79 (m, 16 H,-(CH_2)$_4$-), 3.51 (t, 4 H, CH_2OH), 4.02 (t, 4 H, -CH_2OAr), 4.36 (t, 2 H, OH), 7.02 (d, 4 H, o-phenoxy), 7.56 (d, 4 H, m-phenoxy).

2.3.3 Synthesis of Liquid Crystalline Polyurethane Elastomers (LCPUE)

Conventional polyurethane synthesis conditions were used for the preparation of LCPUE.[11-13]

To a 500-mL four-necked flask equipped with a condenser, thermometer, mechanical stirrer, and argon inlet-outlet were successively added PTMO (M_w= 650, 1000, 2000) (0.007 83 mol), the 1:1 (w/w) mixture of 2,4-tolylene diisocyanate (1.36 g, 0.0007 83 mol) and 2,6-tolylene diisocyanate (1.36 g, 0.0007 83 mol). The reaction mixture was mechanically stirred at 100 $^\circ$C under argon for 2.5 h. Then DMF (15 mL) and Diol-6 (3.02g, 0.007 82 mol) were added, and the reaction was held at 100 $^\circ$C for 50 h. DMF was added as the reaction proceeded to keep the solution viscosity low

Scheme I:
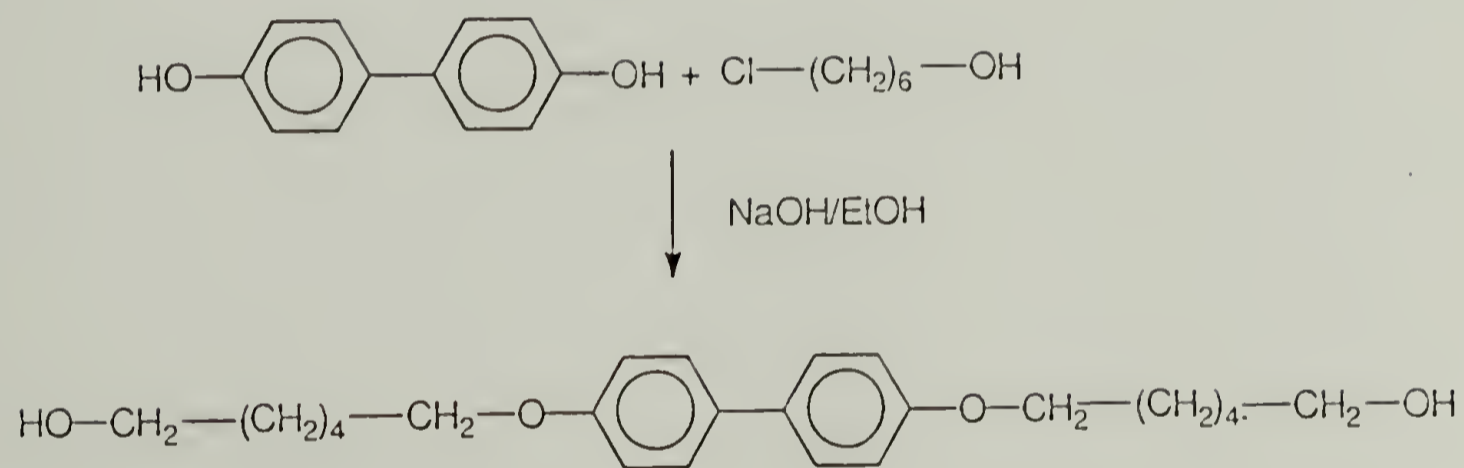
Figure 2.1   The synthesis of mesogenic chain extender 4,4'-bis(6-
            hydroxyhexoxy)biphenyl (Diol-6)
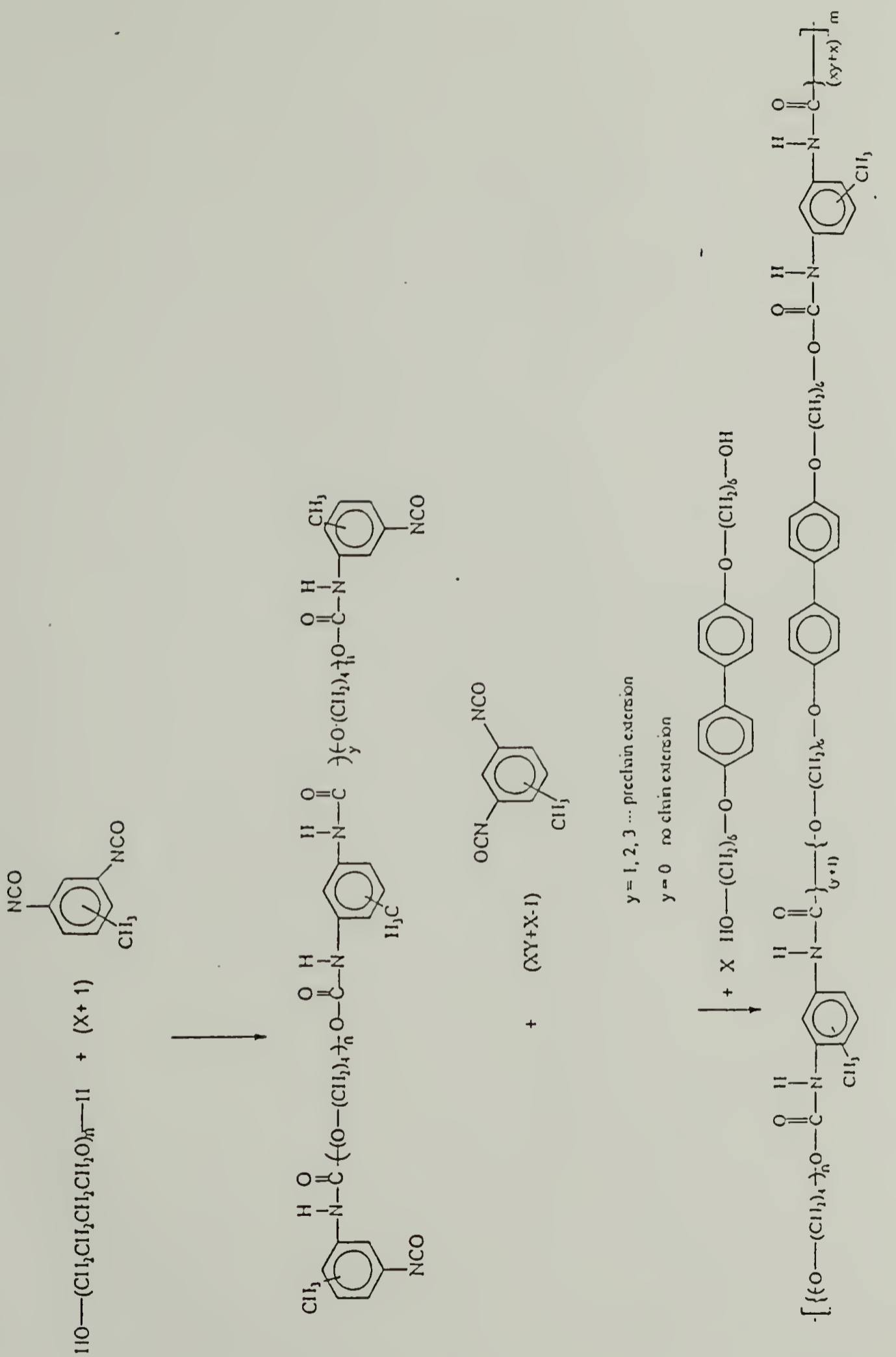
Figure 2.2   The synthesis of Liquid Crystalline Polyurethane Elastomers (LCPUE)

enough to allow stirring. The white polymer was precipitated out by pouring the hot, viscous solution into methanol. After Soxhlet extraction of material in methanol to remove DMF and unreacted starting material, the product was dried in vacuo.

The list of the chemical shifts of the ^{13}C NMR spectrum in LCPUE is given in Table 2.1. The spectrum was obtained with a 20-s recycle delay and the decoupler gated off except during acquisition.

2.3.4 Polymer Characterization Techniques

Molecular weights relative to polystyrene standards were determined by gel permeation chromatography (GPC) in THF and DMF as eluents with flow rates of 1 mL/min. The GPC instrument was equipped with three Polymer Labs columns (10^3, 10^4 and 10^5 Å) for THF as the eluent ($40\,°C$) and four Water Ultrastyragel columns (500, 10^3, 10^4 and 10^5 Å) for DMF as the eluent ($70\,°C$). The measurements were made by using UV and RI detectors, respectively.

A TA instrument 2910 differential scanning calorimeter was used to determine the thermal transitions. Indium was used as a standard for calibration. First-order transitions (e.g., mesophase-isotropic phase, etc.) were taken as the maximum or minimum of the endothermic or exothermic peaks. Glass transitions (T_gs) were taken as the half-height of the change in the heat capacity.

^{1}H and ^{13}C NMR spectra were recorded on a Varian XL-200 and XL-300 spectrometer, respectively. TMS was used as an internal standard.

Optical textures were studied with an Olympus polarizing optical microscope equipped with a Linkam hot stage and an Olympus photocamera.

Table 2.1   Line listing for ^{13}C NMR resonances in Liquid Crystalline Polyurethane Elastomers
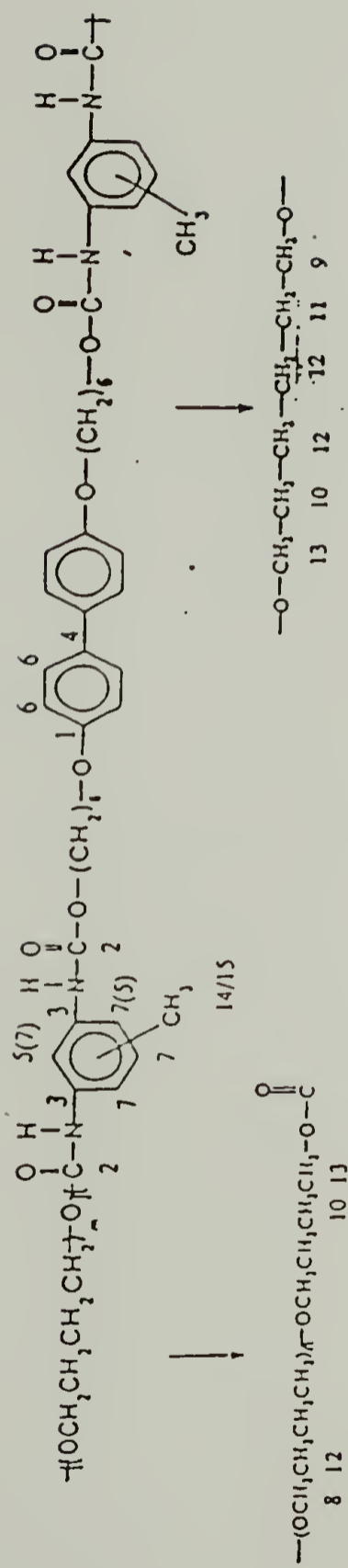
Region	Range,ppm	Specific Key Resonance,ppm	Assignments	Symbol
I	160-140	158.04	Carbon bonded with oxygen in phenoxy	1
		154.25	Carbonyl group of 2,6 urethane group	2
		153.7, 153.61	Carbonyl group of 2,4 urethane group	2
II	140-100	136.72, 136.19, 136.08	Carbon bonded with urethane group in phenyl group	3
		133.23	Carbon between the biphenyl group	4
		130.66	Carbon bonded with CH$_3$ in phenyl group	5
		127.57, 126.51	Carbon bonded with hydrogen in biphenyl group	6
		114.61	Carbon bonded with hydrogen in phenyl group	7
III	74-60	70.76-69.88	-CH$_2$O- in PTMO	8
		67.70	CH$_2$ bonded with phenoxy in Diol-6	9
		65.26	CH$_2$ bonded with the urethane groups	13
IV	30-20	29.12, 28.81	CH$_2$ next to CH$_2$ (67.7 ppm chemical shift) in Diol-6	11
		26.10	-CH$_2$- in PTMO and Diol-6	12
		25.74, 25.61	CH$_2$ next to CH$_2$ (65.26 ppm chemical shift) in PTMO and Diol-6	10
V	20-10	16.96	CH$_3$ of 2,4-TDI	14
		12.04	CH$_3$ of 2,6-TDI	15

22

X-ray powder and fiber diagrams of the polymer were recorded using Ni-filtered Cu Kα radiation in a Statton camera. The X-ray camera length was calibrated with $CaCO_3$.

Tensile tests were performed in an Instron Universal testing machine Model TTBM. The LCPUE was cast into a film between 0.1 and 0.2 mm thick and cut into ring samples 3.94 mm in width. The rings were elongated to break at a rate of 50 mm/min, at room temperature. These tests except for the sample thickness had been carried out in accordance with the specification of ASTM D412-87.

2.4   Results and Discussion

2.4.1   Constitution of the Segmented Polyurethane Elastomers

The reactivity of the isocyanate groups of 2,4- and 2,6-tolylene diisocyanate,[14] by considering the combination of electronic and steric effects, gives the following sequence of reactivity: 4-NCO (2,4-TDI) > 2-NCO (2,6-TDI) > 2-NCO (2,4-TDI with 4-urethane) ≥ 6-NCO (2,6-TDI with 2-urethane). Since equal reactivity of the hydroxyl end groups of PTMO, as well as of the Diol-6 end groups, can be assumed, which is not affected by the conversion of one of two hydroxyl groups into a urethane linkage, the difference of the reactivity of the isocyanate groups in the system has no specific effect on the 2,4- and 2,6-TDI distribution along the chain; i.e., the TDI isomers are randomly built into the chain.

The possible prechain extension of poly(tetramethylene oxide) with TDI during the prepolymer formation[13] is shown in Figure 2.2, and the relatively small amount of residual TDI reacts with Diol-6 in the following chain

23

extension reaction to form longer hard segments. In this context, the polydispersity of the PTMO should also be discussed. The idealized hard-segment structure is perturbed by the incorporation of Diol-6 repeating units, and low molar mass homologues of the H-$[O(CH_2)_4]_n$-OH series, especially with n =1,2, might not contribute to the soft segment of the segmented block copolymer but participate in the liquid crystalline hard domain formation.

Table 2.2 shows the average molar masses and molar mass distributions (MMD) of the polymers as obtained from GPC measurements in two different solvents. The MMD values are close to 2, expected for conventional condensation polymerization. The relative molar masses, compared with polystyrene standards, are comparable to those of conventional polyurethane elastomers. The difference in the molar masses obtained from THF and DMF as solvents (eluents) reflects the fact that THF is a poor solvent for the liquid crystalline hard segments and their possible aggregation in THF, especially evident for the LCPUE 650 sample. This illustrates the importance of the proper choice of a solvent as the eluent in molar mass determination.

2.4.2   Thermal Characterization[15,16]

DSC thermograms for LCPU and LCPUE are shown in parts A and B of Figure 2.3. In the low-temperature region, Figure 2.3A and Table 2.3 show a decrease and narrowing of the T_g of the soft segment of LCPUE with an increase of the soft-segment molar mass. The endotherm in Figure 2.3A represents melting of the soft-segment crystallites in LCPUE 2000. It has been suggested that the critical molar mass required for PTMO soft-segment crystallization in segmented polyurethanes is about 3000.[17] In the present case, this is achieved by prechain extension during the prepolymer formation of LCPUE 2000.[13]

Table 2.2   Molar mass characterization obtained from GPC analysis in THF and DMF solvents

Polymer	Mw	MMD [a]	Mw	MMD
	(in THF Solvent)		(in DMF Solvent)	
LCPUE 650	60,000	2.17	32,100	1.82
LCPUE 1000	75,400	2.00	42,500	1.95
LCPUE 2000	45,700	1.84	33,600	2.01

a) MMD= $\overline{M}w/ \overline{M}n$
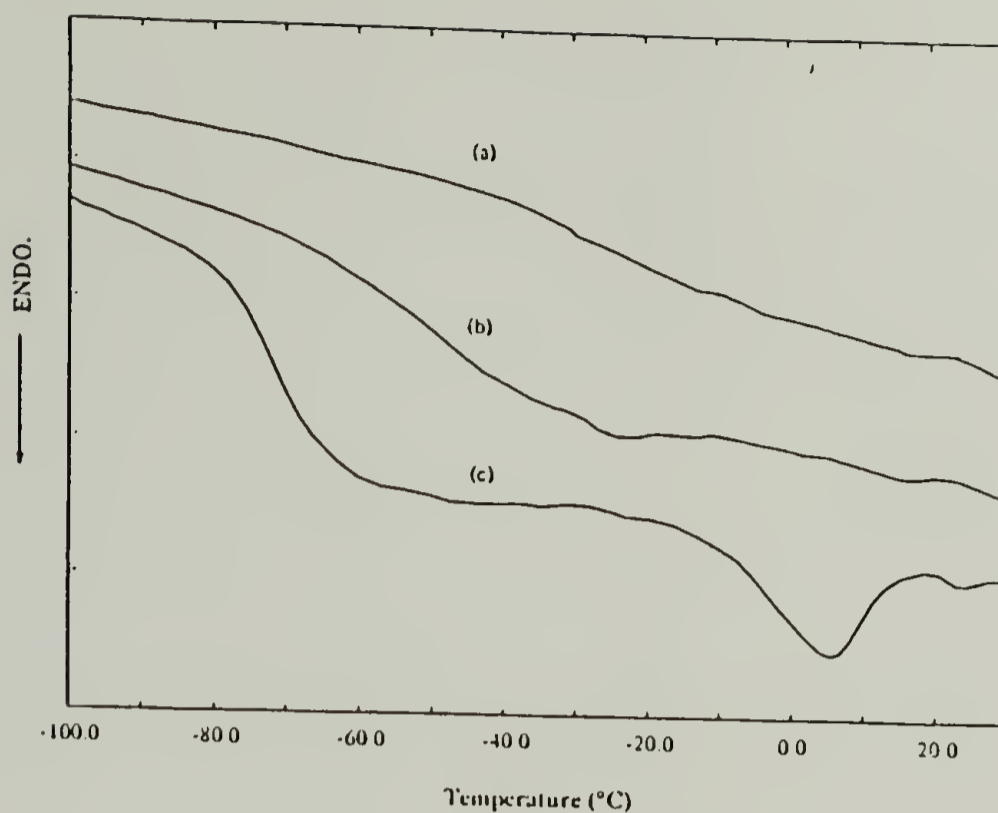
(A)
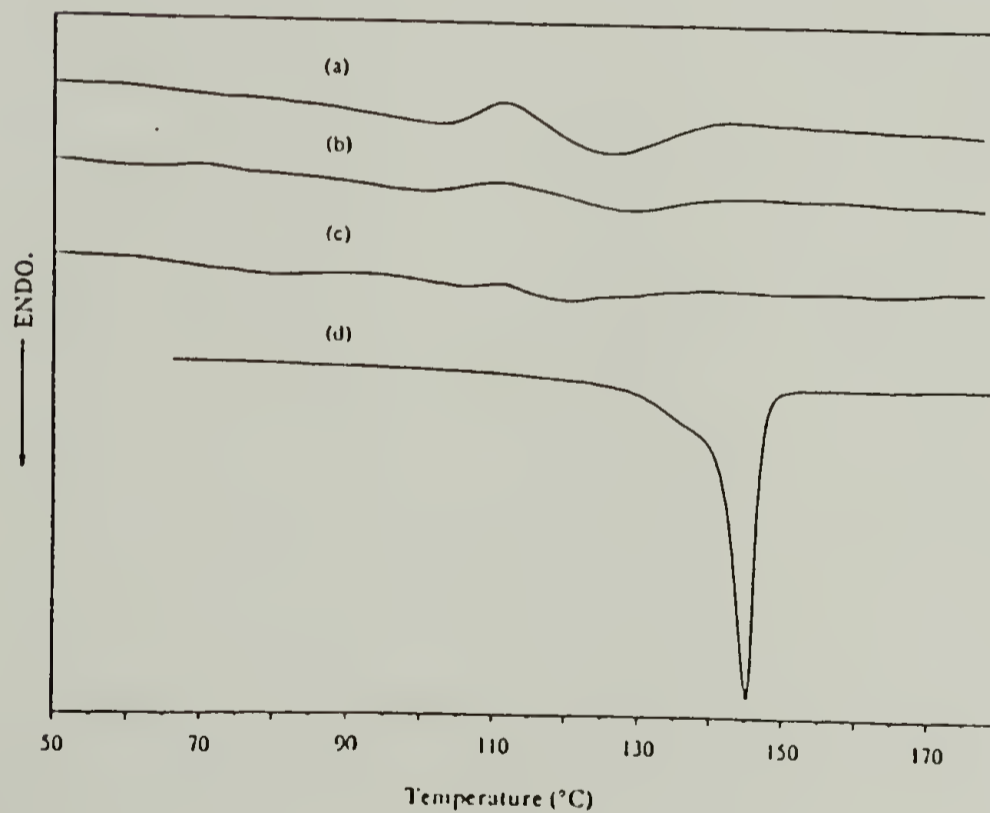
(B)

Figure 2.3   (A) DSC low-temperature thermograms for LCPUE at a
              heating rate of 10 K/min: (a) LCPUE 650, (b) LCPUE 1000,
              (c) LCPUE 2000. (B) DSC high-temperature thermograms
              for LCPUE at a heating rate of 10 K/min: (a) LCPUE 650,
              (b) LCPUE 1000, (c) LCPUE 2000, (d) LCPU

26

Table 2.3   Thermal properties of LCPUE by DSC

Sample	Soft Segment	Hard Segment		
	$T_g/°C$	$T_{i(1)}/°C$ a)	$T_{i(2)}/°C$ b)	ΔH_i mol/KJ c)
LCPUE 650	-25	103	126	12.0
LCPUE 1000	-51	101	128	9.9
LCPUE 2000	-73	105	121	5.1

a) Peak temperature of low endotherm

b) Peak temperature of high endotherm

c) Heat of isotropization of the sample annealed at 105°C 3 hours

In the high-temperature region (Figure 2.3B), a distinct endothermic peak around 145 $^\circ$C is found for LCPU. High-temperature polarizing optical microscopy shows that this corresponds to the isotropization temperature (T_i). Compared with the LCPU homopolymer, the endotherm in LCPUE is shifted to lower temperature and appears to consist of two endotherms separated by an exotherm. The lower temperature endotherm occurs at ca. 100 $^\circ$C, and the higher temperature occurs at ca. 128 $^\circ$C (Table 2.3). High-temperature X-ray powder diffraction patterns show that the second endotherm is related to the mesophase-isotropic phase transition. The depression of T_i relative to that of LCPU is associated with the oligomeric structure of the hard segment in the LCPUE. This is similar to the behavior of the melting points (T_m) of 2,4-TDI and 1,4-butanediol model oligomers with different numbers of repeating units and structural regularity.[18] Monodisperse hard-segment polyurethane elastomer studies[13,19,20] have also shown a decrease of the transition temperature with a decrease of the number of repeating units in the hard segment. Furthermore, the broadening of the endotherm in the LCPUE reflects the lack of uniformity of the mesophase domains. It could be caused by structural irregularity in the mesophase resulting from the incorporation of butanediol and dihydroxydibutyl ether in the hard segments (Figure 2.2, n= 1,2 in PTMO) and/or by the distribution of micromesophase sizes and the influence of the structure of the interfacial region.

Figure 2.4 shows the DSC traces of LCPUE 650 at different heating rates. At the slow heating rate of 2K/min (Figure 2.4, curve a), there is predominantly one broad endotherm at about 120 $^\circ$C, corresponding to the high-temperature original endotherm. As the heating rates are increased, the low-temperature endotherm increases at the expense of the high-temperature endotherm. For the 80 K/min heating rate, the low-temperature endotherm
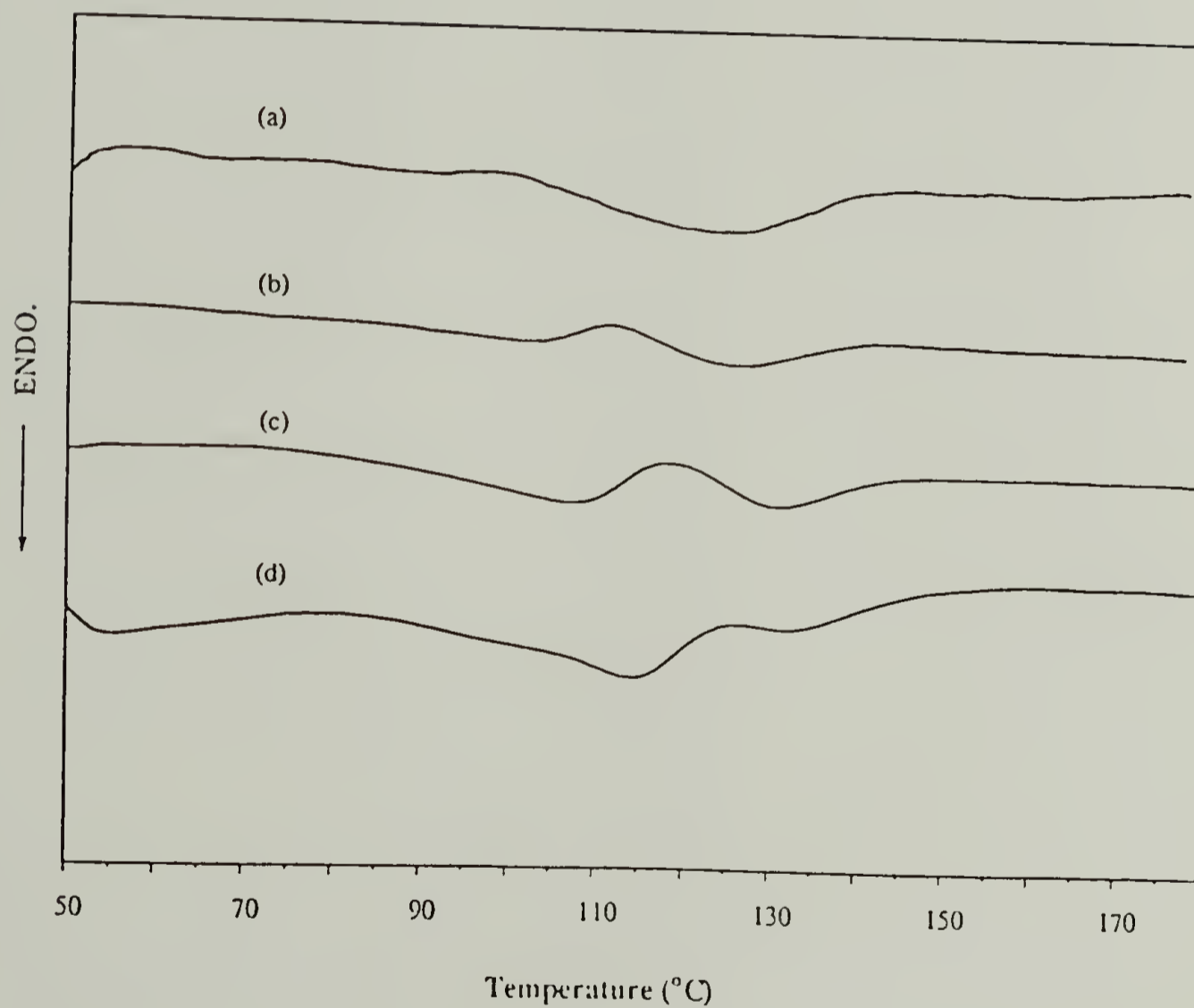
Figure 2.4   DSC thermograms for LCPUE 650 at different heating
rates: (a) 2, (b) 10, (c) 40, (d) 80 K/min

predominantes and the high-temperature endotherm is only visible as a weak shoulder (Figure 2.4, curve d). This behavior can be explained by the existence of two mesophases of different thermodynamic stability in the LCPUE. The melting behavior of model compounds suggests it might be related to 2,4-TDI and Diol -6 isomeric structure. At sufficiently low heating rates, the thermodynamically more stable phase is created during heating by the reorganization of the less stable one. Similar thermal behavior has also been observed for LCPUE 1000 and 2000.

Annealing of LCPUE at 105 $^{\circ}$C, which is above the isotropization temperature of the lower temperature mesophase, narrows the endothermic transition peak and yields the higher temperature mesophase (Figure 2.5). X-ray diffraction patterns of the annealed LCPUE samples show that the reflection at 4.5 Å sharpened substantially, indicating improved lateral packing order in the mesophase. Another interesting phenomenon is the increase of the heat of isotropization of the mesophase with decreasing soft-segment molar mass. This may be due to the contribution of the low molar mass fraction of poly(tetramethylene oxide) in the formation of the mesophase. Especially in LCPUE 650, short oligo(tetramethylene oxide) chains can further extend the hard segments. The effect will decrease as the low molar mass fraction of poly(tetramethylene oxide) decreases when the average molar mass increases.

Figure 2.6 shows that the development of the mesophase is both thermodynamically and kinetically controlled. If the LCPUE 650 sample quenched from the isotropic phase to 65 $^{\circ}$C is heated immediately at a heating rate of 10 K/min (Figure 2.6, curve a), two distinct endotherms are observed separated by an exotherm. Following the same procedure, after quenching the sample to 75 $^{\circ}$C, no endotherm appears in the subsequent heating cycle; but it is only upon annealing for, e.g., 20 min, that the endotherm appears again.
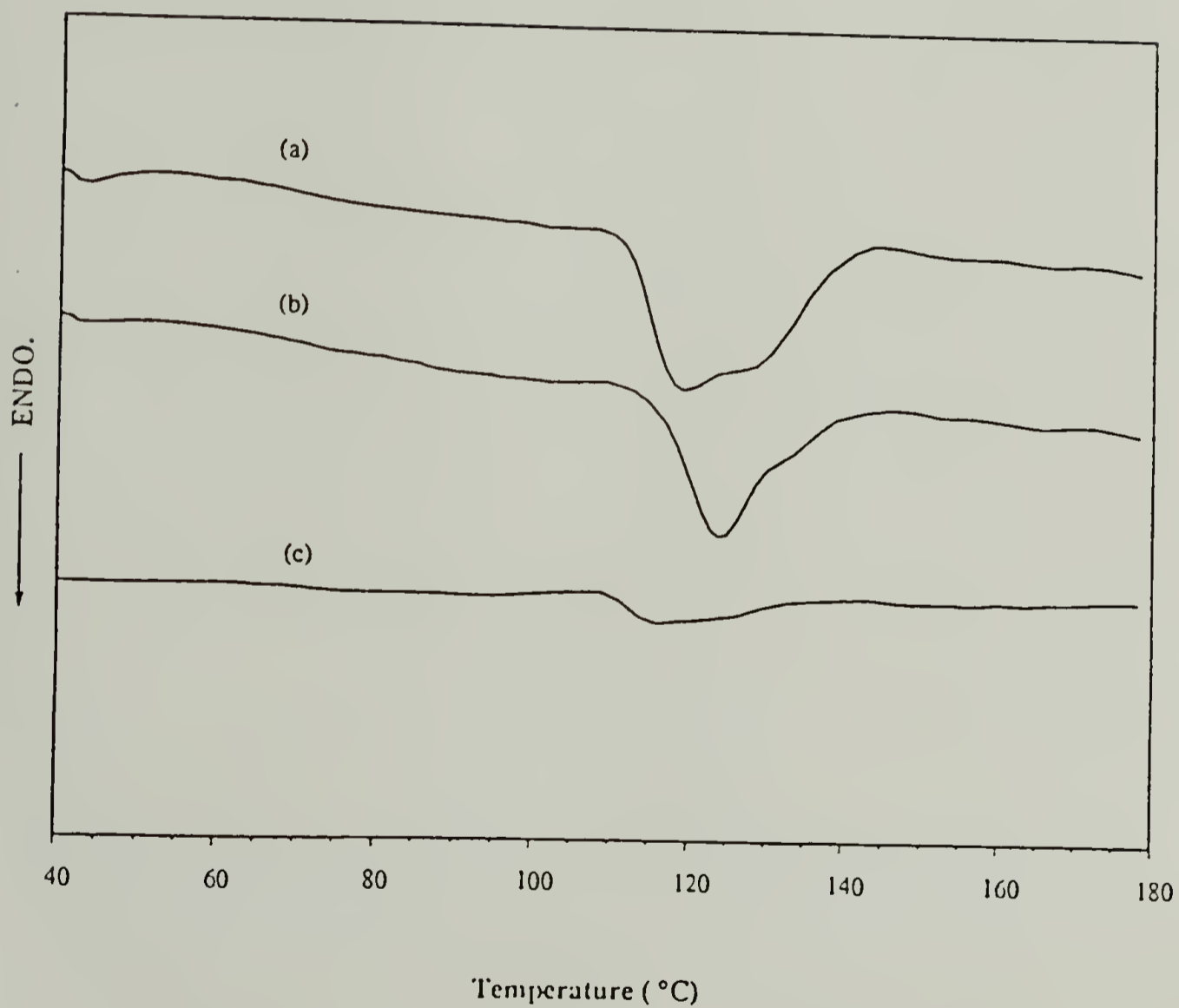
Figure 2.5   DSC thermograms for LCPUE at a heating rate of 10 K/min after
annealing at 105 °C for 3 h: (a) LCPUE 650, (b) LCPUE
1000, (c) LCPUE 2000
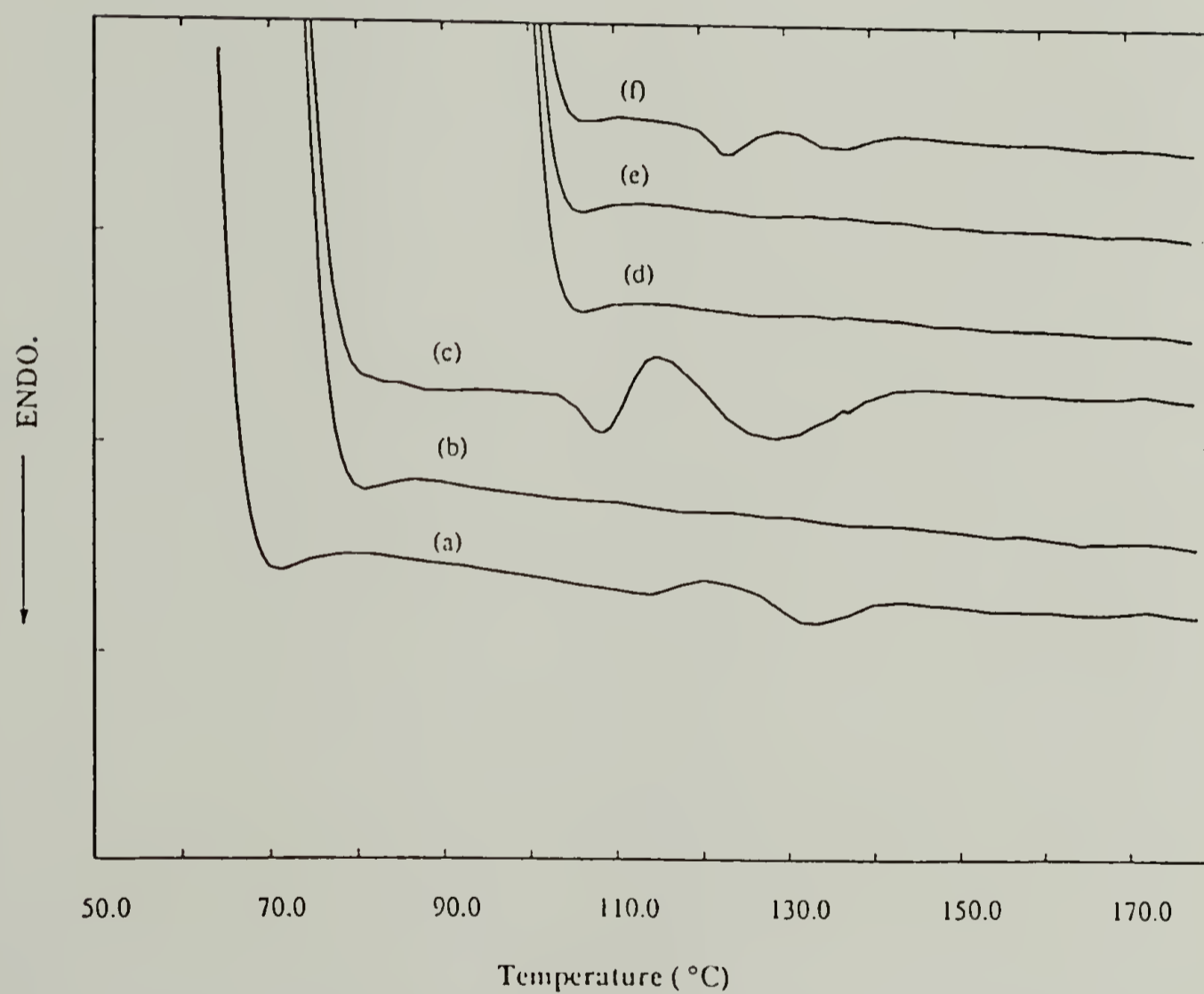
Figure 2.6   DSC thermograms for LCPUE 650 at a heating rate of
10 K/min after quenching the sample from 180 °C to the
following temperature: (a) 65 °C, (b) 75 °C, (c) 75 °C and
annealed at 75 °C for 20 min, d) 100 °C, (e) 100 °C and
annealed at 100 °C for 20 min, (f) 100 °C and annealed at
100 °C for 90 min

Compared to this, a longer annealing time, e.g., 90 min, is required to observe the endothermic transition for the sample quenched to 100 °C. Curves a, b, and d in Figure 2.6 reflect the effect of thermodynamics on mesophase formation in the different supercooled samples. Comparison of curves b and c, as well as d or e and f, reveals the additional kinetic effects in mesophase formation. This systematic varying of the sample thermal history also indicates that the mesophase formation occurs from a liquid-liquid microphase separated system.

2.4.3 Textural Observations with Polarizing Optical Microscopy

The observation of the LCPU sample which is cooled from the isotropic melt (155 °C) shows a Schlieren texture under the polarizing optical microscope (Figure 2.7). Unlike a nematic phase in which the Schlieren texture exhibits singularities with two brushes,[21] this sample shows only singularities with four associated brushes. This suggests a smectic mesophase in the LCPU homopolymer.

For the LCPUE samples, no birefringence is observed under the polarizing optical microscope. This means that the size of the mesophase microdomain is smaller than the wavelength of the polarized light.

2.4.4 X-ray Diffraction

X-ray diffraction patterns are presented in Figure 2.8 for the oriented and unoriented LCPU and LCPUE 1000 samples with different thermal histories.

Two distinct rings are observed in the unoriented LCPU sample (Figure 2.8a); a sharp inner one implies a lamellar spacing of 14.3 Å, which is indicative

33
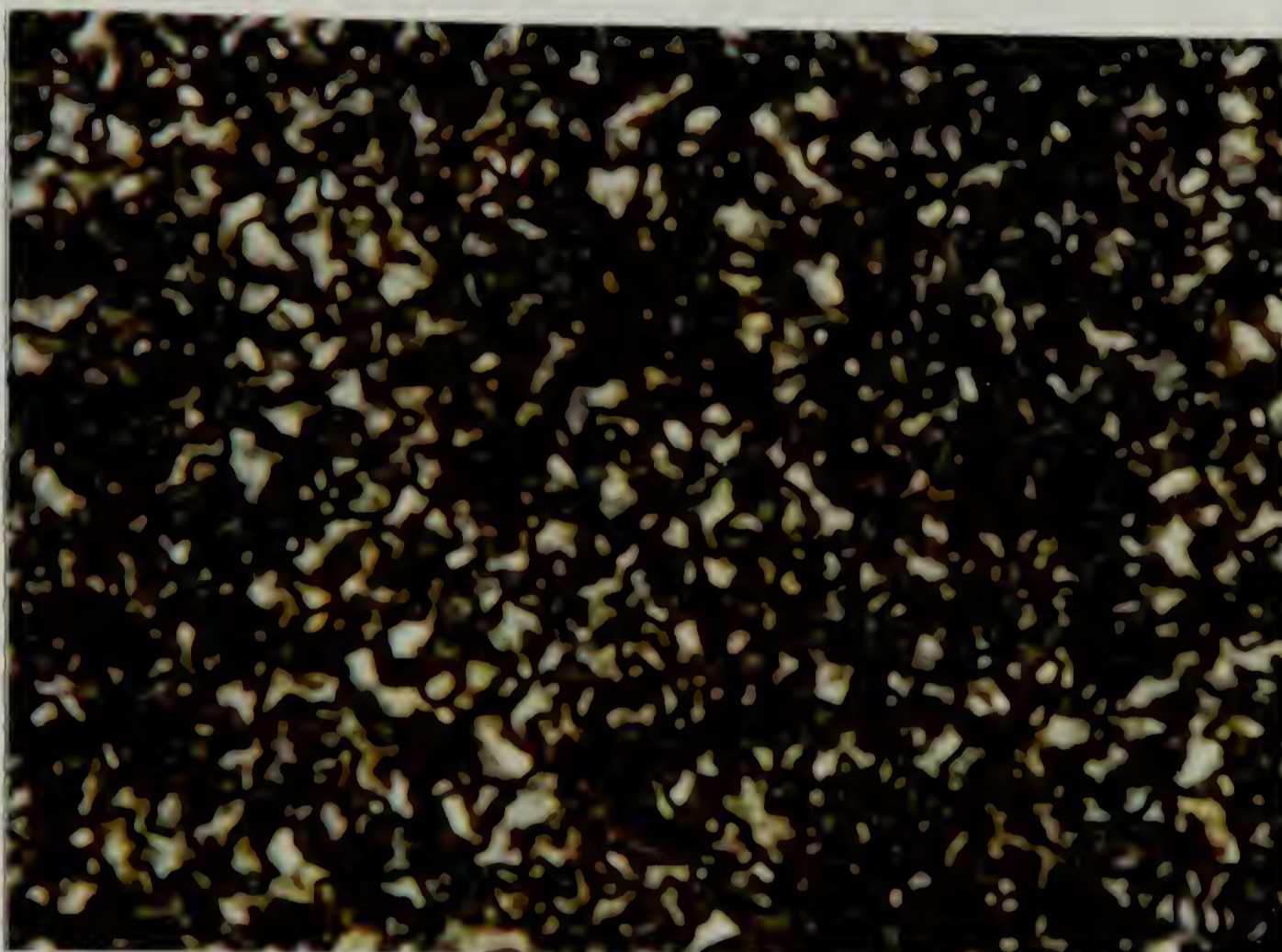
25 μm

Figure 2.7   Polarizing optical micrograph of the LCPU mesophase
obtained on cooling from the isotropic melt
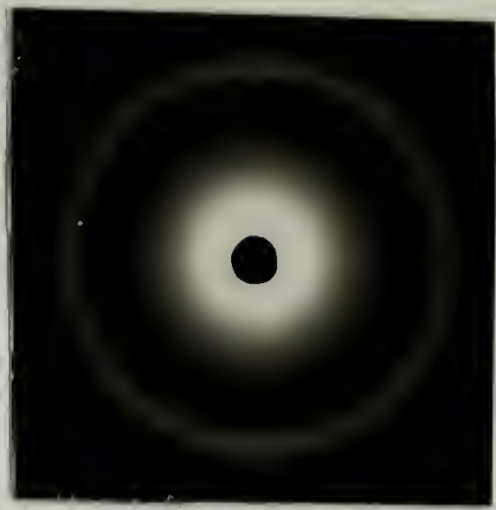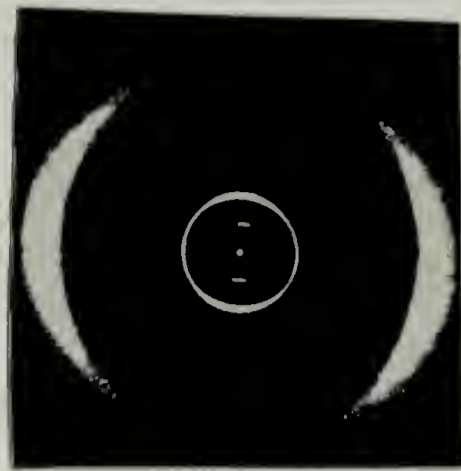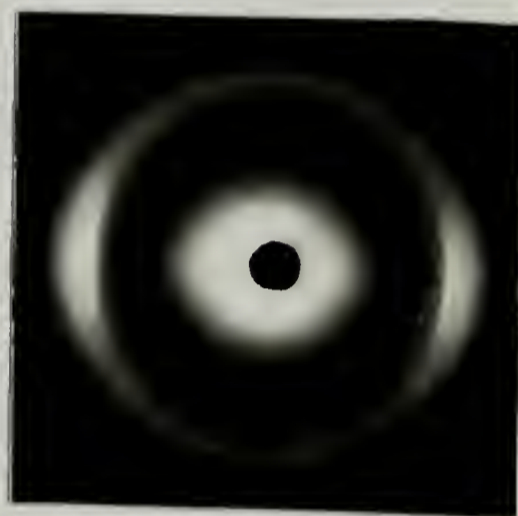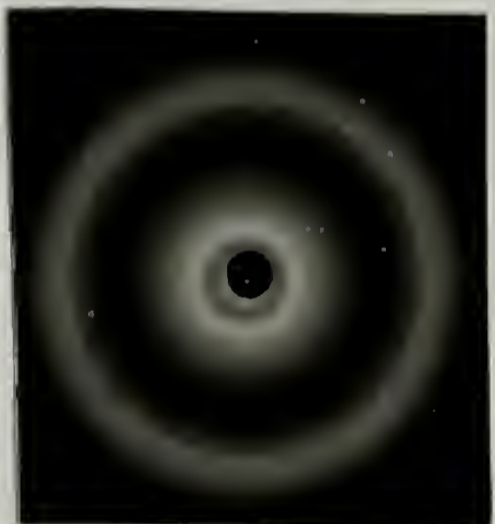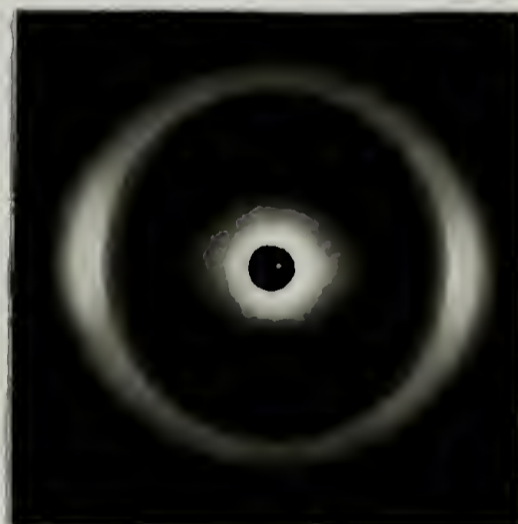
Figure 2.8   Room-temperature X-ray diffraction patterns: (a) LCPU
sample without orientation; (b) LCPU fiber drawn from
the melt; c) unstretched LCPUE fiber drawn from the melt;
(d) stretched LCPUE fiber drawn from the melt; (e)
unstretched annealed LCPUE fiber; (f) stretched annealed
LCPUE fiber

of long-range positional order in the structure. This is consistent with the layered morphology of a smectic phase. The diffuse outer ring occurring at 4.5 Å corresponds to the interchain spacing and reflects the packing of the molecules within the layers of the smectic phase.[22,23]

Figure 2.8b shows the X-ray fiber pattern for the LCPU sample drawn rapidly from the melt. Instead of the outer ring in the unoriented sample, two diffuse equatorial arcs appear and correspond to an interchain spacing of 4.5 Å. Simultaneously, the intensity of the inner ring on the meridional position is increased, and additional reflections are present as well. Together with the Schlieren microscopic texture, these results indicate a smectic phase polydomain morphology.[24]

Parts c and d of Figure 2.8 show the X-ray diffraction patterns for the unstretched and stretched LCPUE 1000 fiber drawn from the melt. The scattering from the liquid crystalline hard domain is superimposed on the scattering of the soft domain. One can discriminate the diffuse outer ring (4.5 Å) resulting from mesophase diffraction and the halo (3.8-4.7 Å) from the PTMO scattering. At 500 % elongation, the increased equatorial arcs illustrate that the liquid crystalline domains are oriented uniaxially. The sharpening of the equatorial reflection at 4.5 Å, which is related to the spacing between the hard segments, suggests that there is an improvement of the lateral packing order in the mesophase. In this context, it has to be pointed out that such as improvement in chain packing can be achieved for multiblock copolymers with semicrystalline polyurethane hard domains only by a combination of stretching and annealing.[25,26] This indicates the ease with which mesophase hard domains can be reorganized by stress, because of their flow properties. Figure 2.9 illustrates a schematic model for the improvement of the packing of the mesophase in a hard domain and its alignment upon elongation.

elongation

(a)

(b)
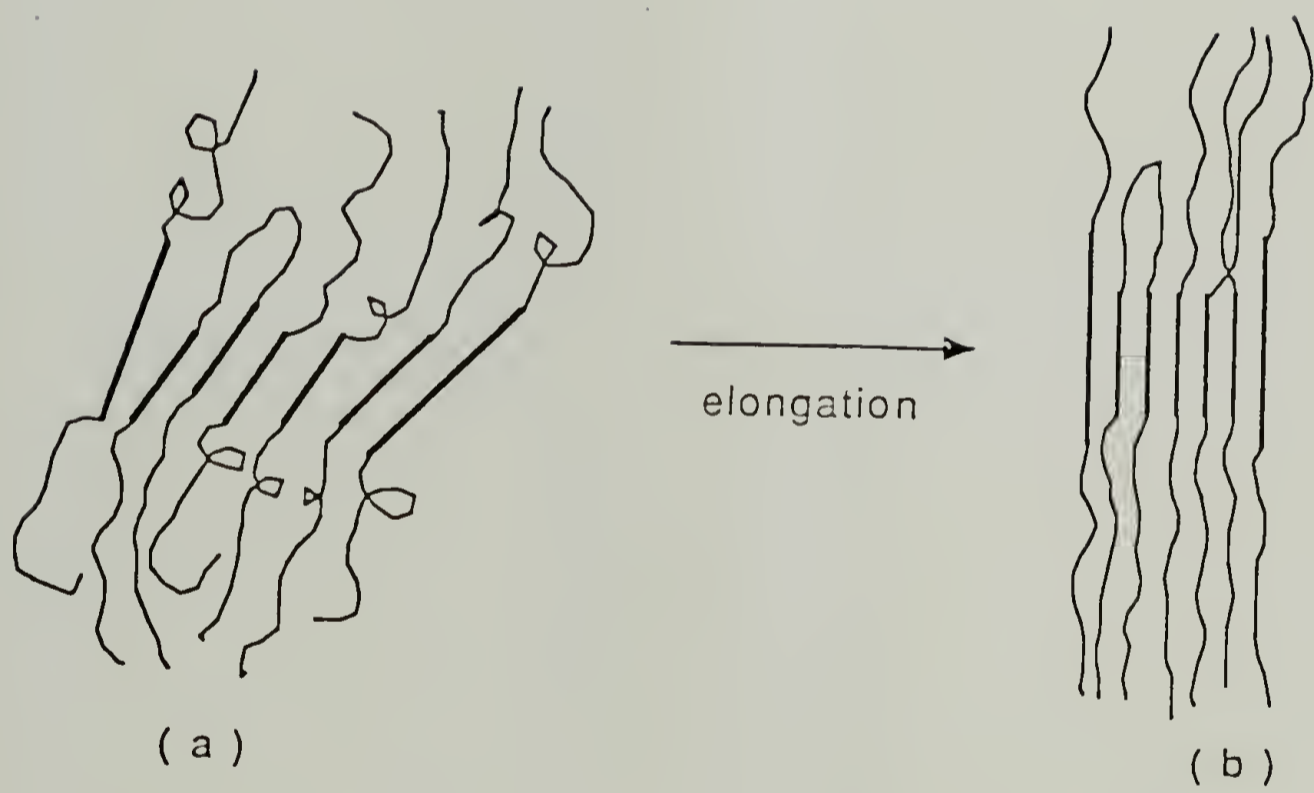
Figure 2.9   Schematic models for the aggregation of liquid crystalline
            hard segments in LCPUE: (a) unoriented sample, (b)
            oriented sample

The effect of annealing on the X-ray diffraction pattern of LCPUE 1000 fiber drawn from the melt is shown in parts e and f of Figure 2.8. A total of 3 h of annealing at 105 °C improves the mesophase order, and a sharp reflection at 4.5 Å is observed. The agreement of the spacing observed with that of the biphenyl distance in a liquid crystalline polyurethane of 2,6-TDI and Diol-6[6] suggests a similarity between the mesophase in the hard domains of the elastomer and the development of a lateral register between the neighboring biphenyl groups during the thermal treatment. As for the unannealed sample, Figure 2.8f illustrates that elongation leads to perfection and orientation of the mesophase.

2.4.5 Tensile Tests

The stress-strain properties of LCPUE are shown in Figure 2.10. It is obvious that the mesophasic hard-segment content has a profound effect upon the stress at a given strain probably due to a filler effect. Since the overall molecular weights of these samples are comparable, the distinct differences in elongation at break can be attributed to the morphological differences in these LCPUE samples. As compared with LCPUE 1000 and 650, the relatively small content of the mesophase in LCPUE 2000 leads to low tensile properties and elongation at break. The superior tensile properties of LCPUE 1000 and 650 may result from the presence of a lamellar or possibly bicontinuous mesophase and an amorphous soft phase.[27]
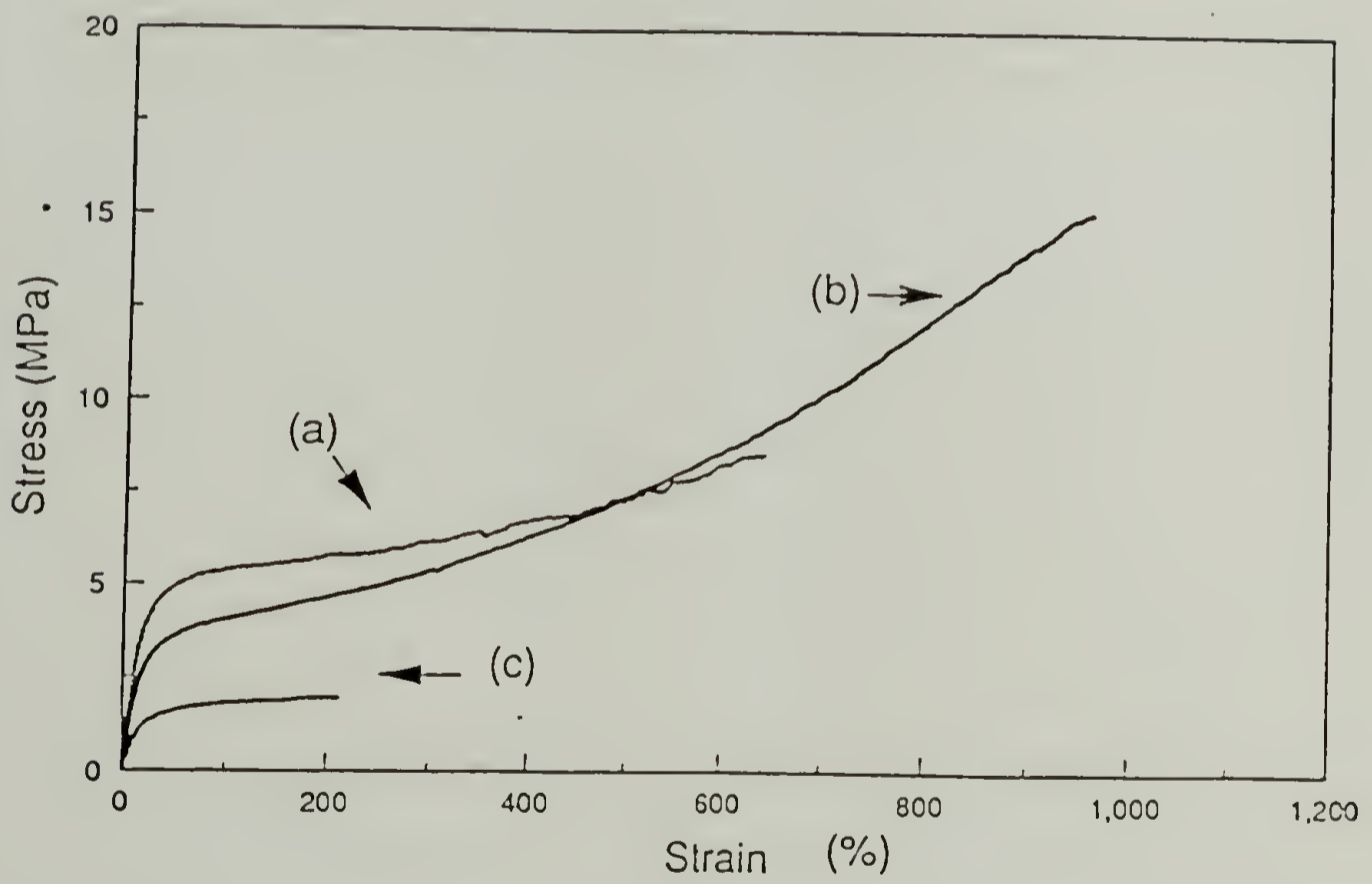
Figure 2.10   Stress-strain curves of LCPUE 650, (b) LCPUE 1000,
(c) LCPUE 2000

2.5   Conclusion

In this type of main-chain liquid crystalline elastomer, the formation of a mesophase is achieved by the self-assembly of the hard segments. The elastic deformation can orient the mesophase and lead to macroscopic anisotropy in the material. The elasticity results from the conformational entropy change of soft segments.

References and Notes

(1)   Finkelmann, H.; Kock, H. J.; Rehage, G. *Makromol. Chem., Rapid Commun.* **1981**, *2*, 317.

(2)   Schatzle, J.; Kaufhold, W.; Finkelmann, H. *Makromol. Chem.* **1989**, *190*, 3269.

(3)   Mormann, W.; Benadda, S. *Polym. Prepr. (Am. Chem. Soc., Div. Polym. Chem.)* **1993**, *34 (2)*, 739.

(4)   Lorenz, R.; Els, M.; Haulena, F.; Schmitz, A.; Lorenz, O. *Angew. Makromol. Chem.* **1990**, *180*, 51.

(5)   Stenhouse, P. J.; Valles, E. M.; Kantor, S. W.; MacKnight, W. J. *Macromolecules* **1989**, *22*, 1467.

(6)   Papadimitrakopoulos, F.; Hsu, S. L.; MacKnight, W. J. *Macromolecules* **1992**, *25*, 4671.

(7)   Iimura, K.; Koiede, N.; Tanabe, H.;.Takeda, M. *Makromol. Chem.* **1981**, *182*, 2569.

(8)   Mormann, W.; Brahm, M. *Macromolecules* **1991**, *24*, 1096.

(9)   Tanaka, M.; Nakaya, T. *J. Macromol. Sci. Chem.* **1987**, *A 24(7)*, 777.

(10)   Stenhouse, P. J. Ph.D. Thesis, University of Massachusetts at Amherst, Amherst, MA. 1992.

(11)   Sandler, S. R.; Karo, W. *Polymer Syntheses I*; Academic Press: New York, 1974; Vol. I, Chapter 8.

(12)   Odian, G. *Principles of Polymerization*, 2nd ed.; John Wiley & Sons: New York, 1981.

(13)   Eisenbach, C. D.; Baumgartner, M.; Gunter,Cl. *Advances in Elastomers and Rubber Elasticity;* Lai, J., Mark, J. E., Eds.; Plenum: New York, 1986; p 51.

(14)   Ferstanding, L. L.; Scherrer, R. A. *J. Am. Chem. Soc.* **1959**, *81*, 4838. Copper, W.; Pearson, R. W.; Parke, S. *Ind. Chem.* **1960**, *36*, 121.

(15)   Seymour, R. W.; Cooper, S. L. *Macromolecules* **1973**, *6(1)*, 48. Miller, J. A.; Lin, S. B.; Hwang, K. S.; Wu, K. S.; Gibson, P. E.; Cooper, S. L. *Macromolecules* **1985**, *18*, 32.

(16)   Cheng, S. Z, D, *Macromolecules* **1988**, *21*, 2475.

(17) Seefried, C. G.; Koleske, J. V.; Critchfield, F. E. *J. Appl. Polym. Sci.* **1975**, *19*, 2493.

(18) Fu, B.; Feger, C.; MacKnight, W. J.; Schneider, N. S. *Polymer* **1985**, *26*, 889.

(19) Harrell, L.L., Jr. *Macromolecules* **1969**, *6(2)*, 607.

(20) Eisenbach, C D.; Nefzger, H. *Multiphase Macromolecular Systems;* Culbertson, B. M., Eds.; Plenum: New York, 1989; p339.

(21) Gray, G. W.; Goodby, J. W. G. *Smectic Liquid Crystals;* Leonard Hill: 1984.

(22) Azaroff, L. V. *Mol. Cryst. Liq. Cryst.* **1987**, *145*, 31.

(23) De Vries, A. *Mol. Cryst. Liq. Cryst.* **1985**, *131*, 125.

(24) Azaroff, L. V. *Mol. Cryst. Liq. Cryst.* **1980**, *60*, 73. Falgueirettes, J.; Delord, P. *Liquid Crystals and Plastic Crystals*; Gray, G. W., Winsor, P. A., Harwood: Sussex, U.K., 1974; Vol. 3, p 62.

(25) Balckwell, J.; Lee C. D. *J. Polym. Sci., Polym. Phys. Ed.* **1983**, *21*, 2169.

(26) Balckwell, J.; Lee C. D. *J. Polym. Sci., Polym. Phys. Ed.* **1984**, *22*, 759.

(27) Thomas, E. L.; Reffner, J. R.; Bellare, J. International Workshop on Geometry and Interface, Sept 1990, C7-363.

CHAPTER 3

A SEGMENTED POLYURETHANE ELASTOMER WITH LIQUID CRYSTALLINE HARD SEGMENTS. 2. RHEOLOGICAL STUDY

3.1   Abstract

The linear viscoelastic properties of a segmented polyurethane referred to as LCPUE 1000 have been studied. LCPUE 1000 is a microphase-separated polymer with submicron mesophases as physical cross-links, and its rheological study indicates a broad transition from a viscoelastic solid to a viscoelastic liquid at the isotropization temperature of the mesophase. Furthermore, it has been found that time-temperature superposition applies in the isotropic state (160 to 110 $^\circ$C). We conclude that the aggregation of liquid crystalline hard segments does enhance the connectivity of the molecular structure, and this is supported by the results of a kinetic study with dynamic mechanical spectroscopy (DMS). Physical gelation studies identify a liquid/solid transition when cooled to 106 $^\circ$C or below and show the characteristic critical behavior at the gel point with a power law relaxation spectrum at low frequencies. Estimates are given for the relaxation exponent and the stiffness of the critical gel.

3.2   Introduction

Segmented polyurethane elastomers are an important class of polymeric materials consisting of thermodynamically incompatible hard and soft segments. The existence of microphase-separated domains, caused by aggregation of the hard and soft segments, has been well established. In order to achieve an anisotropic mesophase[1] in the hard domains, the mesogenic units are introduced as chain extenders.

The rheological behavior of thermotropic liquid crystalline polymers (TLCP) has been studied[2-6] for their unconventional phenomena which depend upon temperature and phase morphology. The viscosity of the nematic phase, for example, is usually considerably smaller than that of the isotropic phase, except at low frequencies or shear rates, where the viscosity grows to very large values which might be explained as a yield stress.

For the present study, the chemical structure of a main-chain TLCP is interrupted by soft segments. This alternating chain structure results in a two-phase morphology comprised of mesophasic hard and amorphous soft domains. A preceding paper[1] describes the synthesis and physical characterization of the material referred to as LCPUE 1000. A DSC experiment with a heating rate of 1.5 K/min shows the glass transition temperature of the soft segment at -51 $^{\circ}$C and the isotropization of the mesophase occurring over a wide range from 110 to 144 $^{\circ}$C. The breadth of the transition originates from the mesophase size distribution and from diffuse interfaces between the mesophasic and the amorphous domains. Here, we use rheological means to probe this thermal process and to further understand the viscoelastic solid/liquid transition.

Gelation or gel formation is a connectivity transition which results in a change of viscoelastic properties. On the molecular scale, this process is caused by cross-linking from either chemical covalent bonds or physical interactions. On the macroscopic scale, the gelation results in a liquid/solid transition, which can be monitored by means of rheology. Here, it should be pointed out that the term "solid" means the rubberlike state of a cross-linked polymeric material. It is not intended to suggest a glassy or even crystalline body with a clearly defined melting temperature.

In physically cross-linking processes, hard segments of macromolecules can aggregate to form physical junctions via hydrogen bonds, van der Waals forces, electrostatic attractions, and others. If the lifetime of the junctions is sufficiently long and molecular clusters grow in size, the polymer will exhibit a liquid/solid transition with a critical behavior at the transition point. The zero-shear viscosity diverges to infinity, and an equilibrium modulus starts to grow from zero after the gel point. Near the gel point, small-amplitude oscillatory shear is the preferred method in rheological experiments since it probes the sample without rupturing the evolving structure. Dynamic mechanical spectroscopy (DMS) is used within the linear viscoelastic range to obtain complex moduli[7]

$$G^* = G' + i\, G'' \tag{1}$$

Where G' represents the in-phase or elastic component and G'' the out-of-phase or dissipative component of G^*.

Chambon and Winter[8,9] have pointed out that, at the critical gel point of a polymer, the frequency dependence of the dynamic moduli follows a power law:

$$G_c' = G_c''/\tan \delta_c = S\,\omega^n\Gamma(1-n)\cos \delta_c \qquad \text{for } 0 < \omega < \omega_0 \qquad (2)$$

where $\Gamma(1-n)$ is the gamma function, S the gel stiffness, ω the frequency, and n the relaxation exponent. The subscript c indicates the validity of the equation at the critical gel point. Furthermore, the loss angle becomes frequency independent at this transition point, and n can be calculated according to:

$$\delta_c = n\pi/2 \qquad\qquad \text{with } \tan \delta_c = (G''/G')_c \qquad (3)$$

Winter and co-workers have used DMS to study physical gelation.[10,11,19] For example, the gelation of a TPE-polypropylene comprised of multiple blocks of stereoregular and stereoirregular sequences is driven by the crystallization of the stereoregular block; the relaxation modulus at the physical gel point obeys the power law (eq 2). The validity of this equation is attributed to the critical gel's structural self-similarity.

3.3   Experimental Section

3.3.1   Materials[1]

The polymer used in this study was synthesized via solution polymerization. In the first stage of the reaction, a prepolymer was prepared from poly(tetramethylene oxide) (M_w= 1000) and the 1:1 mixture of 2,4-tolylene diisocyanate and 2,6-tolylene diisocyanate at 100 $^\circ$C. This was followed by the chain extension of the mesogen 4,4'-bis[(6-hydroxyhexyl)oxy]biphenyl. The resulting polymer, referred to as

46

LCPUE_1000 (Figure 3.1), has 42.3 wt % of hard segments. The average molar mass (M_w) determined by gel permeation chromatography in a THF solvent was found to be 75 400 (relative to polystyrene standards) with a polydispersity index of about 2.

3.3.2 Sample Preparation

Samples for rheological measurements were molded at 150°C under vacuum and then slowly cooled down to room temperature at a rate of 5 K/min.

3.3.3 Rheological Measurements

Small-amplitude oscillatory shear experiments were performed on a Rheometrics dynamic spectrometer (RDS) 7700 using concentric disk fixtures, with a disk diameter of 25 mm and a gap width of about 1 mm after thermal adjustments, which assumed a fixture expansion of 1 μm/K. A nitrogen atmosphere was used to prevent oxidation in the experiments above 80 °C

In order to investigate the material in its linear viscoelastic region, the periodic shear strain was varied from 0.05 to 0.25 in the higher temperature range (100-160 °C) and from 0.0125 to 0.02 in the lower temperature range (0-100 °C). Dynamic shear frequencies ranged from 0.1 to 500 rad/s. The viscoelastic properties of the sample were obtained from the oscillatory strain and its periodical torque response.

The isothermal consecutive frequency sweep (CFS) method allowed us to track the kinetics of the physical gelation process. The measurements were made with a strain of 0.02 in the frequency range of 0.1-10 rad/s.
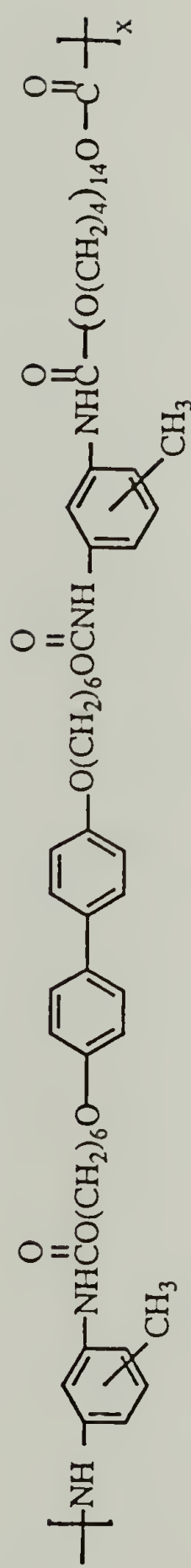
Figure 3.1   Chemical structure of LCPUE 1000

48

Time-temperature superposition and related data analysis were carried out with the IRIS software. The kinetic experiments on the phase transition were analyzed with the GELPRO software of Mours et al.[12]

3.4 Results

3.4.1 Temperature Scans

The dynamic moduli of the LCPUE 1000, measured at a frequency of 10 rad/s and strains of 0.02-0.25, decayed monotonically with increasing temperature; see Figure 3.2. Both heating and cooling scans with a rate of 1.5 K/min indicate a reversible broad transition from a viscoelastic solid behavior to liquid behavior but did not reveal the exact instant of a first-order phase transition. However, this gradual rheological transition occurs in the same temperature range as the thermal events which are associated with the mesophase isotropization in DSC studies.[1] It should also be noted that there is a small "hysteresis loop" between heating and cooling runs in Figure 3.2. Moduli are lower on the cooling run than on the heating run. Figure 3.2. also shows the temperature of crossover ($G'=G''$) at 132 $^{\circ}$C in the heating mode and at 110 $^{\circ}$C in the cooling experiment. The difference in the crossover temperatures and the hysteresis are due to the kinetic effect of the mesophase formation. In reference to the crossover temperature at 110 $^{\circ}$C, the dynamic moduli G^* of the cooling scan have been studied further for both the viscoelastic liquid (160 $^{\circ}$C→110 $^{\circ}$C) and the viscoelastic solid (110 $^{\circ}$C→20 $^{\circ}$C) regions.
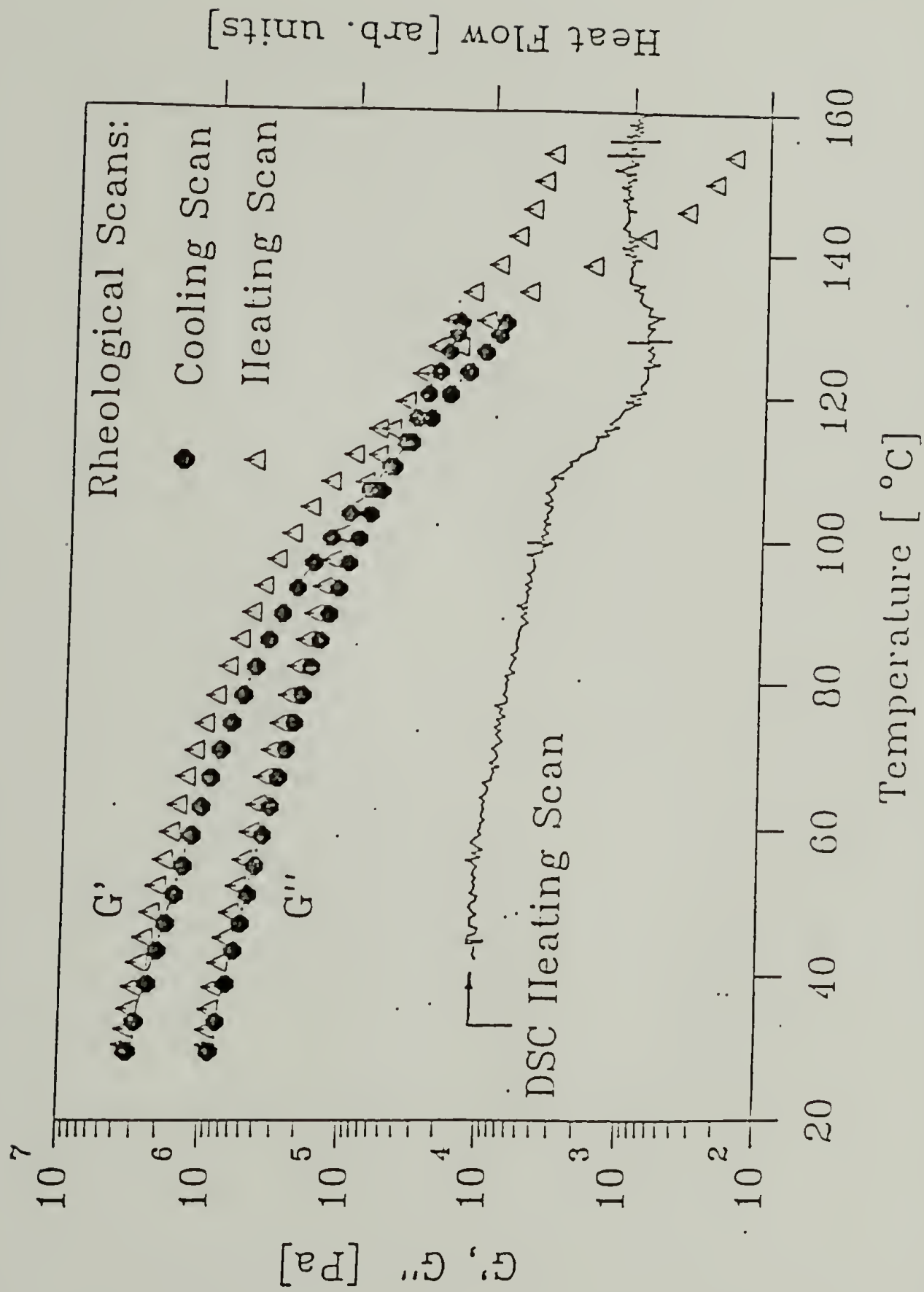
Figure 3.2 Temperature dependence of the shear moduli G' and G", compared with the result of the DSC heating scan (lower curve). The circles represent the cooling scan; triangles represent the heating scan. Frequency: 10 rad/s. Strain varied between 0.2 and 0.0125. Heating and cooling rates were 1.5 K/min in all experiments; the points belonging to the cooling scan are connected by lines.

3.4.2 Viscoelastic Liquid Zone

Figure 3.3 shows the results of isothermal frequency scans at 110, 120, 140 and 160 °C. In order to erase annealing history, samples were brought to the isotropic state at 160 °C after each measurement and then back to the experimental temperature. In Figure 3.3a, a master curve is constructed with a reference temperature of 120 °C. The loss moduli G" are consistently larger than the storage moduli G'. At low frequencies, the slopes of G' and G" are 2 and 1, as expected for a viscoelastic liquid, such as a polymer melt. In Figure 3.3b, the absolute value of complex viscosity $\eta*$ ($\eta* = G*/\omega$) has a constant value of 10^3 Pas at low frequencies and starts to decrease with increasing frequency as the material exhibits shear thinning behavior. Time-temperature superposition is possible (see the master curve at a reference temperature $T_0 = 120$ °C). The temperature shift factors follow the Arrhenius type of temperature dependence with an apparent activation energy of $E_a \approx 60$ kJ/mol.

3.4.3 Viscoelastic Solid Zone

Isothermal frequency scans for various temperatures are shown in Figure 3.4. The values of the storage moduli G' are always larger than those of the loss moduli G", as is characteristic for most viscoelastic solids. The slopes of the modulus-frequency plots are much smaller than those in the viscoelastic liquid zone (Figure 3.3a). A zero slope is approached at low frequencies, as is typical for solids.

3.4.4 Evolution of Viscoelastic Behavior during Physical Gelation

The crossover G' = G" is known to occur not exactly at the gel point[13] but often is close to it. Therefore, it has often been used for rough estimates of
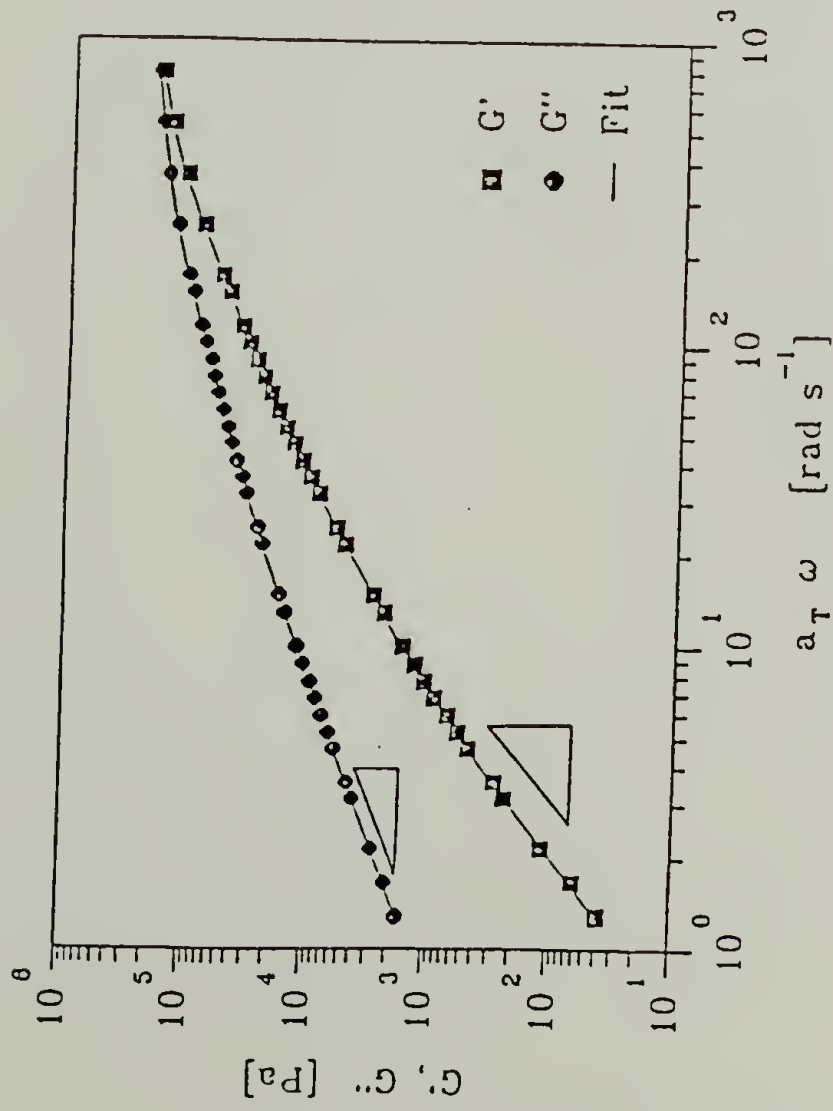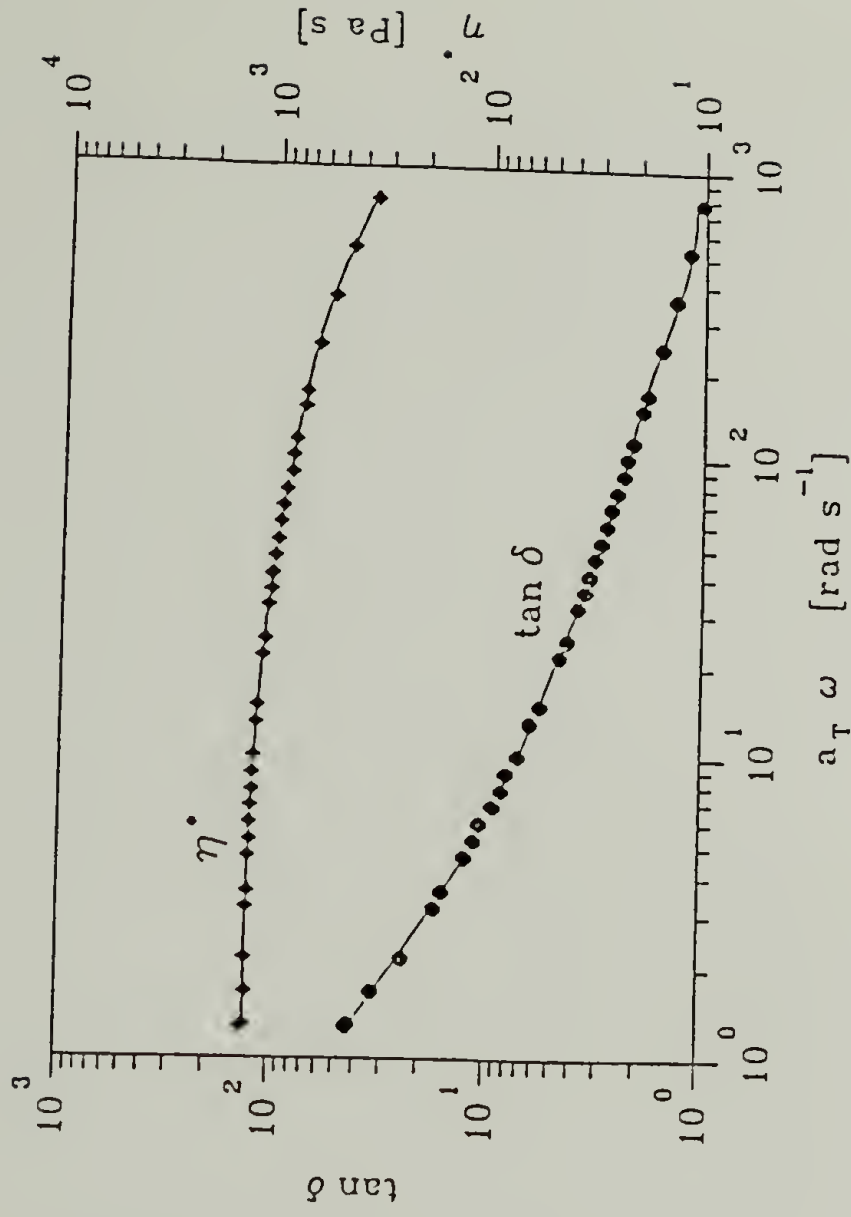
Figure 3.3　(a) Master curve for frequency scans in the upper temperature region (isotropic phase). Measured shear moduli and fitted curve. Reference temperature: 120 °C. Strain varied between 0.05 and 0.2. The straight lines indicate slopes 1 and 2, respectively. (b) Same as part 3a. Measured complex viscosity (diamonds) and tangent of the loss angle (circles), compared with the fitted curve (solid lines).
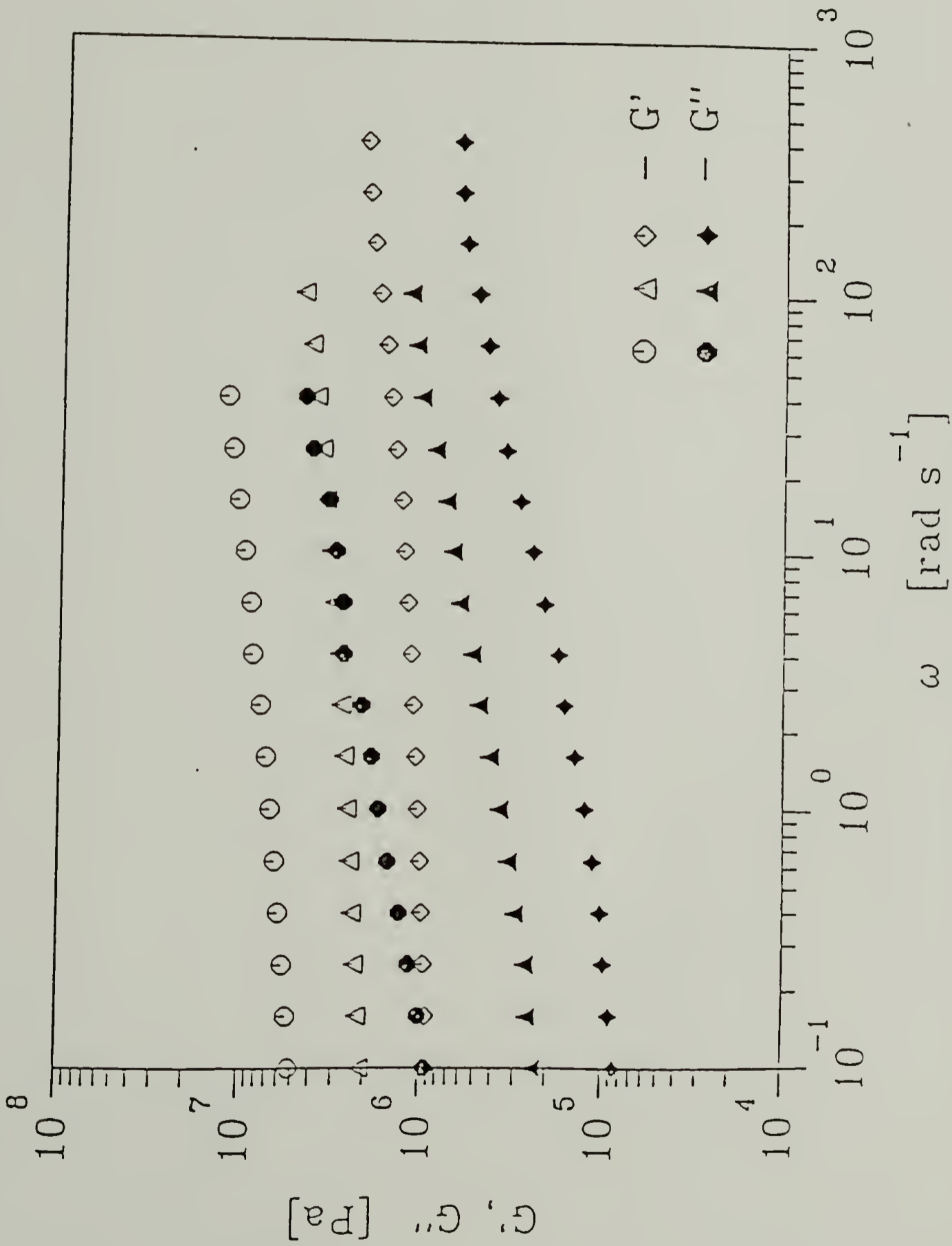
Figure 3.4   Storage and loss moduli according to frequency scans at three different temperatures in the solid state.
Circles: 20 °C. Triangles: 60 °C. Diamonds: 100 °C.   Strain varied between 0.02 and 0.0125.

the gel point. For LCPUE 1000, the gel point is reached with G" being about 10 times larger than G', as will be shown below.

The gelation from the viscoelastic liquid to the viscoelastic solid is strongly dependent on thermal history. The evolution of viscoelasticity was studied by heating the sample to 160 °C, where it forms a polymeric melt, followed by quenching to a temperature below 110 °C. Here we chose 106, 101, and 99 °C for the isothermal gelation process. Figure 3.5a shows the growth of the dynamic moduli versus time at a constant frequency of 0.463 rad/s. The quenching to 99 °C gives the fastest growth of the moduli, indicating the connectivity changes to be caused by physical processes. The observed growth at 106 °C depends on the frequency (Figure 3.5b), being more pronounced at low frequencies.

In spite of its dependency upon temperature and frequency, the gel point, a liquid/ solid transition, can be distinguished by a loss tangent which, at a constant temperature, is independent of frequency. Figure 3.6 shows the tan δ measured at 0.1, 0.215, 0.463, 1.0 and 2.15 rad/s as a function of elapsing time at 106 °C. The crossover of tan δ, which approximately equals 10.1, is observed as frequency independent. The corresponding time is 1090±20 s for the formation of the critical gel. As the time passes, the viscoelastic liquid has increased its elasticity (Figure 3.7). It is further substantiated by the steady increase of the storage modulus G' (Figure 3.8). At the critical gel point, the relaxation exponent n equals 0.937. From eq 2, the value of the gel stiffness S is calculated as 107 Pas^n.

3.4.5 Softening of the Solid State

In the reverse process, the physical gel is "melted" by the isotropization of the mesophase, resulting in a viscoelastic transition from solid to liquid.
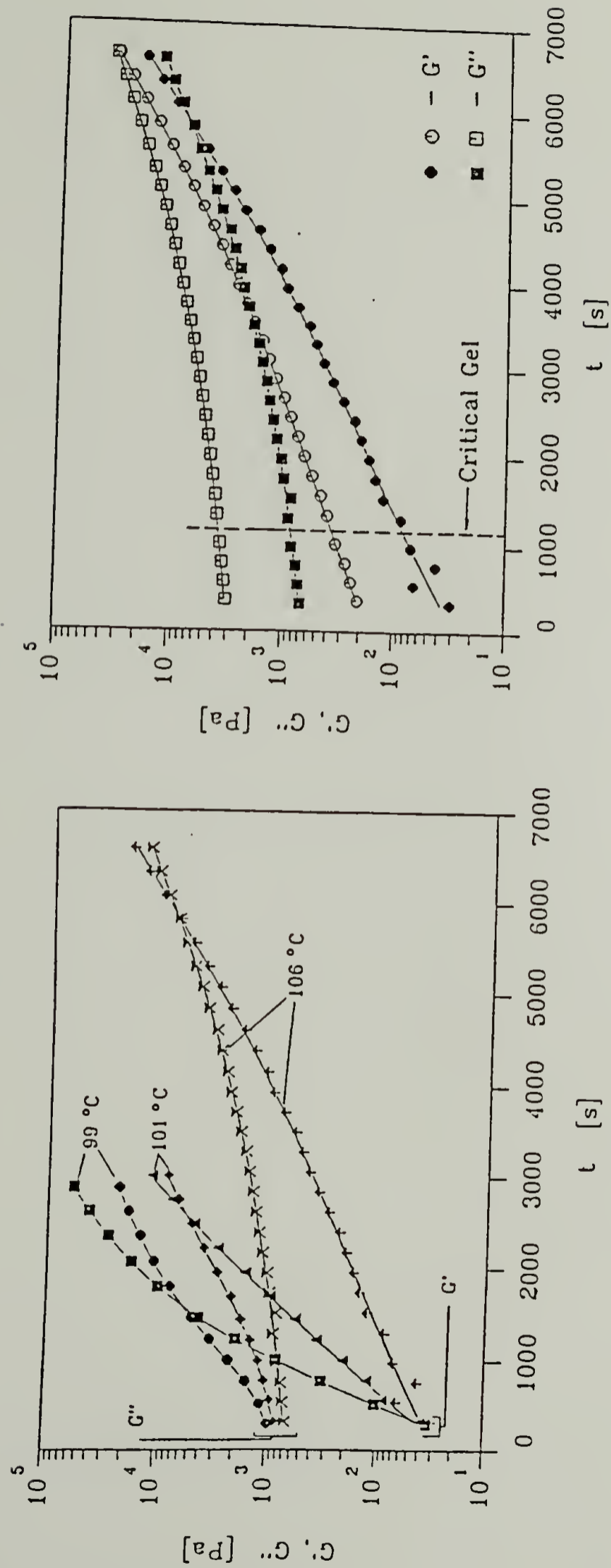
Figure 3.5   (a) Kinetic study of the phase transition liquid/solid. Evolution of the shear moduli with time at a constant frequency. G': squares, 99 °C; triangles, 101 °C; closedcrosses, 106 °C. G'': circles, 99 °C; diamonds, 101 °C; open hourglasses, 106 °C. Strain: 0.02. Frequency: 0.463 rad/s. (b) Frequency dependence of the solidification process at 106 °C. Two frequencies are shown: 0.463 rad/s (filled symbols); 2.15 rad/s (open symbols). The strain was 0.02; the position of the critical gel is indicated by the dashed line in the left part of the figure.
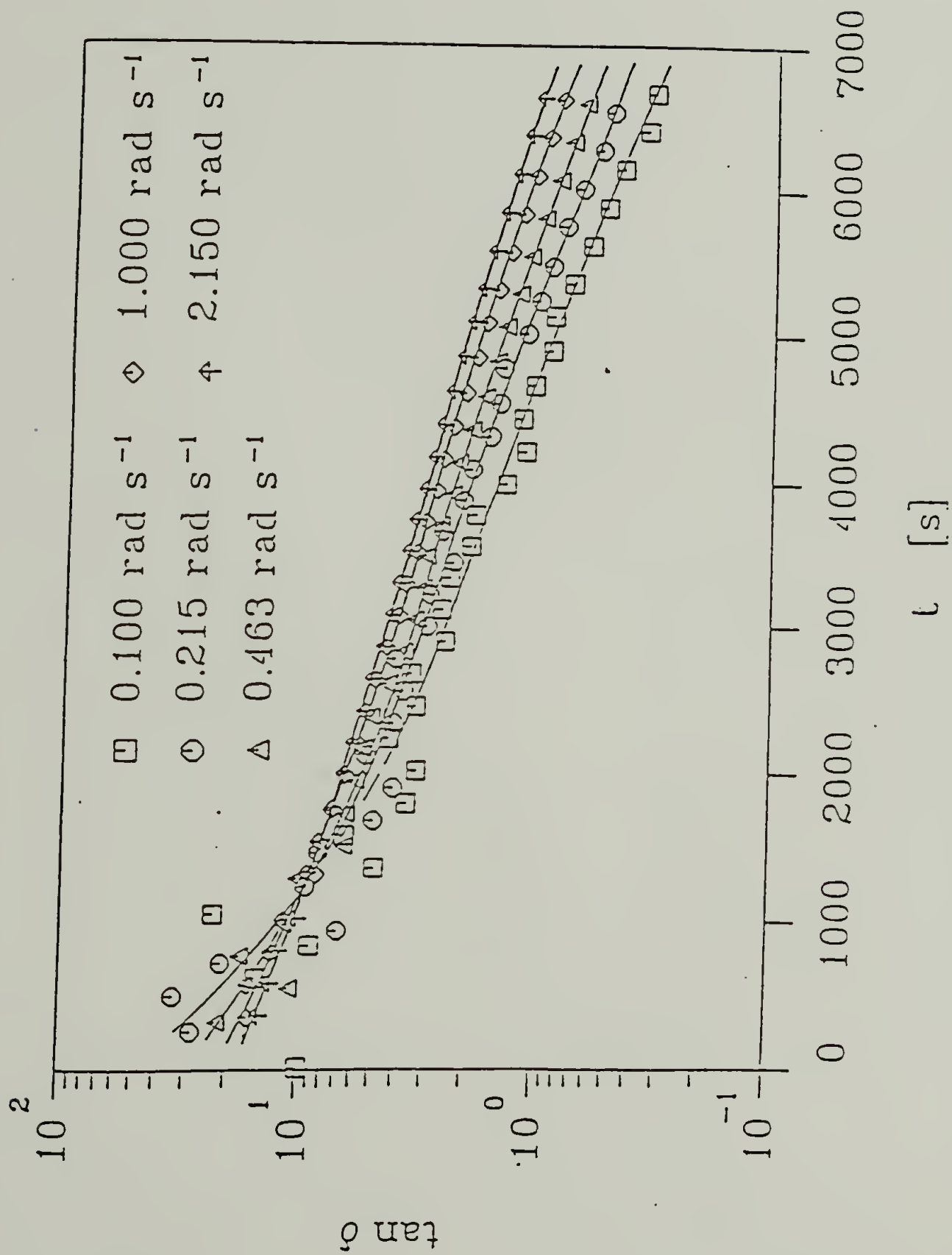
Figure 3.6   Kinetic study at 106 °C. Strain 0.02, tangent of the loss angle vs time. Frequencies (rad/s): squares, 0.10; circles, 0.215; triangles, 0.463; diamonds, 1.00; closed crosses, 2.15.
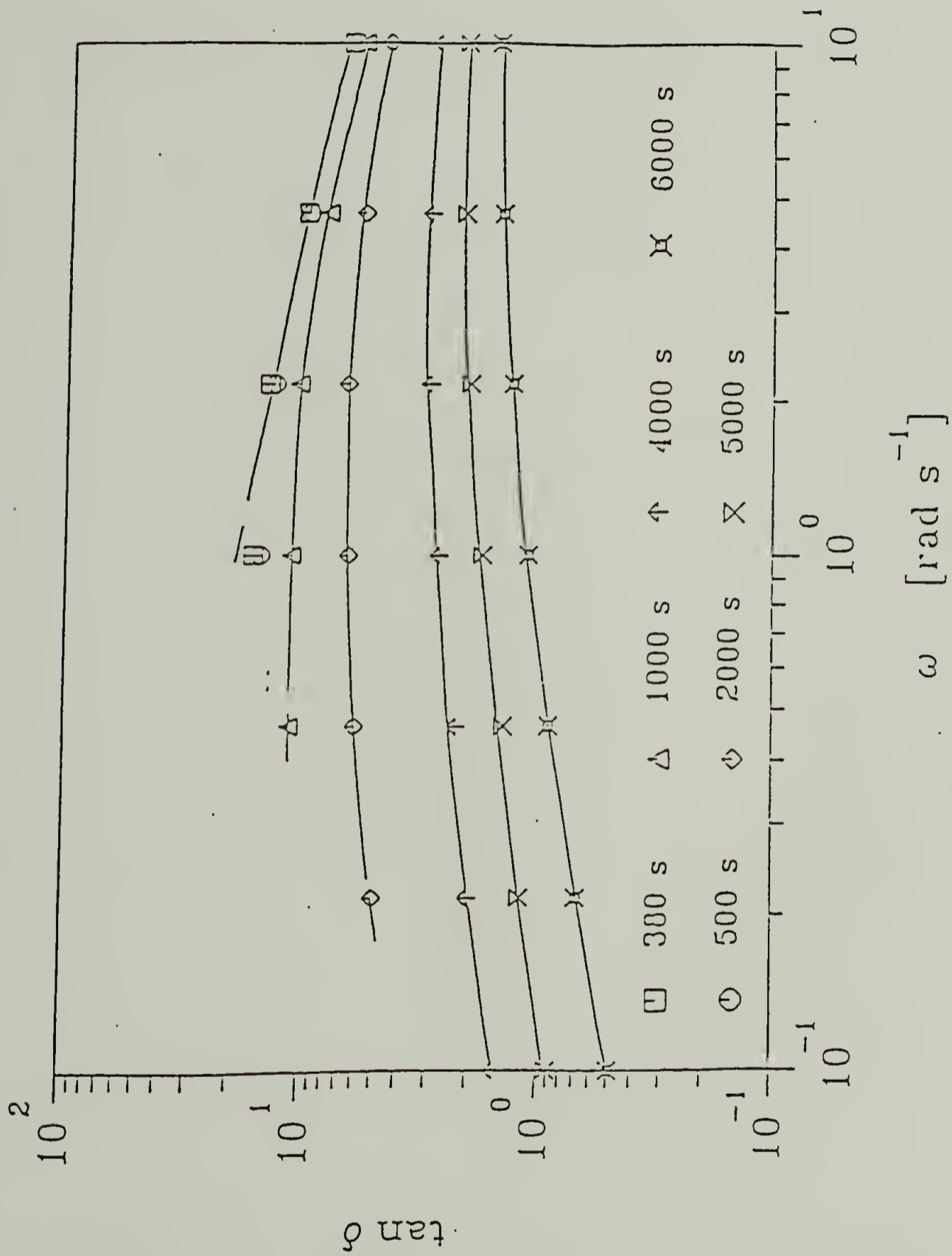
Figure 3.7   Kinetic study at 106 °C. Strain 0.02, tangent of the loss angle vs frequency. Time after starting the observation (s) as indicated in the figure.

57
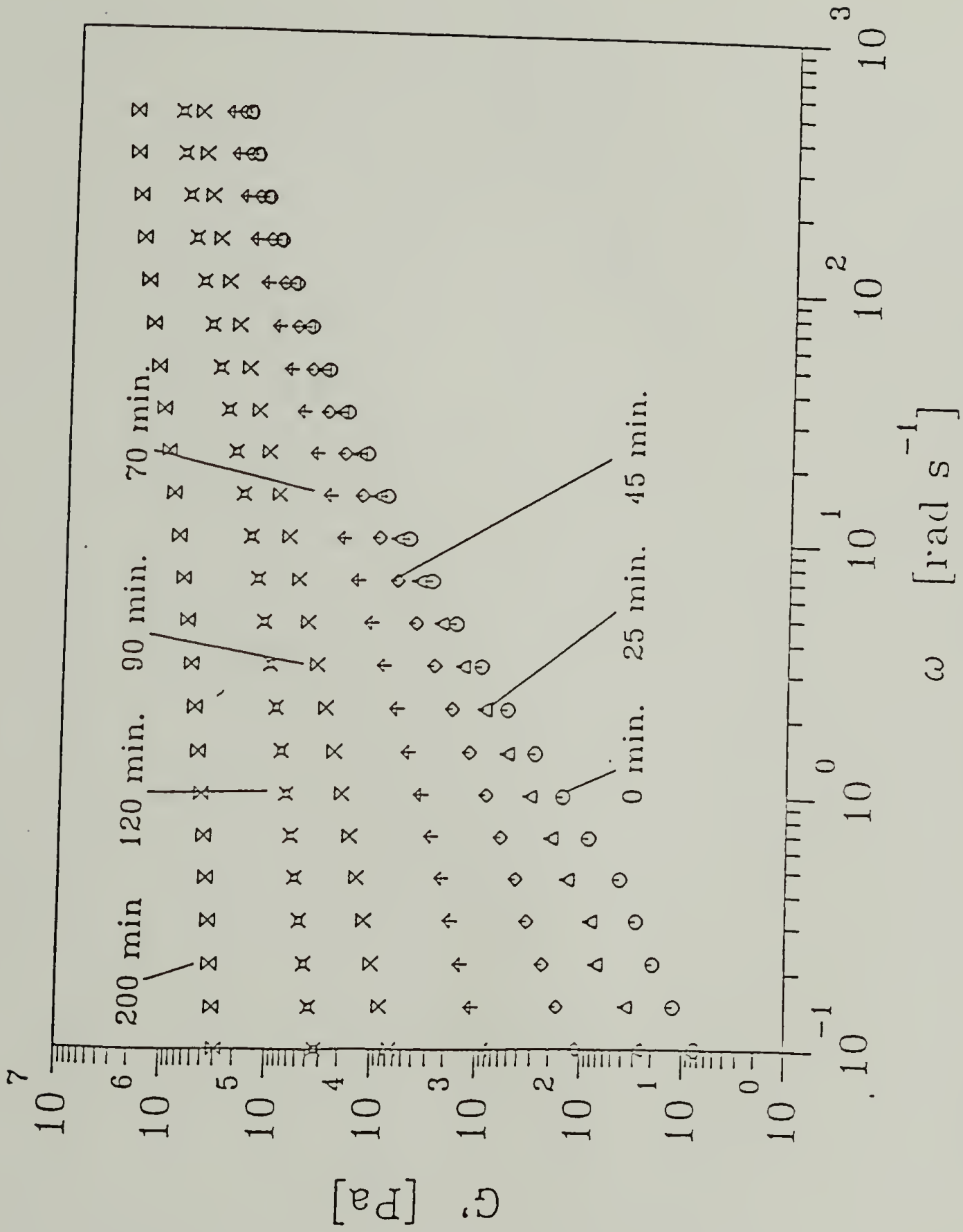
Figure 3.8   Evolution of the storage modulus during the solidification at 106 °C.
Data sets for times up to 200 min after initiating the test.

Five isothermal CFS scans at 125, 132, 136, 143, and 150 °C are given in Figure 3.9. The change of loss tangent versus time is indicated by the arrows in the figure. As the sample is heated above 132 °C, tan δ increases continuously with time, indicating the development of the terminal zone behavior, as is typical for an isotropic fluid. At 125 °C, the decrease of the tan δ values with time shows an increase of the elasticity by annealing.

3.5   Discussion

.   The physical network formation of the segmented copolymer results in a distinct change from a viscoelastic liquid to a viscoelastic solid. This is accompanied by a significant rise in the storage and loss moduli. Submicrometer-sized mesophasic domains are formed and act as physical cross-links. The rheological hysteresis in Figure 3.2 is due to the kinetic effects of ongoing structural reorganization.

In the high-temperature liquid phase, time-temperature superposition behavior shows that the morphology of the polymer remains the same upon cooling from 160 to 110 °C. This does not necessarily imply the existence of a single phase, since even binary separated phases have been reported to obey time-temperature superposition.[14,15] Furthermore, in the cooling scan from 160 °C, a kinetically controlled gelation takes place at temperatures below 110 °C.

The CFS scans in the heating mode show that the isotropization of the mesophase occurs at a higher temperature than its formation. The development of the terminal zone corresponds to the broad isotropization, as observed by DSC.[1] However, in Figure 3.2, the softening effect of

59
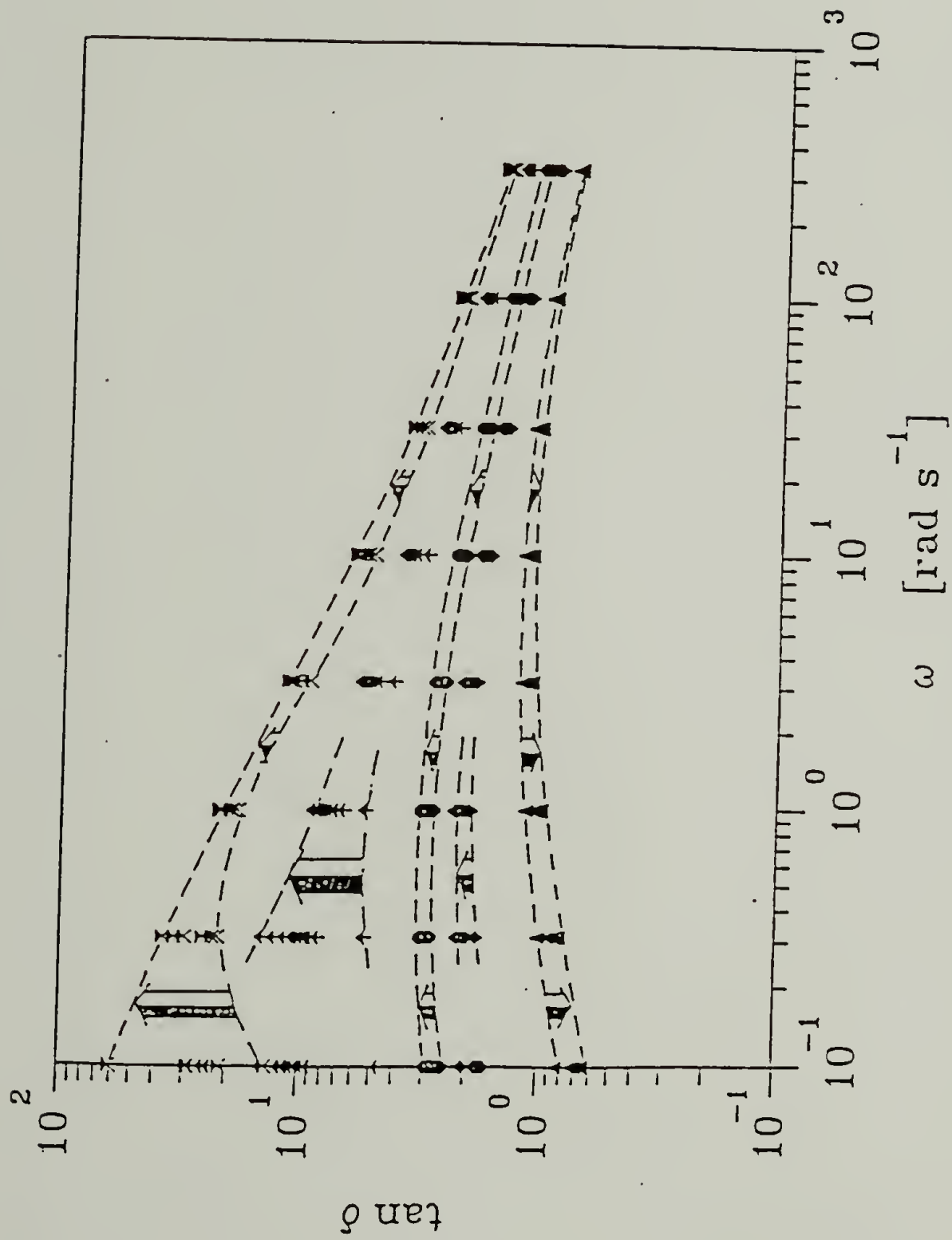
Figure 3.9   Five isothermal CFS scans, characterizing the solid/liquid transition. The arrows indicate the evolution of the loss tangent in time for the isothermal scans. For three experiments (at 125, 136, and 150 °C), dashed lines mark for the the whole frequency window the upper and the lower limit of the range, in which tan δ did change. The temperatures were increased in the following sequence: triangles, 125 °C; circles, 136 °C; diamonds, 132 °C; circles, 136 °C; closed crosses, 143 °C, open hourglasses, 150 °C.

LCPUE 1000 before the isotropization is observed by the gradual decrease of the dynamic moduli. This is largely due to the increased mobility of the soft segments with increasing temperature, and other possible structural changes resulting from the loss of sample connectivity.

A viscoelastic liquid/solid transition caused by physical cross-linking has been identified by the rheological method, and a critical gel was observed at 106 °C. For LCPUE 1000, we find the relaxation exponent n=0.94, a relatively high value, compared with other critical gel data.[16-18] In chemically cross-linking systems, relaxation exponents are between 0.5 and 0.7.[7-9,19] In physically cross-linking systems with crystalline units as hard segments,[10,11] the relaxation exponents are usually between 0.11 and 0.13, with the exception of the PVC plastisol system, which yields a value of 0.8.[20] The relaxation exponent and the gel stiffness of 107 Pas^n indicate a very soft structure with a high degree of internal mobility in LCPUE 1000.

3.6   Conclusion

A broad viscoelastic solid/liquid transition is observed by rheology. A mechanical hysteresis and a crossover ($G'=G''$) temperature difference between heating and cooling scans are due to the kinetically controlled transition. The CFS method has been applied to identify the viscoelastic transition at 106 °C and shows the existence of a critical gel, which obeys a power law. The quantitative analysis yields values for the gel stiffness and the critical exponent, which indicate a soft gel structure with a high degree of mobility.

References and Notes

(1)   Tang, W.; Farris, R. J.; MacKnight, W. J.; Eisenbach, C. D.
        Macromolecules **1994**, *27*, 2814.

(2)   Wissbrun, K. F.; Griffin, A. C. *J. Polym. Sci., Polym. Phys. Ed.*
        1982, *20*, 1835.

(3)   Jackson, W. J., Jr.; Kuhfuss, H. F. *J. Polym. Sci., Polym. Chem. Ed.*
        1976, *14*, 2043.

(4)   Wissbrun, K. F. *J. Rheol.* **1981**, *25(6)*, 619.

(5)   Baird, D. G. *Liquid Crystalline Order in Polymers;* Academic Press:
        New York, 1978; p 237-259.

(6)   Stenhouse, P. J.; Valles, E. M.; Kantor, S. W.; MacKnight, W. J.
        Macromolecules **1989**, *22*, 1467.

(7)   ˙ De Rosa, M. E.; Winter, H. H. *Society of Plastics Engineers, Inc.,*
        Technical Papers; Vol. XXXIX, ANTEC '93 Conference Proceedings,
        New Orleans, Vol. 3. 1993.

(8)   Winter, H. H.; Chambon, F. *J. Rheol.* **1986**, *30 (2)*, 367.

(9)   Chambon, F.; Winter, H. H. *J Rheol.* **1987**, *31(8)* ,683.

(10)   Lin, Y. G.; Mallin, D. T.; Chien, J. C. W.; Winter, H. H.
        Macromolecules **1991**, *24*, 850.

(11)   Richtering, H. W.; Gagnon, K. D.; Lenz, R. W.; Fuller, R. C.; Winter,
        H. H. *Macromolecules* **1992**, *25*, 2429.

(12)   Mours, M.; Winter, H. H. *Rheol. Acta* **1994**, *33*, 385.

(13)   Winter, H. H. *Polym. Eng. Sci.* **1987**, *27(22)*, 1698.

(14)   Han, C. D.; Kim, J. K. *Polymer* **1993**, *34*, 2533.

(15)   Bates, F. S. *Macromolecules* **1984**, *17*, 2607.

(16)   Winter, H. H. *Encyclopedia of Polymer Science and Engineering,*
        supplement vol., second ed.; John Wiley & Sons: New York, 1989; p
        343-351.

(17)   Hsu, S. H.; Jamieson, A. M. *Polymer* **1993**, *34*, 2602.

(18)   Amis, E. J.; Hodgson, D. F.; Yu, Q. *Polym. Prepr. (Am. Chem. Soc.,*
        Div. Polym. Chem.) **1991**, *32(3)*, 447.

(19)   Chambon, F.; Petrovic, Z. S.; MacKnight, W. J.; Winter, H. H.
       Macromolecules **1986**, *19*, 2146.

(20)   Te Nijenhuis, K.; Winter, H. H. *Macromolecules* **1989**, *22*, 411.

CHAPTER 4

SEGMENTED POLYURETHANE ELASTOMERS WITH LIQUID CRYSTALLINE HARD SEGMENTS.
3. INFRARED SPECTROSCOPIC STUDY

4.1   Abstract

Segmented liquid crystalline polyurethanes (LCPUE) have been studied by infrared spectroscopy. The nematic liquid crystalline hard domains act as physical cross-links and can be oriented by the application of mechanical strain. The orientation function achievable in the hard segments results from the combination of mechanical strain and stress-softening. Furthermore, elastic deformation induces the rearrangement of some hard segments in the mesophase into a more ordered packing. High temperature infrared spectra have been correlated with thermal transitions of the LCPUE, and a liquid-liquid microphase separated morphology above the isotropization of the mesophase appears to exist.

4.2   Introduction

Segmented block copolymers with alternating liquid crystalline hard and amorphous soft segments are a new class of thermoplastic elastomers. Due to the chemical structural differences between the hard and soft segments, a microphase-separation occurs, consisting of liquid crystalline hard domains

64

and amorphous soft domains. The liquid crystalline hard domains act as physical cross-links for the network and tend to become macroscopically anisotropic during elongation. Hence, mechanical strain may result in a highly oriented thermoplastic elastomer.[1]

Thermotropic liquid crystalline polyurethanes have been studied for their variable phase behavior and potential application as high-strength fibers.[2-4] In previous studies, Stenhouse et al.[5] obtained an enantiotropic liquid crystalline polyurethane (referred to as LCPU) from 4,4'-bis(6-hydroxyhexoxy)biphenyl with 2,4-tolylene diisocyanate and 2,6-tolylene diisocyanate at equal molar ratio. The LCPU has been further investigated by differential scanning calorimetry (DSC), polarized optical microscopy and wide-angle X-ray scattering (WAXS), and clearly exhibits a smectic mesophase. In WAXS studies,[2] an intense and sharp X-ray diffraction at 14.3 Å is observed and assigned to the 004 layer reflection of the LCPU. One additional weak meridional diffraction at 28.8 Å arises from the 002 layer reflection.

The elastomers described here (referred to as LCPUE) are based on this LCPU structure as the hard segment and poly(tetramethylene oxide) as the soft segment. The mesophase in the LCPUE is formed by the aggregation of the liquid crystalline hard segments. This is experimentally proven on the basis of DSC, WAXS and rheology studies.[1,6] Compared with the smectic mesophase in LCPU, the WAXS pattern shows the disappearance of the sharp low angle reflection in the LCPUE mesophase. This may be attributed to the fact that the liquid crystalline hard domain structure is perturbed by the polydispersity of the hard segments and the incorporation of low molar mass homologues of the poly(tetramethylene oxide) soft segments. The chemical structure modification results in reduced position correlation in the mesophase by smearing out the

65

layered morphology,[7] and consequently leads to a nematic mesophase with an average inter-hard segment lateral packing of 4.5 Å.

The mechanical properties of this type of segmented block copolymer are strongly dependent upon domain structure and orientation. Hence, it is important to determine how each of the domains deforms during the straining process. Infrared dichroism is a useful method to monitor the orientation behavior of specific polymer chain segments, and affords a determination of the degree of domain orientation induced by mechanical deformation.[8]

Infrared spectroscopy is also widely used to study chain-chain interaction and conformational order in polymers.[9,10] The molecular interactions are related to the nature of the phase which determines the relative arrangement of functional groups. Therefore, it is possible to investigate the dependence of the mesophase microstructure on molecular interactions using this technique, and much of the interest has focused on the analysis of absorption bands which are involved in hydrogen bonding. Furthermore, mechanical strain improves the lateral packing of the chains, and reduces the degree of disorder within the mesophase. This increase in order can be monitered by infrared spectroscopy and WAXS.

4.3   Experimental Section

4.3.1 Materials

The polymers were synthesized via solution polymerization. In the first stage of the reaction, a prepolymer was prepared from hydroxy terminated poly(tetramethylene oxide) (PTMO; $M_w = 650$, 1000) and the 1:1 mixture of 2,4-tolylene diisocyanate and 2,6-tolylene diisocyanate at 100 °C. This was

66

followed by chain extension using the mesogen 4,4'-bis(6-hydroxyhexoxy)biphenyl. The resulting polymers (Figure 4.1), referred to as LCPUE 650 and LCPUE 1000, have 65.1 wt% and 42.3 wt% of hard segments, respectively.

4.3.2 Infrared Spectroscopy

Infrared spectroscopic experiments were performed with an IBM Model 32 Fourier transform infrared spectrometer. Data were collected at 2 cm^{-1} resolution with a minimum of 128 scans. The LCPUE films cast from CHCl$_3$ solution were sufficiently thin to be within an absorbance range where the Beer-Lambert law was obeyed.

The applicability of infrared dichroism to thermoplastic elastomers depends on the availability of characteristic absorption bands in the hard and soft domains with known transition moment vectors. In LCPUE samples, the stretching vibration of the N-H part of the urethane linkage of the hard segments, appears at 3286 cm^{-1} and is employed to characterize the orientation of hard domains. The asymmetric C-H stretching absorption occurs at 2935 cm^{-1}, and is used to describe the orientation of soft domains. A small portion of the methylene groups from the chain extender (Diol-6) and the methyl groups from TDI reside in the hard domains (17% in LCPUE 1000 and 25% in LCPUE 650) but do not affect the CH$_2$ asymmetric stretching band significantly, so it can be employed as the characteristic band for the soft segment poly(tetramethylene oxide).

The dichroic ratio D for a particular absorption band is defined by

$$D = \frac{A_{\parallel}}{A_{\perp}}$$

(1)

67
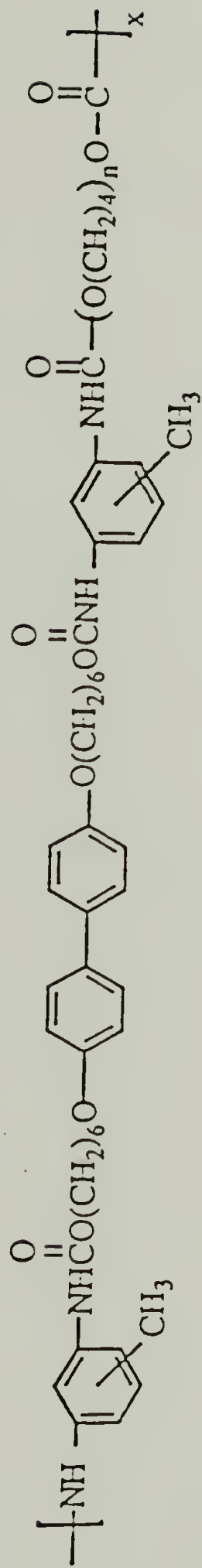
Figure 4.1   Chemical structure of Liquid Crystalline Polyurethane Elastomers

where $A_{\parallel}$ and $A_{\perp}$ are the peak absorbancies of infrared radiation polarized parallel and perpendicular to the stretching direction, respectively.

The orientation function for the absorbing species can be calculated from

$$f = \frac{(D_0+2)\,(D-1)}{(D_0-1)\,(D+2)} \tag{2}$$

where $D_0 = 2\cot^2\alpha$, defined as the dichroic ratio for perfect chain alignment. Here α, the angle between the transition moment of the vibration and the chain axis, is assumed to be 90^0 for both the N-H vibration and the C-H asymmetric stretching bands in LCPUE samples. The orientation function ranges from a value of -0.5 to 1.0, $f = -0.5$ for perfect chain orientation transverse to the stretch direction, $f = 0$ for random chain orientation, and $f = 1.0$ for perfect orientation in the stretch direction.

The orientation function, f, can be further related to an average angle θ by

$$f = \,<3\cos^2(\theta)-1>/2 \tag{3}$$

where θ is the angle between the chain segment and the stretching direction.

Thin LCPUE films were stretched to different strain levels. Polarized and unpolarized IR spectra were recorded 30 min after the deformation had taken place to allow sufficient time to reach orientation equilibrium.

High temperature infrared spectra were obtained by placing LCPUE films between KBr windows, which were clamped between brass holders in a

temperature-controlled cell monitored via thermocouples placed adjacent. The heating rate of the LCPUE sample was controlled as 10 K/min.

4.4   Results and Discussion

4.4.1   IR Dichroism

The orientation function-strain curves of hard and soft domains for LCPUE 1000 are shown in Figure 4.2. Overall there is a clear distinction between the two domain orientations, illustrated by a much higher value for the hard domain.[11] This is largely attributed to the fact that the amorphous PTMO (M_w = 1000) is above its T_g and tends to relax toward random conformations after stress is applied. On the other hand, the orientation function of the soft segments increases gradually to 0.20 with the strain, indicating that PTMO undergoes conformational changes leading to chain orientation. The mesophasic hard domain orientation function is found to be positive and reaches its maximum (f = 0.37) at 600% strain. From this, one can conclude that the mesophase orients parallel to the stretching direction.

It has been reported, in some types of polyurethane block copolymers, that negative orientation of the hard segments is observed up to 400% strain. Cooper and coworkers[12] compared the orientation mechanisms of amorphous and crystalline hard segment regions in MDI-polyurethane elastomers, and found that only crystalline regions showed a transverse orientation at low elongation with respect to the stretching direction. Bonart and coworkers[13,14] correlated this observation with a proposed model. Hard segments were oriented perpendicular to the longer axis of the domain, soft segments were envisioned as being stretched initially to different extents, giving rise to local

70
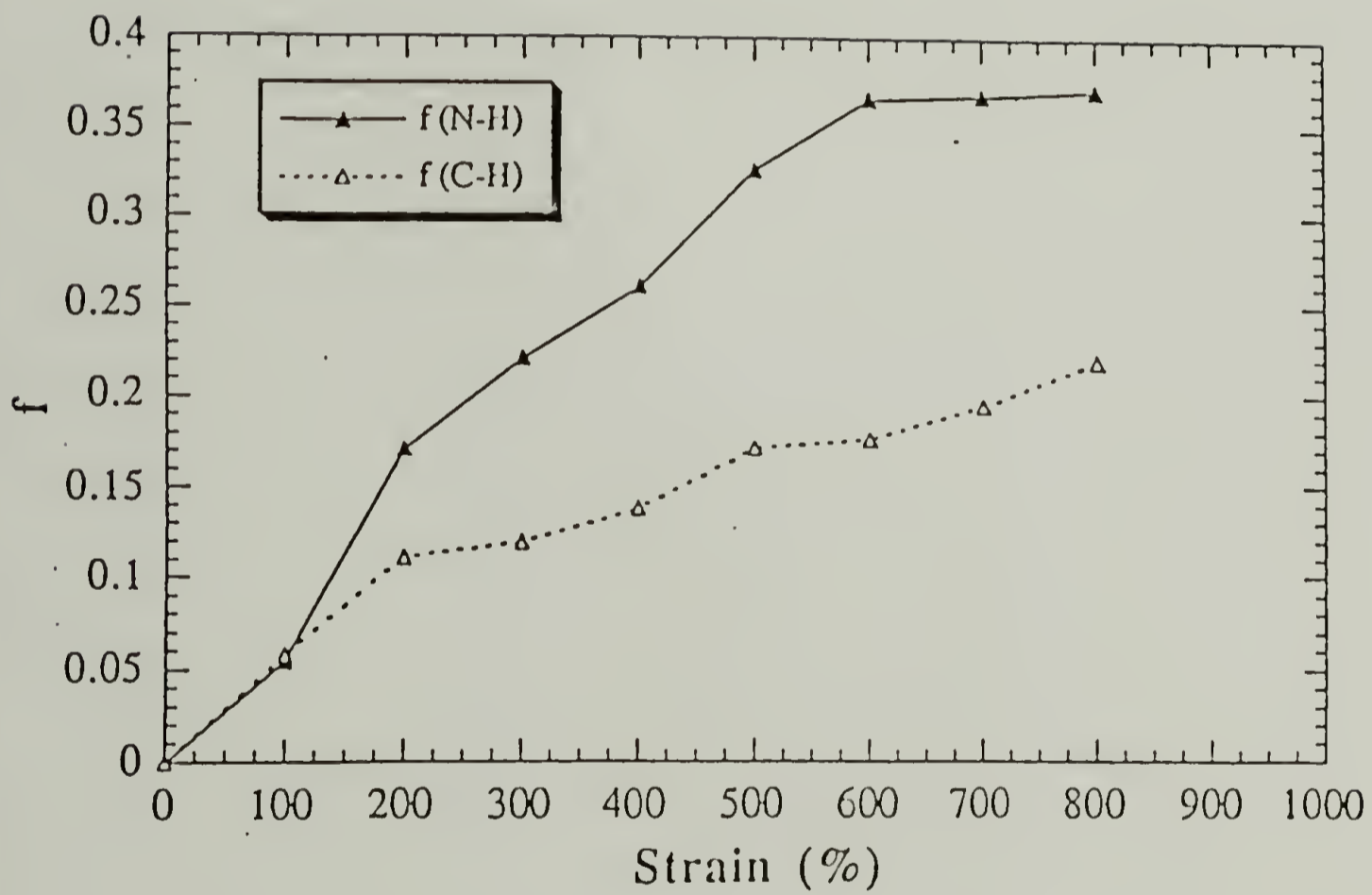
Figure 4.2   Orientation function-strain curves for LCPUE 1000

torques which twisted the hard segments preferentially transverse to the stretching direction, and eventually led to parallel alignments at high strains.

In the current LCPUE 1000 sample, no negative orientation values of the hard domains are observed in the range 0%-100% strain. This suggests that the nematic mesophase (hard domain) is oriented in the direction of stretch even at low strains.

The orientation function of the hard domains is used to calculate the average ordering of the nematic mesophase (eq 3). At 0% strain, $f = 0$ indicating that mesophases orient randomly. At 800% strain, $f = 0.37$ and the angle is 40.4° on average between the stretching axis and the local director of the mesophase.

Figure 4.3 illustrates, in the LCPUE 650 sample, that the orientation of soft segments is little affected by the change of poly(tetramethylene oxide) molar mass. However, the decrease of the hard segment orientation function may be attributed to the morphological difference between the two LCPUE samples caused by the different concentration of soft segments, and the maximum values of the orientation function are strain dependent.

4.4.2 Strain Induced Reorganization

There are two major regions of the infrared spectrum of LCPUE 1000 which are useful for understanding the reorganization of the nematic mesophase. These are the N-H stretching region from 3100 to 3500 cm^{-1} and the amide I region from 1640 to 1780 cm^{-1}.

Amide I Mode

Figure 4.4 shows infrared spectra of LCPUE 1000 in the amide I region as a function of increasing strain. A substantial increase of the intensity of the
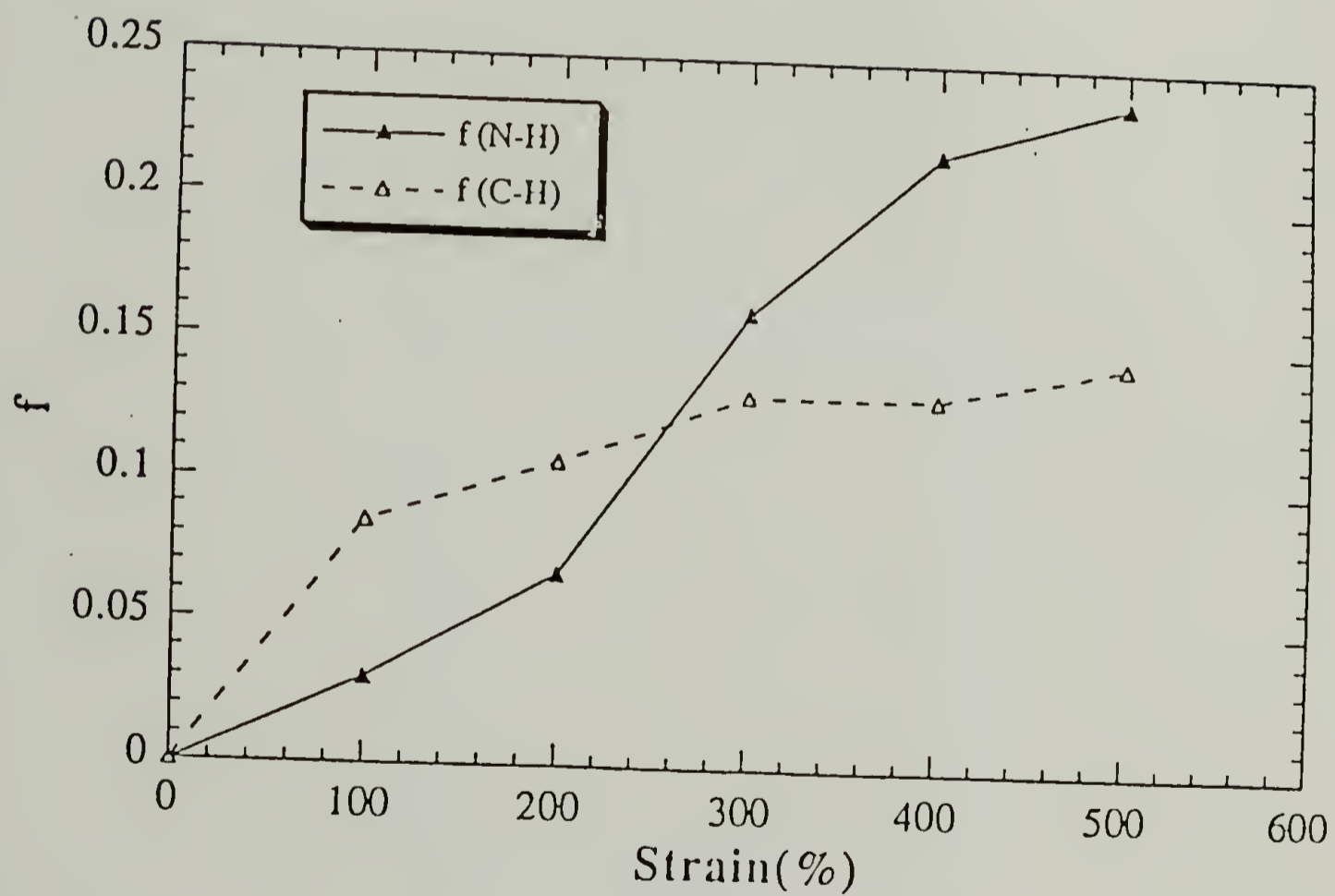
Figure 4.3   Orientation function-strain curves for LCPUE 650

73
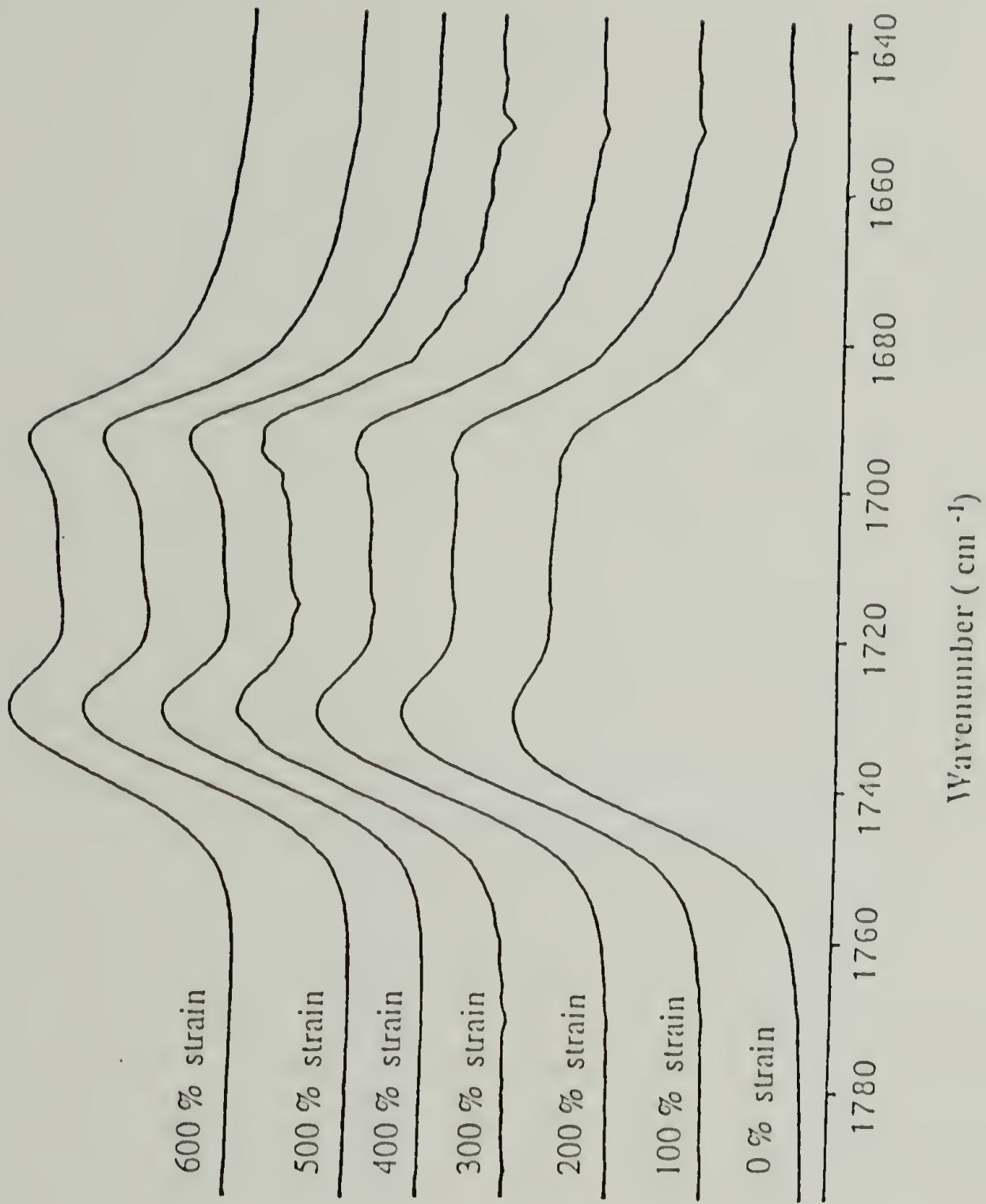
Figure 4.4   IR spectra of LCPUE 1000 recorded from 0 % to 600 % strain in the amide I region

low frequency peak at 1692 cm^{-1} is observed during the elongation. It is well-known that the infrared band of H-bonded urethane carbonyls appears at a lower frequency than that of free urethane carbonyls.[15] Furthermore, semicrystalline samples such as polyamides[16] and polyurethanes[9] have been studied, and it has been found that C=O groups in the amide I band are sensitive to the differences in the pattern of hydrogen bonds that determine the relative arrangement of the C=O groups and the degree of dipole-dipole interactions. The amide I band was resolved into its constituents as hydrogen bonded carbonyl groups in ordered ("crystalline") domains, hydrogen bonded carbonyl groups associated with disordered ("amorphous") conformations and non-hydrogen bonded (free) carbonyl groups.

In LCPUE 1000, thermal analysis and WAXS have previously shown the existence of a mesophase, and suggested the reorganization of some hard segments in the mesophase during mechanical strain.[1] IR spectroscopy provides a more detailed technique to study localized microstructural changes taking place during elongation. In Figure 4.5a, there are three different bands at 1694, 1711 and 1735 cm^{-1} in the amide I region, which correspond to ordered hydrogen bonded, disordered hydrogen bonded and non-hydrogen bonded free carbonyl groups. Other investigators have also observed carbonyl bands at these frequencies in liquid crystalline polyurethanes and ascribed them to different patterns of hydrogen bonds.[9,17] Here, both ordered and disordered hydrogen bonded carbonyl groups exist in the mesophase, while the free C=O groups are at the domain interface and/or within the soft segment matrix. In order to analyze the data quantitatively, curve fitting is employed to resolve the amide I mode into its constituents.[16,17]

The following assumptions are made to permit a logical approach in the procedure of curve fitting:

0 % strain

1800 1780 1760 1740 1720 1700 1680 1660 1640

Wavenumber (cm $^{-1}$)

(a)

600 % strain

1800 1780 1760 1740 1720 1700 1680 1660 1640

Wavenumber (cm^{-1})
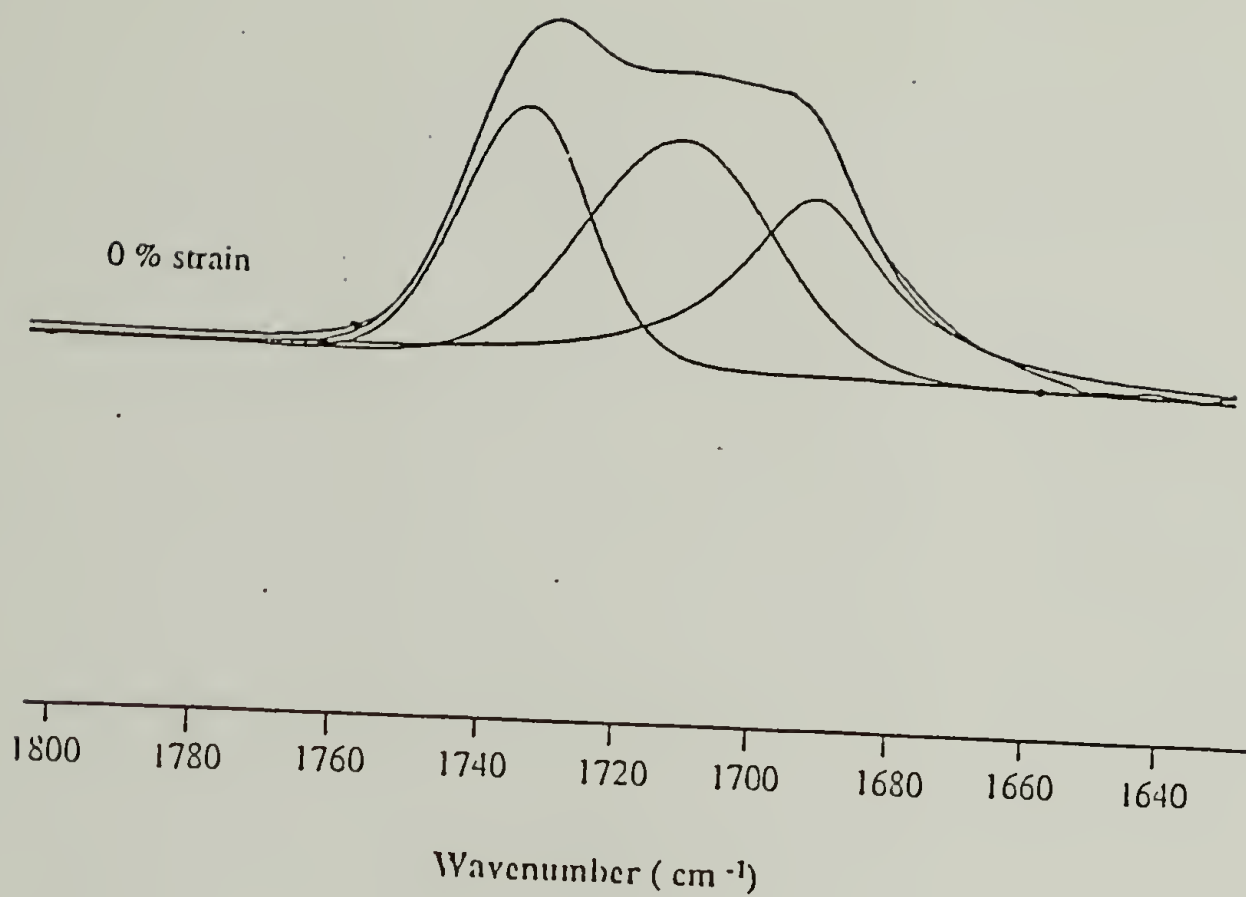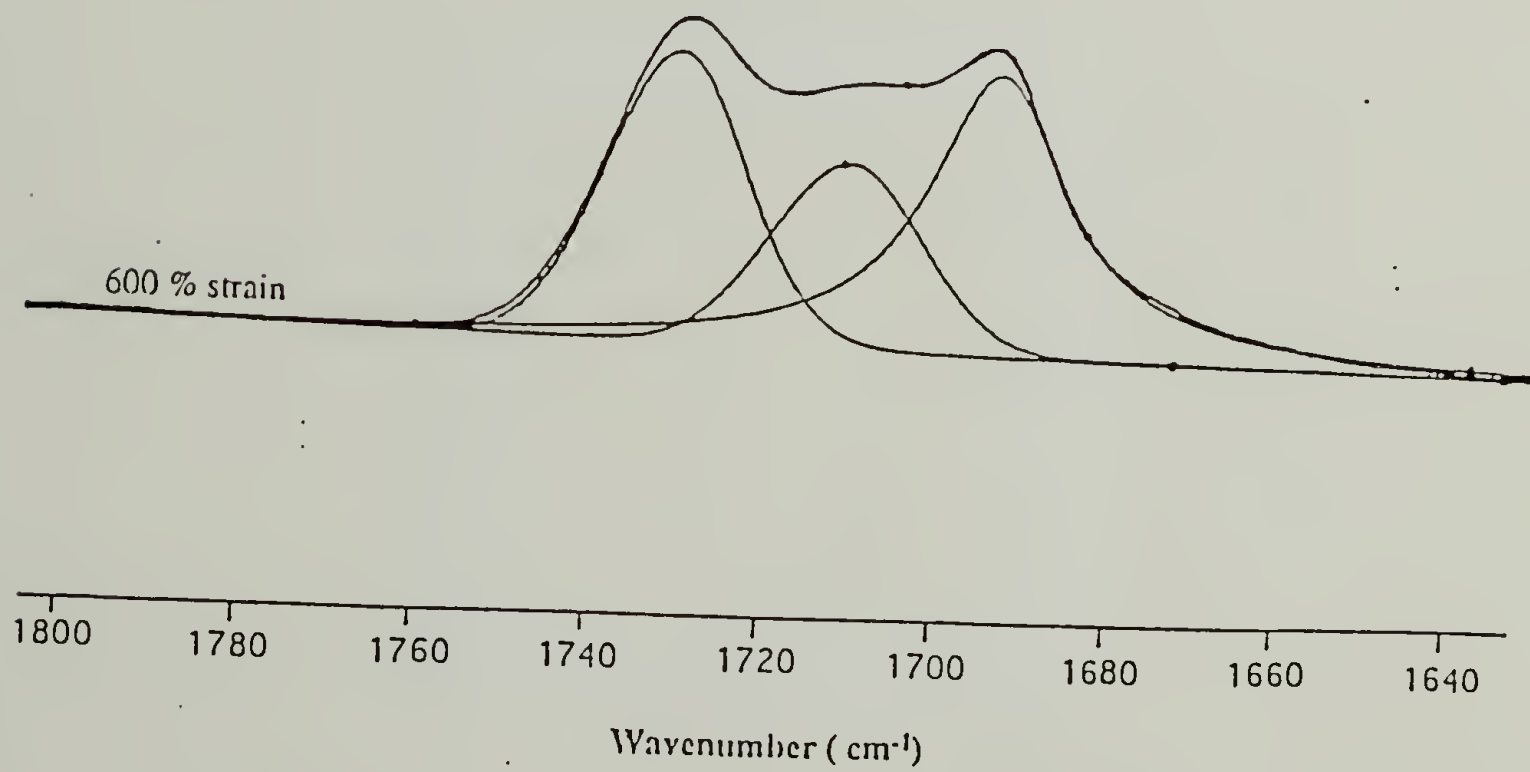
(b)

Figure 4.5   Least-squares curve fitting of the amide I region of LCPUE
1000: (a) at 0 % strain (b) at 600 % strain

1. The band shapes of the non-hydrogen bonded carbonyls and disordered hydrogen bonded ones are assumed to be Gaussian. Together with these two, a Lorentzian band shape is imposed on the ordered H-bonded carbonyl peak. These assumptions afford a "best fit" of the original curve, and the areas of the deconvoluted peaks are reasonable and consistent with other experimental data.

2. The frequency, band shapes and band widths of these three bands are assumed to be unchanged at different strains.

3. Curve fitting is limited to the spectral data of the amide I region between 1780 and 1640 cm^{-1}.

4. The absorption coefficients of these disordered hydrogen bonded and ordered hydrogen bonded carbonyl bands are assumed to be the same and independent of the strength of the hydrogen bonding. The ratio of the H-bonded/non bonded carbonyl band absorption coefficients is listed as being 1.7.[18]

Table 4.1 summarizes the detailed results of the curve fitting of the amide I region in the strain range of 0-600%. At 0% strain (Figure 4.5a), one can observe that the disordered hydrogen bonded amide I band from the nematic mesophase occurs at 1712 cm^{-1}, the "free" band at 1735 cm^{-1} and ordered band at 1692 cm^{-1}. This is consistent with the results from the previous wide angle x-ray studies. Figure 4.6a shows the diffuse outer ring at 4.5 Å resulting from the nematic mesophase diffraction. These two types of hydrogen bonding and other dipolar interactions lead to the aggregation of hard segments, and maintain the structural order within the mesophase. However, cocrystallization of the isomeric 2,4- and 2,6- tolylene diisocyanate hard segments does not occur.[5] This means that no thermodynamically stable crystal phase exists in the hard domains.

(a)

(b)

Figure 4.6   Room-temperature X-ray diffraction patterns: (a) unstretched
              LCPUE 1000 fiber drawn from the melt (b) stretched
              LCPUE 1000 fiber drawn from the melt

Table 4.1   Curve fitting results of the amide I region of LCPUE 1000

| strain | hydrogen bonded | | | | | | | | | | | |
| | ordered | | | disordered | | | "free" | | | | | |
	υ, cm^{-1}	$W_{1/2}$, cm^{-1}	A_0	υ, cm^{-1}	$W_{1/2}$, cm^{-1}	A_d	υ, cm^{-1}	$W_{1/2}$, cm^{-1}	A_f	A_d/A_t	A_o/A_t	A_f/A_t
0%	1692	26.1	3.50	1712	39.0	4.18	1735	26.5	5.36	0.32	0.27	0.41
100%	1693	22.2	4.22	1711	27.5	2.73	1733	25.8	6.55	0.20	0.31	0.49
200%	1694	20.2	4.35	1711	24.8	2.38	1732	26.3	6.94	0.17	0.32	0.51
300%	1694	20.3	4.45	1711	25.1	2.12	1732	24.2	7.23	0.16	0.32	0.52
400%	1694	18.6	4.61	1711	24.2	2.43	1731	23.4	6.39	0.18	0.34	0.48
500%	1694	18.8	4.71	1711	24.6	2.46	1731	22.8	6.10	0.18	0.36	0.46
600%	1694	19.6	4.84	1712	24.2	2.40	1732	22.8	6.00	0.18	0.37	0.45

Upon stepwise increase of the strain to 600% (Figure 4.5b), the area of the disordered hydrogen bonded carbonyl band decreases substantially, and the ordered one becomes significantly increased. This suggests that the rearrangement of some hard segments in the mesophase has been achieved. Mechanical strain reduces the disorder in the meophase by packing the hard segments in a more regular fashion. In Figure 4.6b, WAXS studies show there are two types of diffraction from the mesophase on the equatorial position. The sharp reflection at 4.5 Å corresponds to the ordered lateral hard segment packing. The diffuse arc reflection at about 4.5 Å relates to the continuing presence of disorder in the nematic mesophase.

On the other hand, in Table 4.1, the area of the "free" amide I band has increased with strain. This would suggest the disruption of hydrogen bonding in some segregated hard domains, or hard segments pulling out from the hard domains into the soft matrix. This is responsible for the stress-softening effect.

In order to illustrate the stress softening effect from mechanical hysteresis, LCPUE 1000 film is stretched for the first time to 100%, then the strain is removed and the sample is restretched to 200%. The stress in the second cycle is lower than that in the first up to 100%, after which it continues in a manner following the first cycle. In a third cycle, a softening up to 200% is observed due to the previous strain history. While the infrared spectroscopic studies give a molecular interpretation of this phenomenon, Figure 4.7 shows that the detached hard segments in the soft domains no longer support the stress, giving rise to the observed softening.[19]

N-H Stretching Mode

Figure 4.8 shows infrared spectra in the range of 3100 to 3600 cm^{-1} as a function of increasing strain. At 0% strain, the spectrum is characterized by a
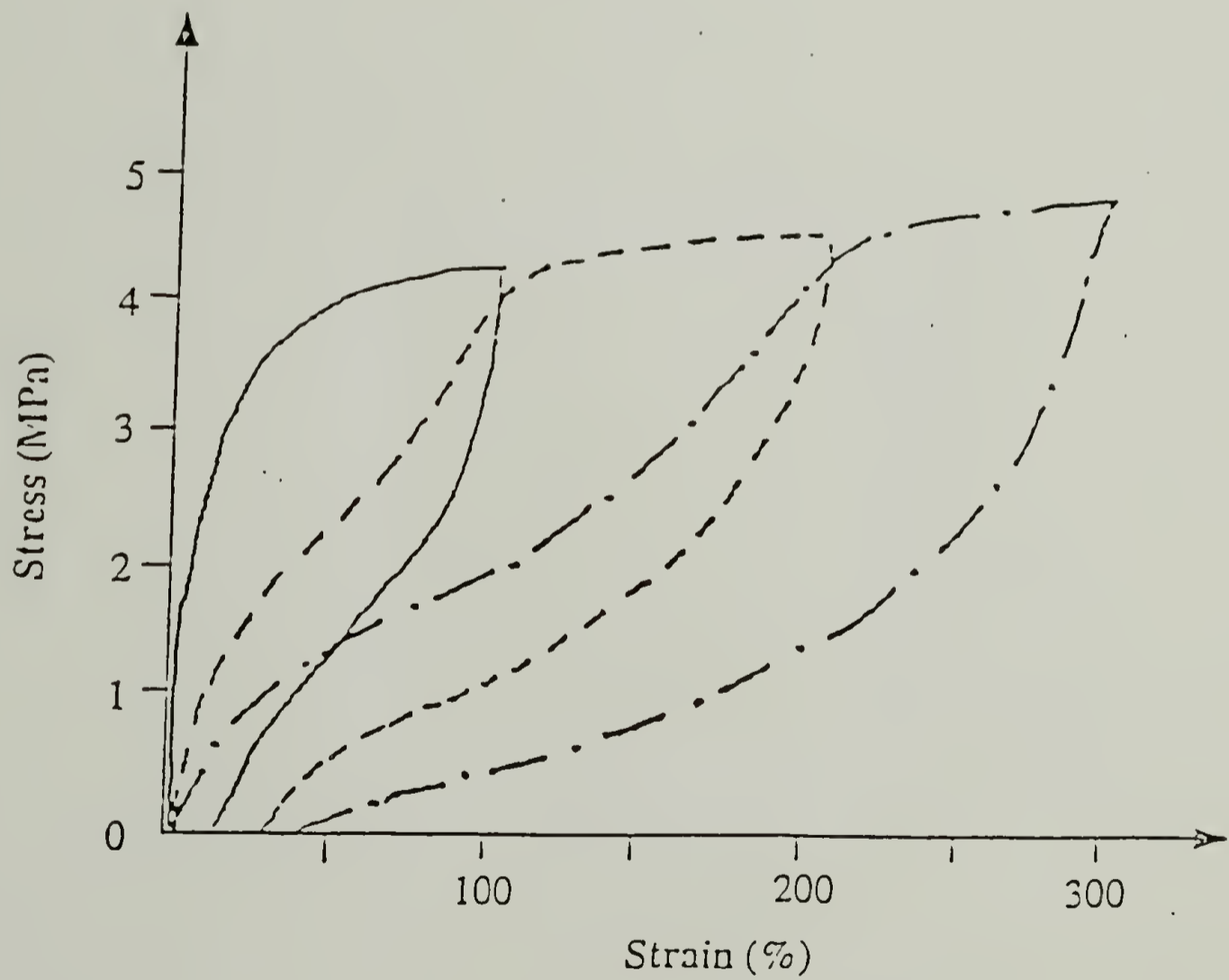
Figure 4.7   Stress-softening of LCPUE 1000
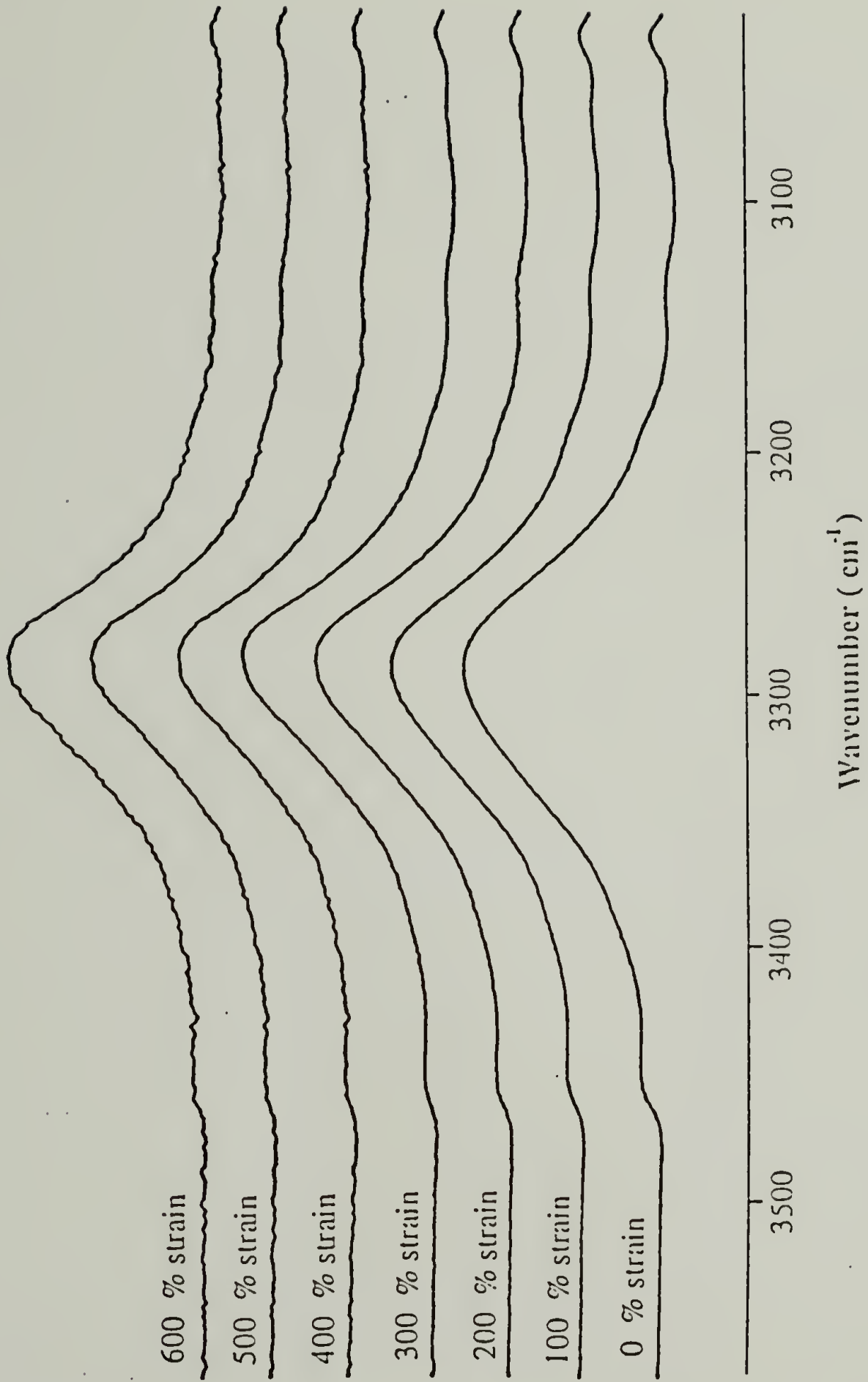
Figure 4.8   IR spectra of LCPUE 1000 recorded from 0 % to 600 % strain in the N-H stretching region

primary band of the hydrogen bonded N-H stretching vibration centered at 3290 cm^{-1}, and it can be approximated as a single Gaussian curve with a width at half-height of 109.8 cm^{-1}. The band of non-hydrogen bonded N-H groups only appears at about 3450 cm^{-1} as a small satellite peak. As strain is increased, there is a steady decrease in the width of the hydrogen bonded N-H stretching band (Table 4.2). Sandorfy[20] and Molis et al[21] reviewed the unusual breadth of the hydrogen bonded N-H stretching mode and concluded that it was due to anharmonic oscillations and disordered phase behavior. Hence, it can be deduced here that the narrowing of the N-H band is another manifestation of the reduction of disorder in the nematic mesophase and phase perfection under mechanical strain.

4.4.3 Temperature Induced Phase Transition

The phase transition of the nematic mesophase in LCPUE 1000 is manifested by two endotherms separated by an exotherm.[1] The lower temperature endotherm occurs at ca. 101 °C, and corresponds to the isotropization of the thermodynamically less stable mesophase. Then, it is followed by the reorganization into the thermodynamically stable mesophase, which isotropizes at ca. 128 °C. IR spectroscopy can be used to monitor the microstructural changes during the thermal processes.

Amide I mode

Three discernible bands in the carbonyl stretching region are observed for LCPUE 1,000 film cast on KBr cell at room temperature. Consistent with the previous study, the highest frequency component at 1734 cm^{-1} corresponds to carbonyls not involved in hydrogen bonding. The other two components, at

Table 4.2   Hydrogen bonded N-H stretching mode of LCPUE 1000

Strain (%)	frequency, cm⁻¹	$W_{1/2}$. cm⁻¹
0	3286	110
100	3286	100
200	3284	96
300	3283	86
400	3283	86
500	3283	85
600	3283	86

1715 and 1694 cm^{-1}, are due to disordered and ordered hydrogen bonded carbonyls within the mesophase, respectively.

Figure 4.9 shows infrared spectra of LCPUE 1000 in the range of 1650-1800 cm^{-1} recorded as a function of increasing temperature. It should be noted that the spectra are plotted on an absolute absorbance scale and consequently the changes in frequency, breadth and relative area can be directly compared. The spectrum at 40 °C is characterized by a strong absorbance at 1734 cm^{-1} and two additional broad bands at lower frequencies. Upon heating the sample to 126 °C, the disordered hydrogen bonded carbonyl band decreases in absolute intensity. This observation can be correlated with the low temperature endothermic transition of LCPUE 1000 sample as shown previously. The disordered hydrogen bonded carbonyl groups originate from the mesophase with less thermodynamic stability.

When the sample is heated to 150 °C, the second stage isotropization occurs. This causes the disappearance of the low frequency band at 1694 cm^{-1}. The ordered hydrogen bonded carbonyls are transformed into free carbonyls and/or disordered hydrogen bonded carbonyls in the amorphous phase. Above 150 °C, the presence of the band at 1715 cm^{-1} suggests that urethane groups can still interact with each other via hydrogen bonding and, indeed, liquid-liquid microphase separation may exist in the isotropic phase.

N-H stretching mode

Figure 4.10 shows infrared spectra in the range of 3100-3600 cm^{-1} plotted on an absolute scale. As temperature is increased from 40 to 170 °C, the broad hydrogen bonded N-H stretching band shifts to higher frequency. This can be attributed to the fact that, during the isotropization process, N-H groups dissociate and transform into "free" ones. Coleman and Molis studied
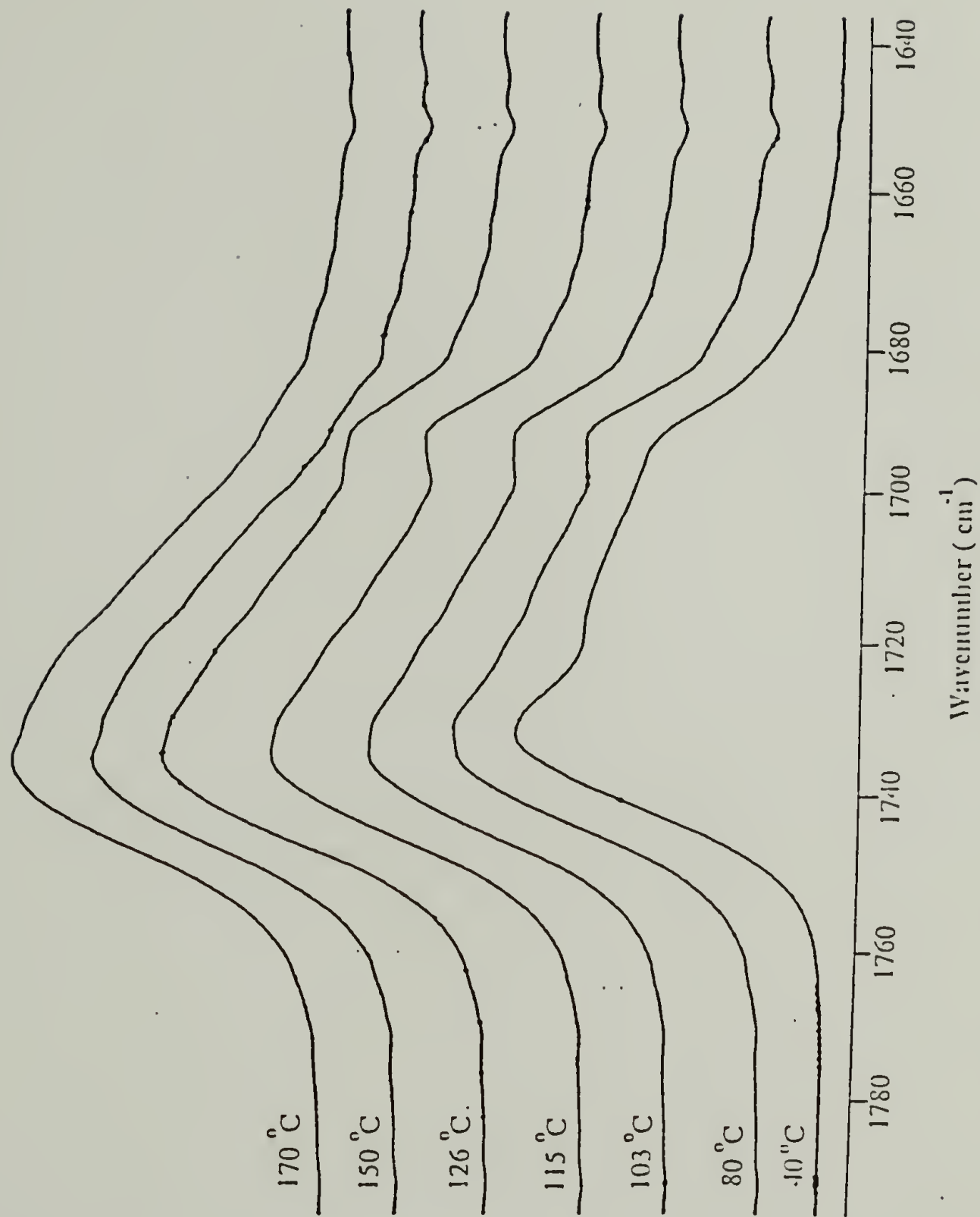
Figure 4.9   IR spectra of LCPUE 1000 recorded from 40 °C to 170°C in the amide I region
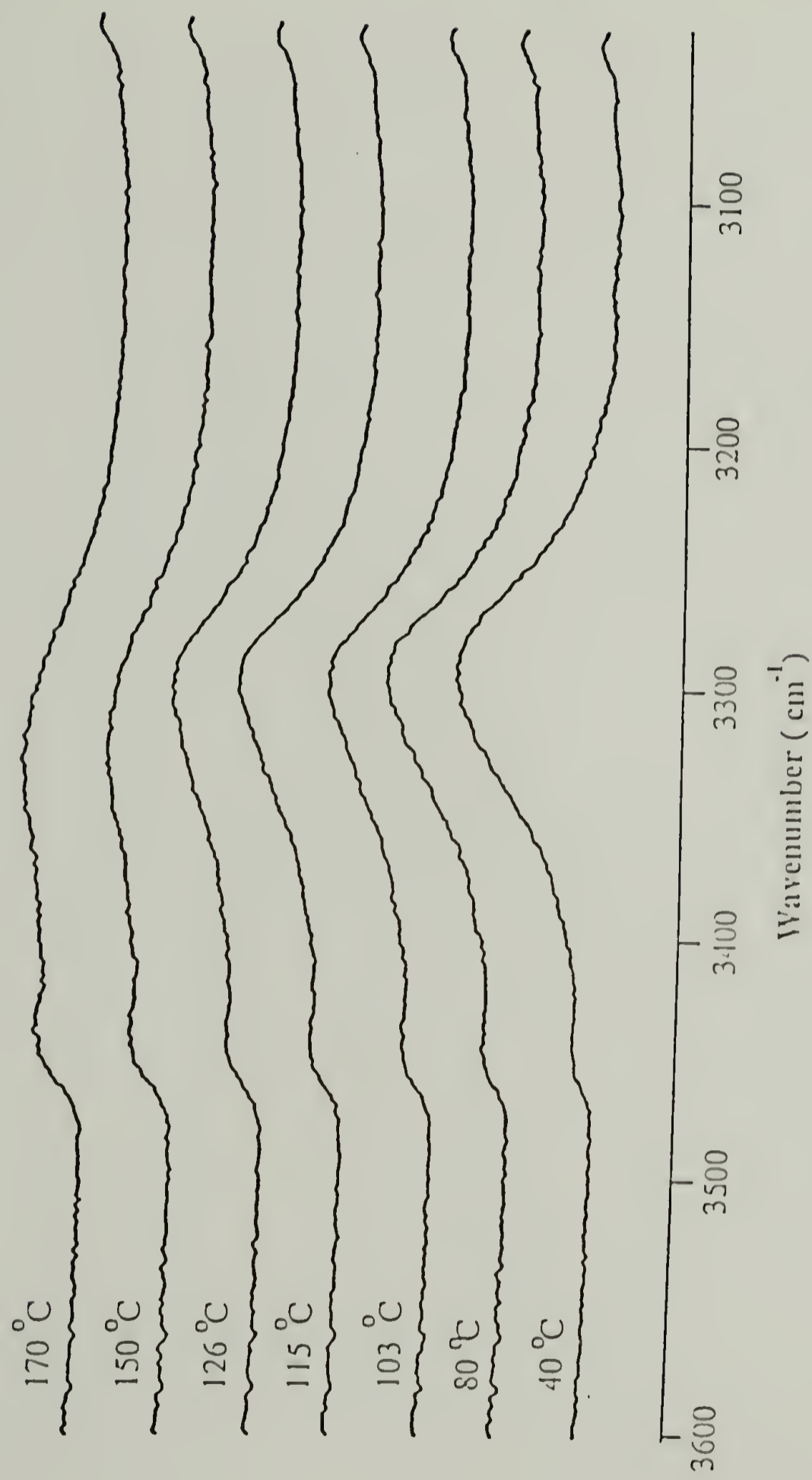
Figure 4.10   IR spectra of LCPUE 1000 recorded from 40 °C to 170°C in the N-H stretching region

the dependence of the N-H absorption coefficient on frequency in amorphous polyamides[18] and polyurethanes,[21] respectively. Their results indicate that the absorption coefficient doubles over the 40 cm^{-1} range from 3360 cm^{-1} to 3320 cm^{-1}. The reduction of the total area of the N-H band in LCPUE 1000 is another example of a substantial decrease of absorptivity with increasing N-H stretching frequency.

4.5 Summary and Conclusion

In summary of results of the infrared investigation of LCPUE, it is apparent that mechanical strain tends to orient the nematic mesophase, which acts as physical cross-links of the network, in the direction of stretching.

The amide I mode is well resolved into three constituents corresponding to ordered hydrogen bonded, disordered hydrogen bonded and free C=O. In the unstrained sample, the large amount of disordered hydrogen bonded carbonyl band is more evidence for the lack of short range positional order in the LCPUE mesophase. Elastic deformation reduces the disorder in the mesophase, shown by a substantial area increase of the hydrogen bonded amide I band at 1694 cm^{-1}.

The carbonyl stretching and N-H stretching vibrations in the high temperature IR spectra reflect microstructural changes during thermal transitions. The presence of disordered hydrogen bonded carbonyl groups above the isotropization transition of the mesophase suggests the existence of liquid-liquid microphase separated morphology.

Very high values (> 0.4) of the hard segment orientation function cannot be attained by straining, and this is largely due to mechanical relaxation accompanying the stress-softening effect.

References and Notes

(1)   Tang, W.; Farris, R. J.; MacKnight, W. J.; Eisenbach, C. D. *Macromolecules* **1994**, 27, 2814.

(2)   Papadimitrakopoulos, F.; Hsu, S. L.; MacKnight, W. J. *Macromolecules* **1992**, 25, 4671.

(3)   Iimura, K.; Koiede, N.; Tanabe, H.; Takeda, M. *Makromol. Chem.* **1981**, *182*, 2569.

(4)   Mormann, W.; Brahm, M. *Macromolecules* **1991**, 24, 1096.

(5)   Stenhouse, P. J. Ph.D. Thesis, University of Massachusetts at Amherst, Amherst, MA. 1992.

(6)   Wedler, W.; Tang, W.; Winter, H. H.; MacKnight, W. J.; Farris, R. J. *Macromolecules* **1995**, 28, 512.

(7) · Donald, A. M.; Windle, A. H. *Liquid Crystalline Polymer;* Cambridge University Press: Cambridge, U.K. 1992.

(8)   Zbinden, R. *The Infrared Spectroscopy of High Polymers,* Chap. V; Academic Press: New York, 1964.

(9)   Pollack, S. K.; Shen, D. Y.; Hsu, S. L.; Wang, Q.; Stidham, H. D. *Macromolecules* **1989,** 22, 551.

(10)   Pollack, S. K.; Smyth, G.; Papadimitrakopoulos, F.; Stenhouse, P. J.; Hsu, S. L.; MacKnight, W. J. *Macromolecules* **1992**, 25, 2381.

(11)   Estes, G. M.; Seymour, R. W.; Cooper, S. L. *Macromolecules* **1971**, 4, 452.

(12)   Seymour, R. W.; Allegrezza, A. E, Jr.; Cooper, S. L. *Macromolecules* **1973**, 6, 896.

(13)   Hoffmann, K.; Bonart, R. *Makromol. Chem.* **1983**, *184*, 1529.

(14)   Bonart, R.; Hoffman, R. *Colloid Polym. Sci.* **1982**, 260, 268.

(15)   MacKnight, W. J.; Yang, M. *J. Polym. Sci., Polym. Symp.* **1973**, 42, 817.

(16)   Skrovanek, D. J.; Painter, P. C.; Coleman, M. M. *Macromolecules* **1986**, *19*, 699.

(17)   Papadimitrakopoulos, F.; Sawa, E.; MacKnight, W. J. *Macromolecules* **1992**, 25, 4682.

(18) Coleman, M. M.; Graf, J. F.; Painter, P. C. *Specific Interactions and the Miscibility of Polymer Blends;* Technomic Publishing Co., Inc.: Lancaster, PA, 1991.

(19) Aklonis, J. J.; MacKnight, W. J. *Introduction to Polymer Viscoelasticity*, 2nd ed.; John Wiley and Sons: New York, 1983.

(20) Sandorfy, C. *The Hydrogen Bond, II* ; Schuster, P. ; Zundel, G.; Sandorfy, C. Eds.; North Holland Publishing Co.: Amsterdam, 1976.

(21) Molis, S. E. Ph.D. Thesis, University of Massachusetts at Amherst, Amherst, MA. 1986.

(22) The width at half height of the resolved bands varies with the degree of strain, particularly in the disordered band. This is a common problem when strongly overlapping bands are curve resolved.

CHAPTER 5

SEGMENTED POLYURETHANE ELASTOMERS WITH MONODISPERSE LIQUID CRYSTALLINE HARD SEGMENTS. 4. SYNTHESIS AND CHARACTERIZATION

5.1 Abstract

Segmented polyurethane elastomers with monodisperse isomerically pure hard segments (PUE) and isomerically mixed hard segments (LCPUE) have been synthesized by treating amine-terminated hard segments with poly(oxytetramethylene) bischloroformate in the presence of an acid acceptor. Differential scanning calorimetry and wide-angle X-ray scattering experiments show the existence of crystalline phases in the isomerically pure hard domains of PUEs and a mesophase in the isomerically mixed hard domains of LCPUE, respectively. Copolymerization and/or blending of the pure isomers (PUE) destablize the crystalline phase, forming an enantiotropic mesophase in the elastomer. Furthermore, Infrared spectroscopy shows the predominant presence of ordered hydrogen bonded carbonyls in the crystalline phase and disordered hydrogen bonded carbonyls in the mesophasic phase, respectively.

5.2 Introduction

Segmented liquid crystalline polyurethane elastomers (LCPUE) are block copolymers composed of alternating liquid crystalline hard and

92

amorphous soft segments. The thermodynamic incompability between the hard and soft segments results in the aggregation of hard segments, forming liquid crystalline domains acting as physical cross-links in the network. Due to the nature of liquid crystalline phase, LCPUEs may be sensitive to external mechanical, electric and magnetic fields, and exhibit properties characteristic of both physically cross-linked elastomers and liquid crystalline materials over a wide temperature range before the isotropization of the liquid crystalline hard domains occurs. In previous papers, we have concluded that the flow characteristics of the liquid crystalline phase in the LCPUEs was responsible for the unusually large elongation at break.[1,2] Furthermore, strain induced hard segment reorganization into more stable cross-links, and resulted in elastomers which could sustain high stress.[3] Thus, LCPUE is not only interesting from a processing point of view, but also because of the possibility to achieve a highly oriented and perfected structure by mechanical deformation.

The hard segment structure and polydispersity influenced the packing order in the domains acting as multifunctional cross-links in segmented polyurethane elastomers (PUE).[4-9] Therefore, it seemed to be important to investigate the structure-property relationships with regard to the hard domain ordering aspect in LCPUE. Our previous studies showed that both the isomerically pure 2,4-tolylene diisocyanate and 2,6-tolylene diisocyanate/4,4'-bis(6-hydroxyhexoxy)biphenyl based polyurethanes were crystallizable.[10] Copolymers obtained by using two isomeric mixtures and/or blends of the isomerically pure polyurethanes destabilized the crystalline phase, and led to the formation of an enantiotropic liquid crystalline phase.[11] The polyurethane elastomers discussed here contain these isomeric polyurethane structures as the monodisperse hard segments, therefore, the

93

resulting hard domains are crystalline and liquid crystalline, respectively. The properties of these elastomers are compared in order to understand the phase behavior of the hard domains.

Furthermore, in order to discriminate between the influence of isomeric compositions and the effects of hard segment size or length distribution, we synthesized model polyurethane elastomers (PUE **10a, 10b** and LCPUE **11**) with monodisperse hard segments. The syntheses and characterization are reported in this paper and correlated with the structural features.

5.3   Experimental Section

5.3.1   Materials

2,4-Tolylene diamine and 2,6-tolylene diamine (both Fluka) were purified through sublimation at 90 $^\circ$C (0.02 mbar). Benzyl chloroformate (Fluka) and phosgene (Messer-Griesheim) were used as received. The syntheses of 4,4'-bis(6-hydroxyhexoxy)biphenyl (**4**)[1] and α-chlorocarbonyl-ω-chlorocarbonyloxypoly(oxytetramethylene) (**9**)[7,12] were carried out as described elsewhere. Chloroform (techn. grade) was refluxed over P_2O_5 for several hours and freshly distilled prior to use.

The syntheses of the isomeric segmented polyurethane elastomers (**10a, 10b** and **11**) are outlined in Figures 5.1, 5.2 and 5.3.
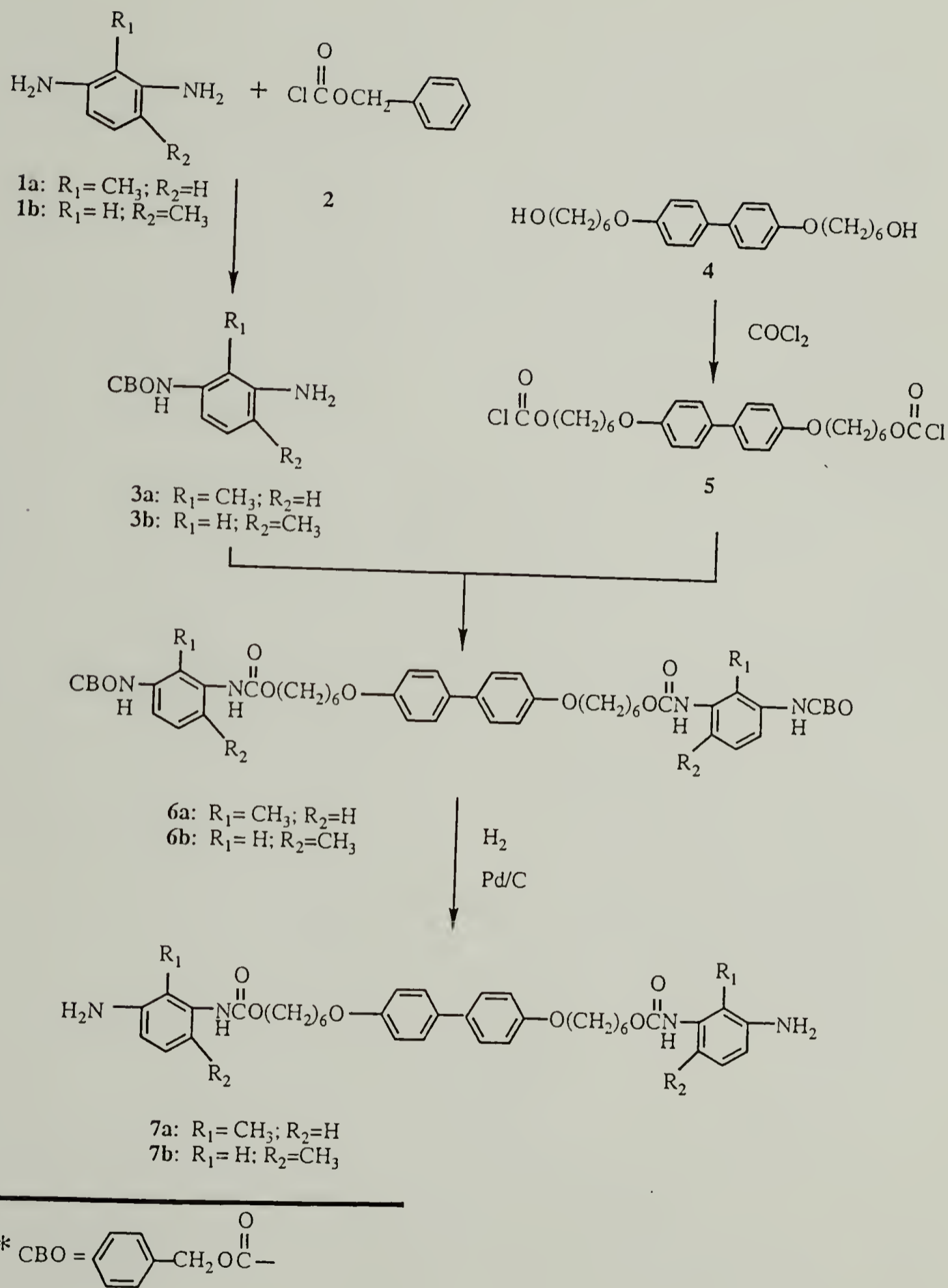
Figure 5.1 The synthesis of amine-terminated oligourethane hard segment
model compounds

95

$H(O(CH_2)_4)_{14}OH$

8

$COCl_2$

$$Cl-\overset{\overset{O}{\|}}{C}-(O(CH_2)_4)_{\overline{14}}\,O-\overset{\overset{O}{\|}}{C}-Cl$$

7a or 7b

9

$$\left[-HN-\underset{R_2}{\overset{R_1}{\bigcirc}}-NH\overset{\overset{O}{\|}}{C}OR O\overset{\overset{O}{\|}}{C}NH-\underset{R_2}{\overset{R_1}{\bigcirc}}-NH\overset{\overset{O}{\|}}{C}(O(CH_2)_4)_{14}O\overset{\overset{O}{\|}}{C}-\right]_x$$
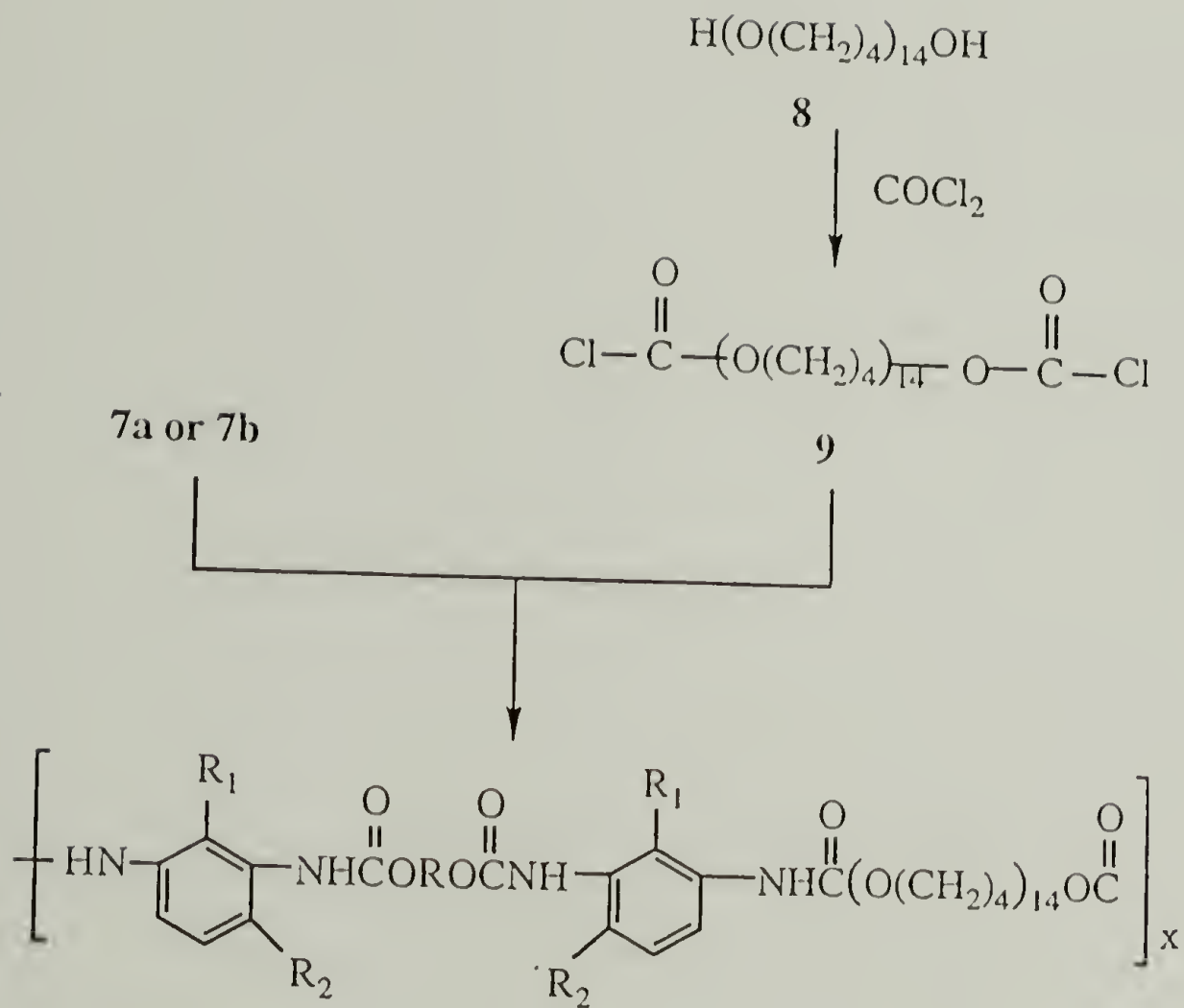
10a: $R_1= CH_3$; $R_2=H$
10b: $R_1= H$; $R_2=CH_3$

with $R= -(CH_2)_6O-\bigcirc\!\!\!-\!\!\!\bigcirc-O(CH_2)_6-$
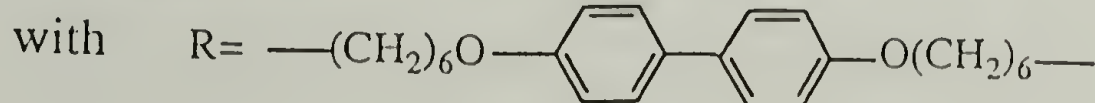
Figure 5.2   The synthesis of isomerically pure segmented polyurethane elastomers (PUE)
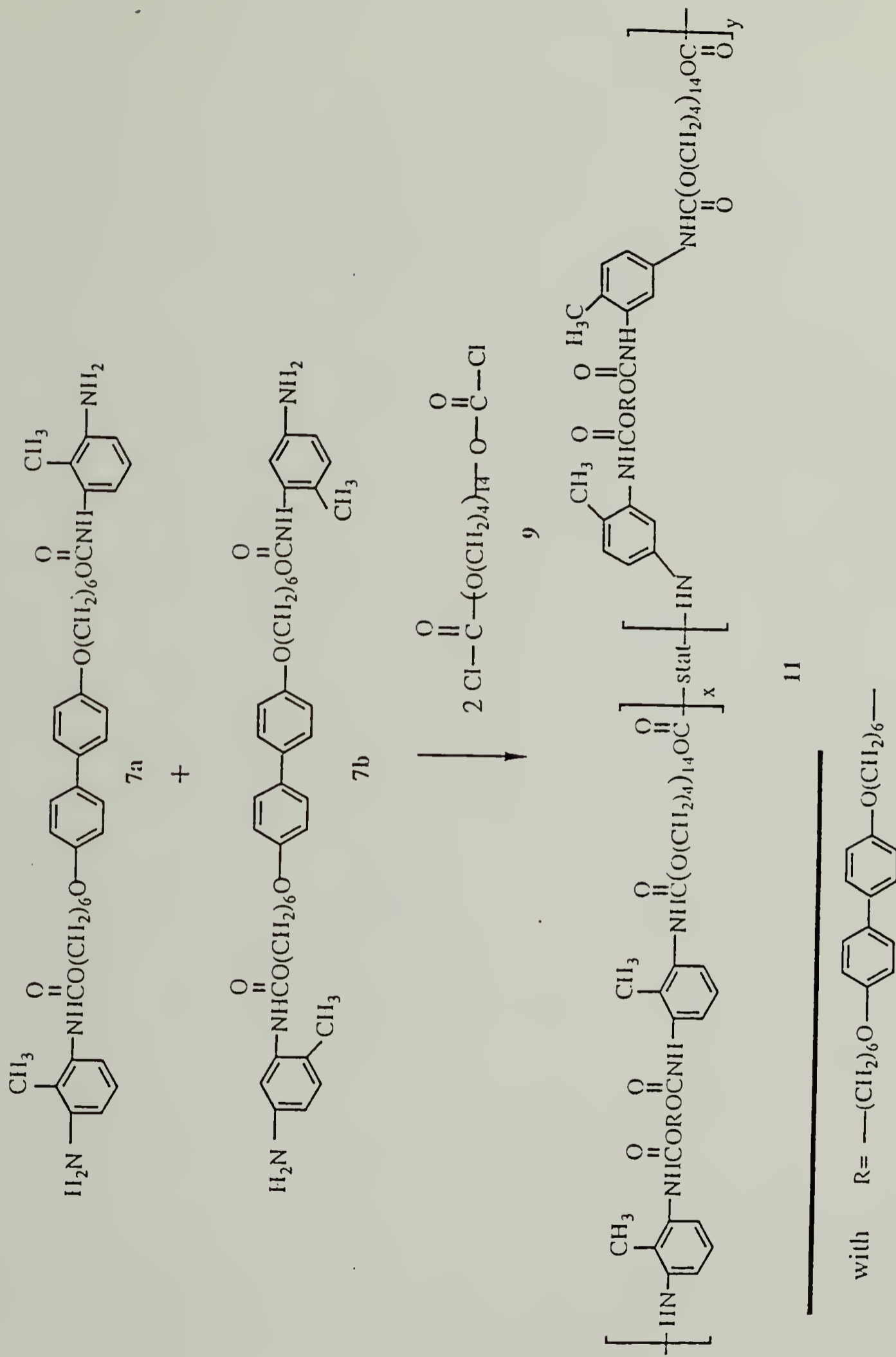
Figure 5.3   The synthesis of isomerically mixed Liquid Crystalline Polyurethane Elastomers (LCPUE)

5.3.2 Synthesis

2-Amino-6-benzyloxycarbonylimino toluene (3a) and 2-amino-4-benzyloxycarbonylimino toluene (3b)

A solution of 10 g (81.9 mmol) diamine **1a** or **1b** in methanol was acidified (pH 3-4) with 4 N HCl, then 14 g (81.9 mmol) benzylchloroformate (**2**) in methylene chloride and a 4 N aqueous sodium hydroxide solution were added dropwise so that the pH remained in the range of 3. After the addition was completed, the reaction mixture was alkalized and stirred overnight. The solution was again acidified and washed several times with chloroform to extract diprotected diamine. After the mixture was brought to pH 12 with concentrated NaOH solution, crude **3a** or **3b** was extracted with chloroform, and dried over Na_2SO_4. The solvent was then removed on a rotary evaporator. Recrystallization from ethanol/cyclohexane yielded 22% **3a** and 31% **3b**, respectively.

3a: IR (KBr): 3456, 3363 (NH); 1720 cm^{-1} (C=O).

^{1}H-NMR (CDCl$_3$): δ= 2.0 (s, -C$\underline{H}_3$, 3H); 3.57 (br, -N$\underline{H}_2$, 2H); 5.18 (s, C$_6$H$_5$C$\underline{H}_2$O-, 2H); 6.40 (s, -N$\underline{H}$COO-, 1H); 6.52 (d, >C=C$\underline{H}$-, 1H); 7.02(m, >C=CH-C$\underline{H}$=C$\underline{H}$-, 2H); 7.34 (m, C$_6$$\underline{H}_5CH_2$O-, 5H).

C$_{15}$H$_{16}$N$_2$O$_2$ (256.3)			
	Calc. C 70.29	H 6.29	N 10.93
	Found C 70.29	H 6.26	N 10.94

3b: IR (KBr): 3454, 3368 (NH); 1728 cm^{-1} (C=O).

^{1}H-NMR (CDCl$_3$): δ= 2.0 (s, -C$\underline{H}_3$, 3H); 3.55 (br, -N$\underline{H}_2$, 2H); 5.16 (s, C$_6$H$_5$C$\underline{H}_2$O-, 2H); 6.53 (d, >C=C$\underline{H}$-, 1H); 6.65 (s, -N$\underline{H}$COO-, 1H); 6.90 (s, >C=C$\underline{H}$-, 1H); 6.93 (d, >C=C$\underline{H}$-, 1H); 7.34 (m, C$_6$$\underline{H}_5CH_2$O-, 5H).

C$_{15}$H$_{16}$N$_2$O$_2$ (256.3)			
	Calc. C 70.29	H 6.29	N 10.93
	Found C 70.36	H 6.36	N 10.87

4,4'- Bis(chloroformylhexoxy)biphenyl (5)

It was obtained in 92% yield by stirring diol-6 (**4**) with a five fold excess of phosgene in THF for 4h and removing the remained phosgene and solvent at high vacuum.

5: IR (KBr): 1789 cm^{-1} (C=O).

^{1}H-NMR (CDCl$_3$): δ= 1.50 (m, -OCH$_2$CH$_2$C$\underline{H}_2$-, 8H); 1.80 (m, -OCH$_2$C$\underline{H}_2$-, 8H); 3.98 (t, -C$_6$H$_4$OC$\underline{H}_2$-, 4H); 4.33 (t, ClOCOC$\underline{H}_2$-, 4H); 6.92 (d, >C=C$\underline{H}$-, 4H); 7.45 (d, -C$\underline{H}$=C<, 4H).

4,4'-Bis[(3-benzyloxycarbonylimino)(2-methyl)phenylene(1-imino carbonyloxyhexyloxy)]-biphenyl (6a) and 4,4'-bis[(5-benzyloxy carbonylimino)(2-methyl)phenylene(1-iminocarbonyloxyhexyloxy)]-biphenyl (6b)

The bischloroformate **5** (4 g, 7.8 mmol) dissolved in 50 ml dioxane was added dropwise to a 50 ml CHCl$_3$ solution of the amine **3a** or **3b** (4.6 g, 18 mmol). Then, a 1 M aqueous solution of Na$_2$CO$_3$ (20 ml, 20 mmol) were added to complete the reaction. The organic layer was washed with 2 N HCl, aqueous NaHCO$_3$ (5%) and water, and finally dried over Na$_2$SO$_4$. Removing the solvent on a rotary evaporator led to the pure urethane **6a** (yield 99%) or **6b** (yield 93%).

6a: IR (KBr): 3310 (NH); 1712 cm^{-1} (C=O).

^{1}H-NMR (DMSO-d$_6$): δ= 1.45 (m, -OCH$_2$CH$_2$C$\underline{H}_2$-, 8H); 1.73 (m, -OCH$_2$C$\underline{H}_2$-, 8H); 2.04 (s, -C$\underline{H}_3$, 6H); 3.98 (t, -C$_6$H$_4$OC$\underline{H}_2$-, 4H); 4.05 (t, -OCOC$\underline{H}_2$-, 4H); 5.12 (s, C$_6$H$_5$C$\underline{H}_2$O-, 4H); 6.96 (d, >C=C$\underline{H}$-, 4H); 7.12 (m, >C=C$\underline{H}$-C$\underline{H}$=C$\underline{H}$-C<, 6H); 7.38 (m, C$_6$$\underline{H}_5CH_2$O-, 10H); 7.50 (d, >C=C$\underline{H}$-, 4H); 8.07 (s, -N$\underline{H}$OCOCH$_2CH_2$-, 2H); 9.04 (s, C$_6H_5CH_2$OCON$\underline{H}$-, 2H).

6b: IR (KBr): 3304 (NH); 1712 cm^{-1} (C=O).

^{1}H-NMR (CDCl$_3$): δ= 1.48 (m, -OCH$_2$CH$_2$C$\underline{H}_2$-, 8H); 1.77 (m, -OCH$_2$C$\underline{H}_2$-, 8H); 2.17 (s, -C$\underline{H}_3$, 6H); 3.99 (t, -C$_6$H$_4$OC$\underline{H}_2$-, 4H); 4.17 (t, -OCOC$\underline{H}_2$-, 4H); 5.16 (s, C$_6$H$_5$C$\underline{H}_2$O-, 4H); 6.36 (s, C$_6$H$_5$CH$_2$OCON$\underline{H}$-, 2H); 6.67 (s, -N$\underline{H}$OCOCH$_2$CH$_2$-, 2H); 6.91 (d, >C=C$\underline{H}$-, 4H); 7.07 (d, >C=C$\underline{H}$-CH=, 2H); 7.20 (d, >C=C$\underline{H}$-, 2H); 7.36 (m, C$_6$$\underline{H}_5CH_2$O-, 10H); 7.44 (d, >C=C$\underline{H}$-, 4H); 7.79 (d, >C=C$\underline{H}$-, 2H).

C$_{56}$H$_{62}$N$_4$O$_{10}$ (951.1)   Calc.   C 70.72   H 6.59   N 5.89

Found C 70.75   H 6.52   N 5.84

4,4'-Bis[(3-amino)(2-methyl)phenylene(1-iminocarbonyloxyhexyloxy)]-biphenyl (7a) and 4,4'-bis[(5-amino)(2-methyl)phenylene (1-iminocarbonyloxyhexyloxy)]-biphenyl (7b)

6a or **6b** was dissolved in a 1:1 (v/v) mixture of glacial acetic acid and dioxane, and hydrogenated for 4h under a H$_2$- pressure of 10 bar at 55 °C with Pd/C as a catalyst. After removing the catalyst by filtration and most of the solvent by evaporation, crude **7a** or **7b** was precipitated from the residue upon the addition of concentrated aqueous NaOH solution (pH~13). The product was extracted with chloroform, the organic phase was dried over Na$_2$SO$_4$ and then evaporated to dryness. Yield **7a**: 40%, yield **7b**: 91%.

7a: IR (KBr): 3450, 3329 (NH); 1712 cm^{-1} (C=O).

^{1}H-NMR (DMSO-d$_6$): δ= 1.04 (m, -OCH$_2$CH$_2$C$\underline{H}_2$-, 8H); 1.67 (m, -OCH$_2$C$\underline{H}_2$-, 8H); 2.03 (s, -C$\underline{H}_3$, 6H); 3.97 (t, -C$_6$H$_4$OC$\underline{H}_2$-, 4H); 4.03 (t, -OCOC$\underline{H}_2$-, 4H); 4.80 (br, -N$\underline{H}_2$, 4H); 6.46 (m, >C=C$\underline{H}$-CH=C$\underline{H}$-C<, 4H); 6.79 (t, >C=CH-C$\underline{H}$=CH-C<, 2H); 6.97 (d, >C=C$\underline{H}$-, 4H); 7.51 (d, >C=C$\underline{H}$-, 4H); 9.60 (s, -N$\underline{H}$COO-, 2H).

7b: IR (KBr): 3454, 3329 (NH); 1701 cm^{-1} (C=O).

^{1}H-NMR (CDCl$_3$): δ= 1.49 (m, -OCH$_2$CH$_2$C$\underline{H}$$_2$-, 8H); 1.77 (m, -OCH$_2C\underline{H}$$_2$-, 8H); 2.10 (s, -C$\underline{H}$$_3$, 6H); 3.63 (br, -N$\underline{H}$$_2$, 4H); 3.99 (t, -C$_6H_4OC\underline{H}$$_2$-, 4H); 4.17 (t, -OCOC$\underline{H}$$_2$-, 4H); 6.33 (s, -N$\underline{H}$OCOCH$_2CH_2$-, 2H); 6.36 (d, >C=C$\underline{H}$-, 4H); 6.68 (d, >C=C$\underline{H}$-CH=, 2H); 6.95 (d, >C=C$\underline{H}$-, 4H); 7.30 (s, >C=C$\underline{H}$-, 2H); 7.43 (s, >C=C$\underline{H}$-, 2H).

General procedure for the synthesis of the isomerically pure segmented polyurethane elastomers (PUE 10a, 10b) and isomerically mixed liquid crystalline polyurethane elastomer (LCPUE 11)

The oligourethane hard segment (**7a**, or **7b**, or a 1:1 mole ratio mixture of **7a** and **7b**) in dioxane/chloroform 1:1 (v/v) was reacted with the soft segment precursor POTM-bischloroformate (**9**) in a 1:1 mole ratio, and a more than two fold excess of a 1M aqueous sodium carbonate solution was added as a HCl-scavenger.[8,9,12] After stirring overnight, the organic layer was washed with water until it was neutral. The polymer can be isolated by precipitation of the reaction mixture in methanol at -20 °C, filtering off and freeze drying from benzene.

Preparation of isomeric blends

Blends were prepared by codissolving the 2,4- PUE and 2,6- PUE at 50°C in DMF, followed by precipitating into methanol at 0°C, filtering, and vacuum drying.

The list of the chemical shifts of the ^{1}H NMR spectra of the polymer **10a, 10b** and **11** is given in Table 5.1. Table 5.2 shows the average molar

101

Table 5.1   Line listing for ^{1}H NMR resonances in Liquid Crystalline Polyurethane Elastomers

region	range, ppm	specific chemical shift (δ), ppm	multiplicity	assignment
I	8.0–6.8	7.76	s	1
		7.48–7.43	d	2
		7.25–7.15	m	3,4,5
		7.10–7.00	m	6,7
		6.96–6.90	d	8
II	6.8–6.0	6.69	s	9
		6.42	s	10,11
III	4.3–3.2	4.17	t	12
		3.99	t	13
		3.41	t	14
IV	2.2–1.0	2.19	s	15
		2.14	s	16
		2.00–1.40	m	17,18

Table 5.2   Molar mass characterization obtained from GPC analysis in CHCl$_3$ Solvent

Polymer	M_w	MMD [a]
2,6- PUE **10a**	43 500	1.23
2,4- PUE **10b**	23 200	2.17
LCPUE **11**	37 500	2.36

[a] $MMD = \dfrac{\overline{M_w}}{\overline{M_n}}$

masses and molar mass distributions (MMD) of the polymers as obtained from GPC measurements in $CHCl_3$.

5.3.3 Polymer Characterization Techniques

Molecular weights relative to polystyrene standards were determined by gel permeation chromatography (GPC) in $CHCl_3$ as an eluent (30 $^\circ$C) with a flow rate of 1 ml/min. The GPC instrument was equipped with four Water Ultrastyragel columns (500, 10^3, 10^4, and 10^5 Å), and the measurements were made by using a Waters 410 RI detector.

^{1}H NMR spectra were recorded on a Varian XL-200 spectrometer. TMS was used as an internal standard.

A TA instrument 2910 differential scanning calorimeter was used to determine the thermal transitions. Indium was used as a standard for calibration. First-order transitions (e.g., mesophase-isotropic phase, crystalline-isotropic phase, etc.) were taken as the maximum or minimum of the endothermic or exothermic peaks.

X-ray powder diffraction patterns of the polymers were recorded using Ni-filtered CuKa radiation in a Statton Camera. The X-ray camera length was calibrated with $CaCO_3$. In order to erase thermal histroy, X-ray samples were brought to the isotropic state at 180 $^\circ$C and then back to the room temperature by the cooling rate of 10 K/min.

Infrared spectroscopic experiments were performed with an IBM Model 32 Fourier transform infrared spectrometer. Data were collected at 4 cm^{-1} resolution with a minimum of 48 scans. The sample films cast from $CHCl_3$ solution on KBr windows were sufficiently thin to be within an absorbance range where the Beer-Lambert law was obeyed.

5.4   Results and Discussion

5.4.1   Constitution of the Isomeric Segmented Polyurethane Elastomers

A polydisperse hard segment length distribution is obtained in the conventional polyurethane synthesis, resulting from the statistics of polycondensation reactions, i.e., particularly from the residual amount of diisocyanate monomer in the prepolymer mixture, which also reacts in the chain extension step.[5] Harrell[7] and Eisenbach[8,9,12] treated amine-terminated hard segments with poly(oxytetramethylene) bischloroformate in the presence of an acid acceptor, and synthesized well-defined segmented model polyurethanes with molecularly uniform hard segments. It was found that the narrowing of the hard segment size distribution changed the superstructure of the macromolecular system and the material properties. It is our intent to investigate isomeric structure-property relationships in LCPUEs without other structural influences, such as hard segment polydispersity. Therefore, monodisperse hard segment intermediates were synthesized in a stepwise manner (Figure 5.1), and then employed as building blocks in the LCPUE synthesis. Based on the different reactivity of the amine groups of 2,4- and 2,6-tolylene diamine,[13] it is possible to protect only one of the two amino groups in **1a** or **1b** when the pH is controlled carefully during the reaction. The benzyloxy terminated oligourethanes **6a** and **6b** are obtained by reacting **3a** and **3b** with diol-6-bischloroformate (**5**), respectively. After the removal of the CBO-protecting groups, the diamines **7a** and **7b** can be isolated, which are introduced into the PUE via a condensation reaction (Figure 5.2).

The copolymerization (Figure 5.3) results in a random distribution of 2,4- and 2,6-substituted tolylene along the chain, which eventually may influence the structure of the hard domain, i.e., the mixing of two kinds of

105

isomeric hard segments into one physical cross-linking region.[11] The ^{1}H NMR in Figure 5.4 shows that the chemical shifts (δ) of methyl groups in 2,4- PUE and 2,6- PUE are 2.19 and 2.14, respectively. The slight downfield shift in 2,4-PUE could be explained by more deshielding of -CH_3, resulting from the inductive effect of ortho- and para- urethanes. The different chemical shifts and their peak integrations illustrate the equal molar ratio of 2,4- and 2,6-substituted tolylene in both LCPUE copolymer and 50/50 blend.

5.4.2 Thermal Characterization

Figure 5.5 shows DSC thermograms for isomeric polyurethane elastomers at a heating rate of 10 K/min. The endotherms in both 2,4- and 2,6-PUEs (**10b** and **10a**, curves a and d) represent the melting of hard domain crystallites. This assignment is in agreement with previous results that 2,4-TDI-Diol-6 and 2,6-TDI-Diol-6 based polyurethanes were found to be crystallizable.[10,11] Molecular symmetry of these hard segments and strong intermolecular forces (e.g. hydrogen-bonding and dipole-dipole interaction) provide a driving force for crystallization in the hard domain; thus, attainment of hard segment close packing leads directly to a three-dimensional crystalline structure. Another notable feature of 2,6- PUE is its symmetrical urethane linkages, brought about by the position of the methyl group in 2,6-substituted tolylene. This causes an increase of the melting temperature (T_m) and heat of fusion (ΔH) (Table 5.3), as compared to those of 2,4- PUE.

The molecular symmetry of the hard segments along the chain in the isomeric pure PUE **10a** and **10b** is significantly disturbed in the copolymer **11** with its random sequence of 2,4- and 2,6-TDI based hard segments; this is expected to destabilize the crystalline phase relative to the liquid crystalline phase, thus forming an enantiotropic mesophase. It is in agreement with X-ray

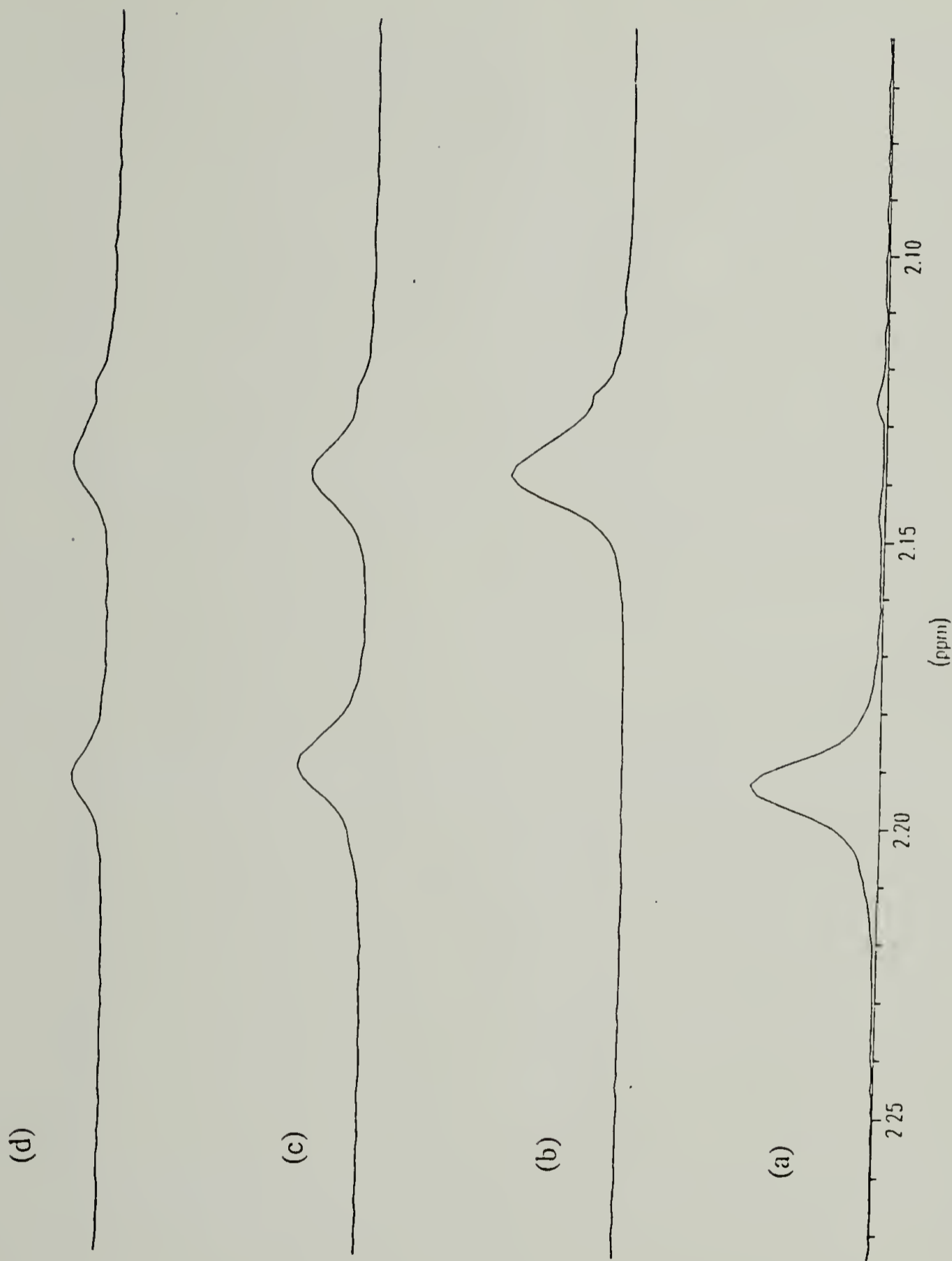Figure 5.4 1H NMR spectra of methyl groups in isomeric polyurethane elastomers: (a) 2,4- PUE **10b** (b) 2,6- PUE **10a** (c) LCPUE **11** (d) a 50/50 blend of **10a/10b**.
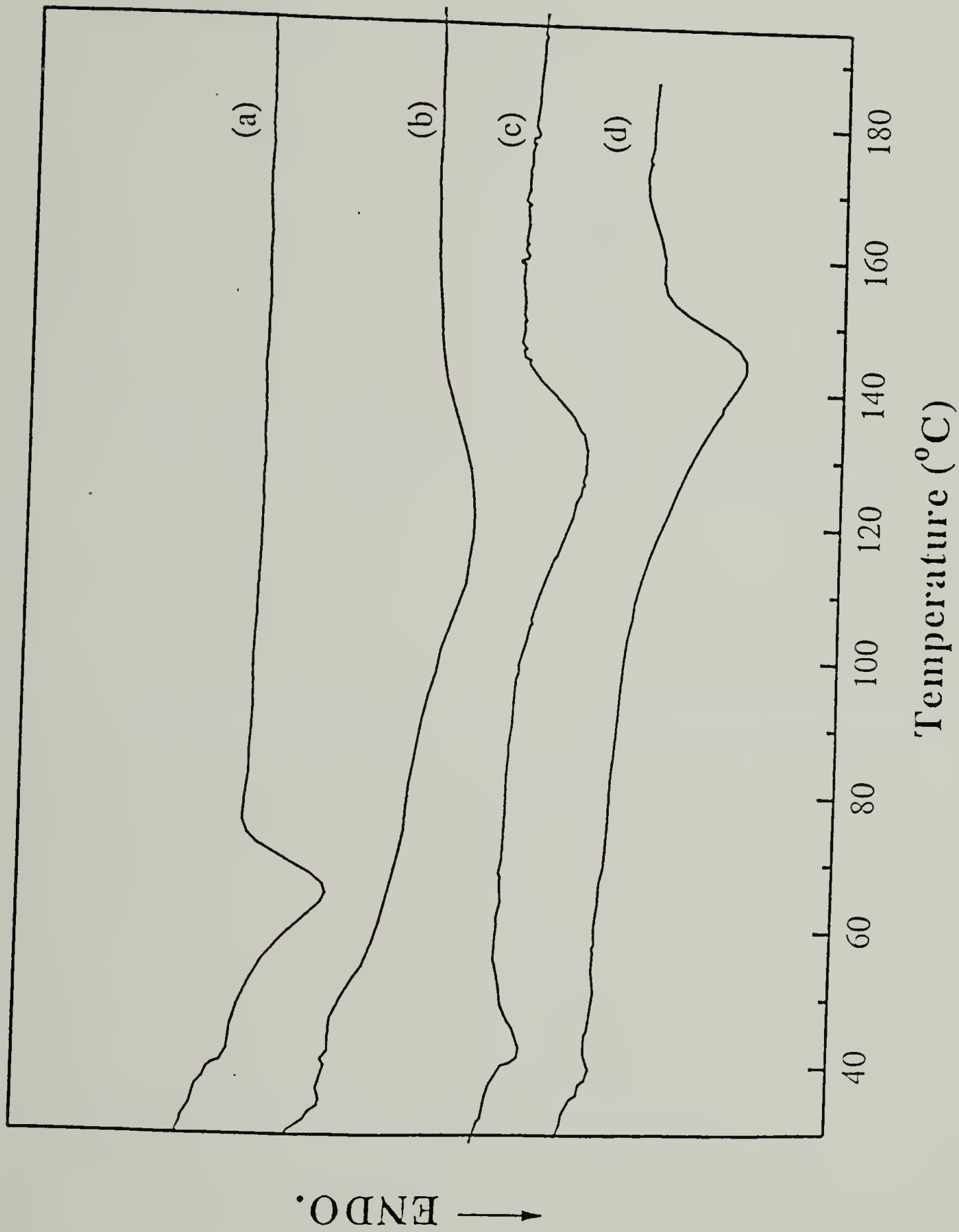
Figure 5.5   DSC thermograms for isomeric polyurethane elastomers at a heating rate of 10 K/min: (a) 2,4- PUE **10b**
(b) LCPUE **11** (c) a 50/50 blend of **10a/10b** (d) 2,6- PUE **10a**.

Table 5.3 - Thermal properties of isomeric polyurethane elastomers by DSC

Sample	$T_m/°C$	$T_i/°C$	ΔH (kJ/mol)[a]
2,4 - PUE **10b**	65.0		18.7
2,6 - PUE **10a**	143		32.1
LCPUE **11**		118	19.5
50/50 Blend (w/w) of **10a** and **10b**		131	15.7

a) The heat of fusion is related to the molar hard segment weight fraction

diffraction pattern shown in Figure 5.7c. Compared with the melting transition of 2,6- PUE, the endotherm in LCPUE **11** (curve b) which corresponds to the isotropization of the mesophase is shifted to lower temperature with a decreased enthalpy. The unusual breadth of this endotherm reflects the lack of uniformity of the mesophasic domains. It could be caused by the domain size distribution and the influence of the structure of the interfacial region.

Blending of 2,4- PUE and 2,6- PUE in equal molar ratio and an additional thermal treatment of sample change the original crystalline structure of each isomer. Compared with thermal data of isomerically pure 2,6- and 2,4- PUEs, the shift of transition temperature and change of enthalpy in a 50/50 blend (curve c) clearly illustrate a large degree of mixing of two kinds of hard segments into the physical crosslinks. The mixing of the isomers is a result of transurethanification, which occurs at the high temperature. It scrambles the distribution of isomers on the polymeric chains, thus an enantiotropic mesophase is formed. The isotropization of mesophase in the blend occurs at a higher temperature than that in the copolymer, and it may suggest the residual crystallites of 2,6- PUE exist. A small endotherm occurs at ca. 45°C, and may suggest the residual crystallites of 2,4- PUE exist.

Figure 5.6 shows that the isotropization of LCPUEs with monodisperse and polydisperse hard segments occurs in the same temperature range from 80 °C to 144 °C. However, there is a distinct exotherm in the polydisperse sample heating trace, separating the isotropization into two parts. According to our previous studies, this was attributed to the reorganization of polydisperse hard segments into thermodynamically more stable phase during heating, followed by complete isotropization at higher temperature.[1]
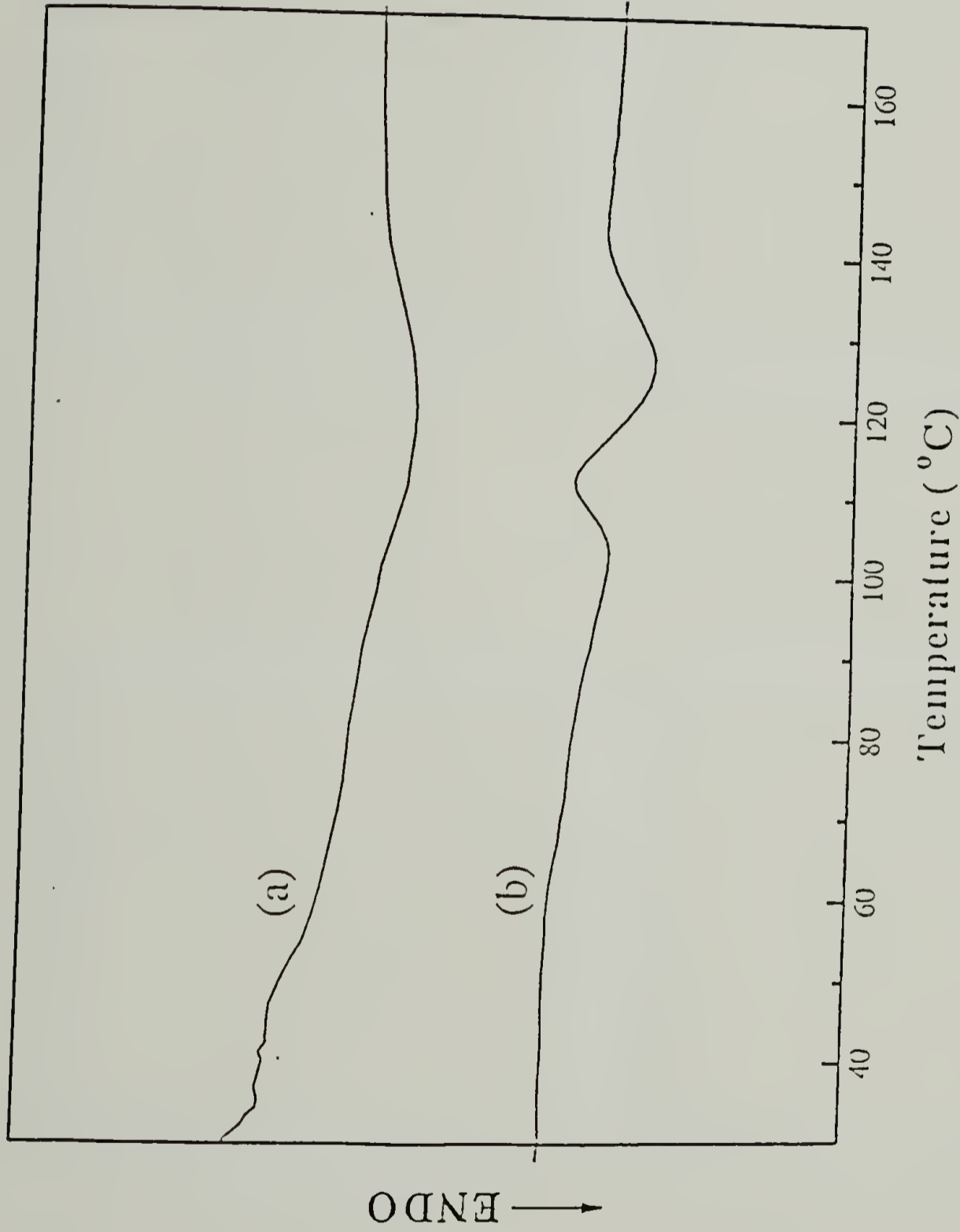
Figure 5.6   DSC thermograms for LCPUEs with an overall equimolar 2,4- and 2,6-TDI content in the hard segments at a heating rate of 10 K/min: (a) LCPUE 11 with monodisperse and isomerically mixed 2,4- and 2,6- TDI-based hard segments (b) with polydisperse hard segments and random incorporation of 2,4 and 2,6-TDI.
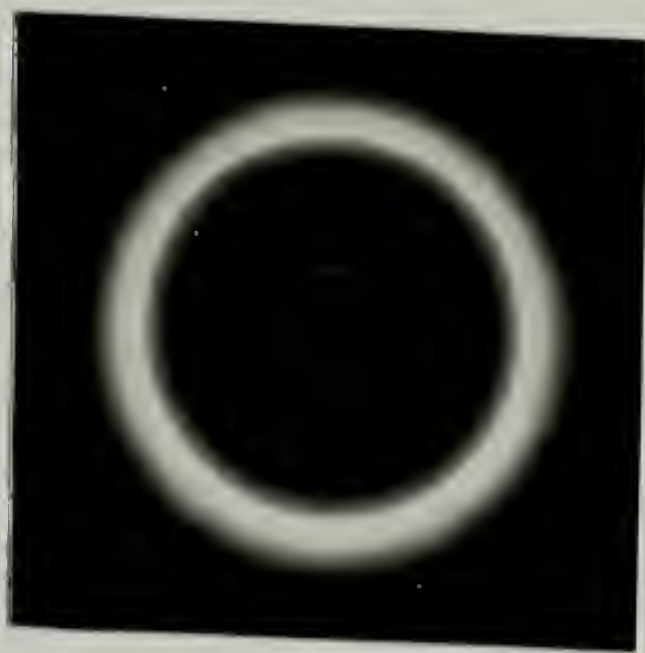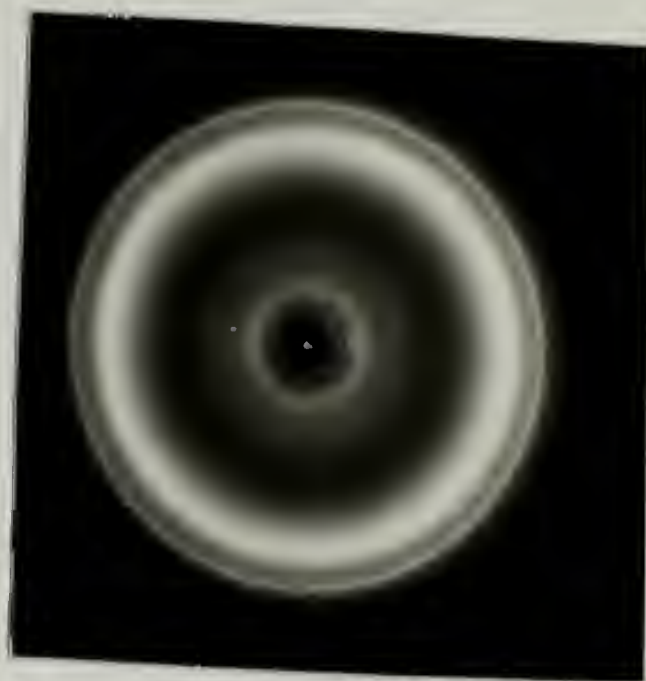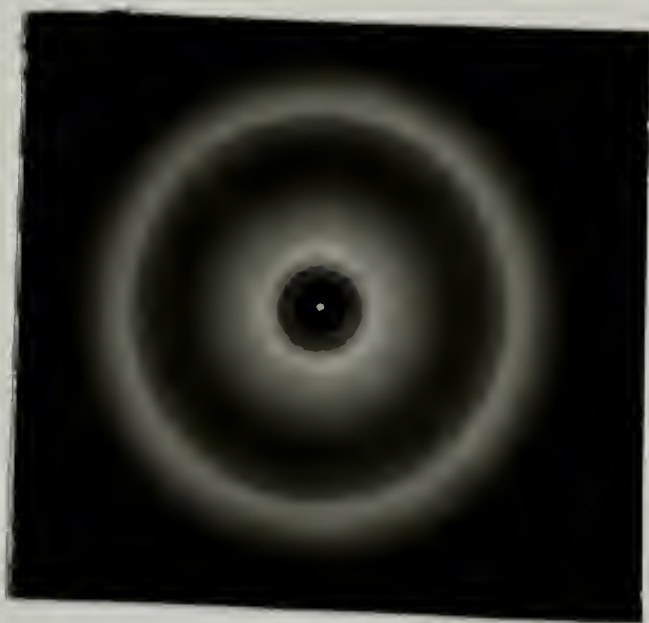
Figure 5.7 Room-temperature X-ray diffraction patterns of unoriented isomeric polyurethane elastomers: (a) 2,6- PUE **10a** (b) 2,4- PUE **10b** (c) LCPUE **11** (d) a 50/50 blend of **10a/10b**

Obviously, such a thermal reorganization does not occur in the monodisperse sample.

5.4.3 X-ray Diffraction

In order to understand the segmental conformation, Eisenbach et al.[9,12] studied the occurrence of the extended or folded hard segments in segmented polyurethanes, and determined that it was influenced by the flexibility of units between the urethane gro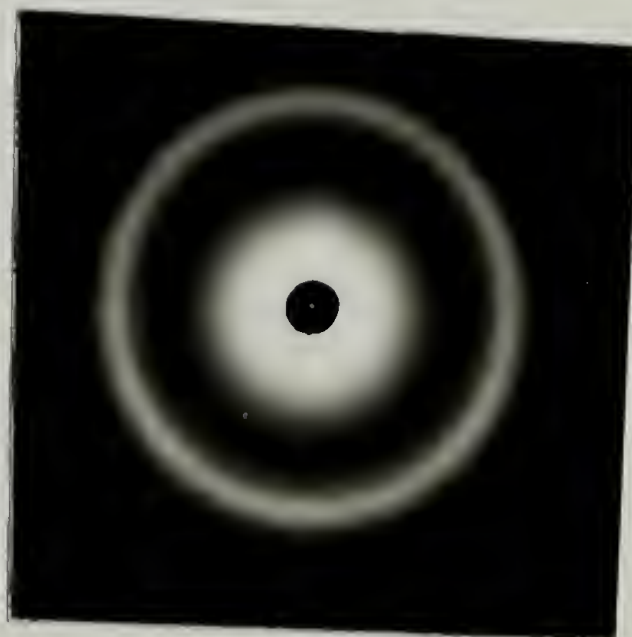ups. Papadimitrakopoulos et al.[10] investigated the structures of homopolymers of 2,4- PUE and 2,6- PUE hard segments. The absence of gauche conformations in the hexamethylene spacer was confirmed, and this led to fully extended conformations of each hard segment.

Figures 5.7a and b show the X-ray diffraction patterns of unoriented 2,4- and 2,6- PUEs at room temperature. The well-defined rings in these patterns manifest the crystalline characteristics of hard domains. The major features of 2,6- PUE (**10a**) are a strong, broad reflection at d=18.2 Å and a strong, sharp one at d=4.8 Å. In addition, three weak reflections at d=5.5 Å, 4.5 Å and 3.1 Å are observed. Four repeats of 18.2 Å give a length of 72.8 Å, which is close to the C-axis length of 73.2 Å in a fully extended 2,6- PUE hard segment dimer.[10] Thus, one may conclude that the monodisperse hard segments crystallize in the fully extended conformation, and the 18.2 Å spacing can be explained as a strong 002 reflection from highly ordered hard segment crystals in 2,6- PUE.

The diffraction pattern of 2,4- PUE (**10b**) is different from that of 2,6- PUE. It shows a strong, sharp reflection at d=3.9 Å, two strong, broad ones at d=4.5 Å and d=17.8 Å. Two weak reflections are also observed at 2.5 Å and 2.9 Å. The different diffraction patterns arise from the unequivalent hard segment packing in isomeric PUEs, attributed to the steric effect that the

methyl group of the tolylene ring asserts on the carbonyl groups of the urethane linkages. The methyl group in 2,6- PUE is ortho to both urethane groups, and causes them to rotate out of the plane of the phenyl. The equilibrium torsional angle of the phenyl-urethane is determined from the combined effect of phenyl-urethane steric interactions, H-bonding and chain packing. However, in 2,4- PUE, only one urethane group is ortho to the methyl group, and the second one is not influenced by the steric effect. Thus, it causes the different crystalline packing of isomeric hard domains.

Two diffuse reflections (d=4.5 Å and d=17.8 Å) are observed in the LCPUE copolymer X-ray diffraction results (Figure 5.7c). The outer ring occurring at 4.5 Å corresponds to the chain spacing and reflects the irregular packing of the hard segments within the mesophase. The crystalline phase in the copolymer is destabilized, and a mesophase is formed.

The effect of blending on domain structure is shown in Figure 5.7d. One can observe a sharp reflection at d=3.9 Å, two broad ones at d=4.5 Å and d=17.8 Å. It indicates that those isomeric hard segments are able to mix after transurethanification to form a mesophase in hard domain. However, the additional reflection at d=3.9 Å and the thermal trace (curve C in Figure 2) may suggest the existence of residual isomerically pure crystallites.

5.4.4 Infrared Spectroscopy

Infrared spectroscopy is widely used to study chain-chain interactions and conformational order in polymers. The molecular interactions are related to the nature of the phase which determines the relative arrangement of functional groups. Therefore, one may investigate the dependence of the mesophase and/or crystalline microstructure on molecular interactions using this technique.

114

Figure 5.8 shows the infrared spectra of isomeric polyurethane elastomers in the amide I region. One can clearly observe three different urethane carbonyl absorbances at 1735, 1712 and 1692 cm^{-1}, corresponding to non-hydrogen bonded, disordered hydrogen bonded and ordered hydrogen bonded carbonyls, respectively. From our previous studies,[3] both ordered and disordered hydrogen bonded C=O groups can be present in both mesophase and crystalline phase. However, the predominant presence of ordered C=O occurs in the crystalline phases, as indicated by the spectra of 2,6- and 2,4- PUEs. Crystallizable hard segments aggregate and form an ordered three-dimensional lattice, interacting by hydrogen bonding formed between them.

In the mesophase, the disordered hydrogen bonded C=O groups are dominant. The irregular packing of hard segments prevents them from interacting in an ordered pattern.

The presence of C=O groups at 1735 cm^{-1} in all samples indicates that some urethane groups are free from hydrogen bonding, and may exist at the interface and/or within the soft segment matrix.

5.5   Conclusion

The aggregation of isomerically pure hard segments results in crystalline physical cross-links in both 2,4- and 2,6- PUEs. Molecular symmetry of these isomers and the ordered hydrogen bonding provide a driving force for crystallization in the hard domain. The difference of 2,4- PUE and 2,6- PUE crystalline phases is attributed to the unequivalent steric effect
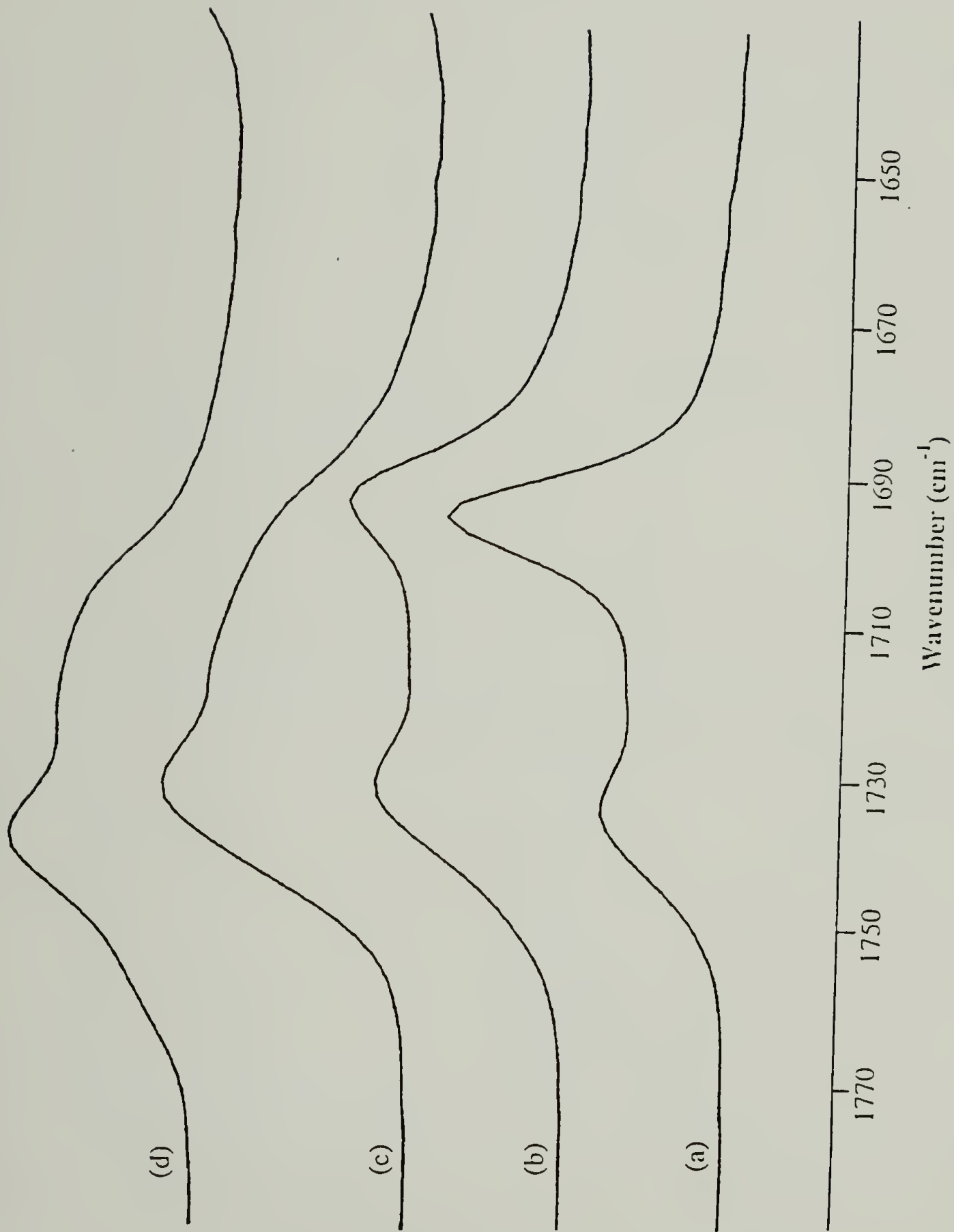
Figure 5.8   IR spectra of isomeric polyurethane elastomers in the amide I region: (a) 2,6- PUE **10a** (b) 2,4- PUE **10b** (c) LCPUE **11** (d) a 50/50 blend of **10a/10b.**

that the methyl group of the tolylene ring asserts on the carbonyl groups of the urethane linkages.

The aggregation of isomerically mixed hard segments results in mesophasic physical cross-links in LCPUE and a 50/50 blend of isomers. An enantiotropic mesophase is formed by copolymerization and/or blending. The predominant presence of disordered hydrogen bonded carbonyl groups further illustrates the irregular packing of hard segments within the mesophase.

References and Notes

(1)   Tang, W.; Farris, R. J.; MacKnight, W. J.; Eisenbach, C. D. *Macromolecules* **1994**, 27, 2814.

(2)   Wedler, W.; Tang, W.; Winter, H. H.; MacKnight, W. J.; Farris, R. J. *Macromolecules* **1995**, 28, 512.

(3)   Tang, W.; MacKnight, W. J.; Hsu, S. L. *Macromolecules* June 1995, in press.

(4)   Fu, B.; Feger, C.; MacKnight, W. J.; Schneider, N. S. *Polymer* **1985**, 26, 889.

(5)   Eisenbach, C. D.; Baumgartner, M.; Gunter,Cl. *Advances in Elastomers and Rubber Elasticity;* Lai, J., Mark, J. E., Eds.; Plenum: New York, 1986; p 51.

(6)   Christenson, C. P.; Harthcock, M. A.; Meadows, M. D.; Spell, H. L.; Howard, W. L.; Creswick, M. W.; Guerra, R. E.; Turner, R. B. *J. Polym. Sci. Phys. Ed.* **1986**, 24, 1401.

(7)   Harrell, L. L., Jr. *Macromolecules* **1969**, 6(2), 607.

(8)   Eisenbach, C. D.; Nefzger, H. *Multiphase Macromolecular Systems;* Culbertson, B. M., Eds.; Plenum: New York, 1989; p339.

(9)   Eisenbach, C. D.; Stadler, E. *Macromol. Chem. Phys.* **1996**, in press.

(10)   Papadimitrakopoulos, F.; Hsu, S. L.; MacKnight, W. J. *Macromolecules* **1992**, 25, 4671.

(11)   Stenhouse, P. J. Ph.D. Thesis, University of Massachusetts at Amherst, Amherst, MA. 1992.

(12)   Eisenbach, C. D.; Hayen, H.; Nefzger, H. *Makromol. Chem., Rapid Commun.* **1989**, 10, 463.

(13)   Ferstanding, L. L.; Scherrer, R. A. *J. Am. Chem. Soc.* **1959**, 81, 4838.

CHAPTER 6

CONCLUSIONS AND FUTURE WORK

6.1   Conclusions

The formation of a mesophase in segmented liquid crystalline polyurethanes is achieved by the self-assembly of the hard segments. Wide-angle X-ray scattering and infrared spectroscopic studies of LCPUE show that the elastic deformation can orient the mesophase and lead to macroscopic anisotropy in the material.

A broad viscoelastic solid/liquid transition is observed by rheology. The isothermal consecutive frequency sweep method has been applied to identify the viscoelastic transition at $106 \, ^{\circ}C$ and shows the existence of a critical physical gel.

Infrared spectroscopic stuides show that the amide I mode of LCPUE is well resolved into three constituents corresponding to ordered hydrogen bonded, disordered hydrogen bonded and free C=O. In the unstrained sample, there is the large amount of disordered hydrogen bonded carbonyl band. Elastic deformation reduces the disorder in the mesophase, shown by a substantial area increase of the ordered hydrogen bonded amide I band at 1694 cm^{-1}.

Molecular symmetry and ordered hydrogen bonding of monodisperse isomerically pure hard segments in both 2,4- and 2,6- PUEs provide a driving force for crystallization in the hard domain. The difference of 2,4- PUE and 2,6- PUE crystalline phases is attributed to the unequivalent steric effect that

the methyl group of the tolylene ring asserts on the carbonyl groups of the urethane linkages.

An enantiotropic mesophase is formed by copolymerization and/or blending of isomerically mixed hard segments in LCPUE and a 50/50 blend of isomers. The predominant presence of disordered hydrogen bonded carbonyl groups further illustrates the irregular packing of hard segments within the mesophase.

6.2   Future Work

The potential applicability of LCPUE as one of the commercial thermoplastic elastomers has been a matter of great interest. As an outcome of this thesis, one may conclude that the good mechanical properties of these materials result from the inherent ability of the liquid crystalline domain to form easily an elongated superstructure under mechanical fields. Evidently, future work is needed to compare the structure-property relationships of segmented polyurethane elastomers with liquid crystalline, crystalline and glassy hard domains. By varying the chemistry of the hard segment, one may synthesize 2,6-TDI-Diol-6 (crystalline) and 2,4-TDI-butanediol (glassy) based segmented polyurethanes, and directly correlate the effect of the hard phase upon the mechanical properties of each material.

Liquid crystalline elastomers (LCE) have attracted considerable attention for their stress-induced optical properties. Finkelmann et al[1-4] studied chemically cross-linked liquid crystalline side-chain polymers, and found the material demonstrated the combined properties known from both low molecular weight liquid crystalline materials and conventional elastomers.

Furthermore, mechanical deformations of the network led to a macroscopic orientation of the liquid crystalline phase and converted a turbid polydomain sample to an optically transparent monodomain. It seems interesting to conduct a parallel study in main-chain liquid crystalline elastomers, in which the aggregation of mesogenic units forms as physical cross-links. One may also observe these mechanically induced optical properties, which can be used as passive optical sensors and for storage application.

References and Notes

(1)   Finkelmann, H.; Brand, H. R. *Trends in Polymer Science* **1994**, *Vol. 2,* No.7, 222.

(2)   Benne, I.; Semmler, K.; Finkelmann, H. *Macromolecules* **1995**, *28*, 1854.

(3)   Schatzle, J.; Kaufhold, W.; Finkelmann, H. *Makromol. Chem.* **1989**, *190*, 3269.

(4)   Kaufhold, W.; Finkelmann, H.; Brand, H. R. *Makromol. Chem.* **1991**, *192*, 2555.

BIBLIOGRAPHY

(1)   Folkes, M. J. *Processing, Structure and Properties of Block Copolymers*; Elsevier Applied Science Publishers: New York, 1985.

(2)   Legge, N. R.; Holden, G.; Schroeder, H. E. *Thermoplastic Elastomers*; Hanser Publishers: New York, 1987.

(3)   Willwerth, L.; Anzuoni, A. *Modern Plastics Encyclopedia 97*; McGraw Hill: New York, 1988.

(4)   Gray, G. W.; Winsor, P. A. *Liquid Crystals and Plastic Crystals*; John Wiley & Sons: New York, 1974.

(5)   Pearce, E. M.; Schaefgen, J. R. *Contemporary Topics in Polymer Science*; Plenum Press: New York, 1977.

(6)   Hartshorne, N. H. *The Microscopy of Liquid Crystals*; Microscope Publications Ltd.: London, 1974.

(7)   Sandler, S. R.; Karo, W. *Polymer Syntheses I*; Academic Press: New York, 1974.

(8)   Odian, G. *Principles of Polymerization*, 2nd ed.; John Wiley & Sons: New York, 1981.

(9)   Lai, J., Mark, J. E., Eds. *Advances in Elastomers and Rubber Elasticity*; Plenum: New York, 1986.

(10)   Culbertson, B. M., Eds. *Multiphase Macromolecular Systems;* Plenum: New York, 1989.

(11)   Gray, G. W.; Goodby, J. W. G. *Smectic Liquid Crystals*; Leonard Hill: New York, 1984.

(12)   Baird, D. G. *Liquid Crystalline Order in Polymers*; Academic Press: New York, 1978.

(13)   Zbinden, R. *The Infrared Spectroscopy of High Polymers*; Academic Press: New York, 1964.

(14)   Coleman, M. M.; Graf, J. F.; Painter, P. C. *Specific Interactions and the Miscibility of Polymer Blends*; Technomic Publishing Co., Inc.: Lancaster, PA, 1991.

(15)   Aklonis, J. J.; MacKnight, W. J. *Introduction to Polymer Viscoelasticity*, 2nd ed.; John Wiley and Sons: New York, 1983.

(16) Schuster, P. ; Zundel, G.; Sandorfy, C. Eds. *The Hydrogen Bond, II*; North Holland Publishing Co.: Amsterdam, 1976.